January 2016

# Dissecting the Multifaceted Relationship Between Maize and Cochliobolus carbonum race 1

Kevin Chu
*Purdue University*

# DISSECTING THE MULTIFACETED RELATIONSHIP BETWEEN MAIZE AND *COCHLIOBOLUS CARBONUM* RACE 1

by

**Kevin Lee Chu**

**A Dissertation**

*Submitted to the Faculty of Purdue University*

*In Partial Fulfillment of the Requirements for the degree of*

**Doctor of Philosophy**


Department of Botany and Plant Pathology

West Lafayette, Indiana

December 2016

# THE PURDUE UNIVERSITY GRADUATE SCHOOL
# STATEMENT OF DISSERTATION APPROVAL

Dr. Gurmukh S. Johal, Chair
Department of Botany and Plant Pathology
Dr. Tesfaye Mengiste
Department of Botany and Plant Pathology
Dr. Robert E. Pruitt
Department of Botany and Plant Pathology
Dr. Steven R. Scofield
Department of Agronomy

**Approved by:**
Dr. Christopher Staiger
Head of the Departmental Graduate Program

# ACKNOWLEDGEMENTS

I would like to thank my advisor Dr. Gurmukh Johal for the opportunity to work in his lab as well as his advice and support over the years. I have developed much as a scientist while working in Dr. Johal's lab. I would also like to thank my committee members Dr. Tesfaye Mengiste, Dr. Robert Pruitt, and Dr. Steve Scofield and our collaborators Dr. Brian Dilkes and Dr. David Rhodes for their scientific guidance and time throughout my research.

I would especially like to thank past and present lab members including Alyssa DeLeon, Norman Best, Rajdeep Khangura, Dr. Antje Klempien, Dr. Sandeep Marla, and Dr. Bala Venkata for their aid, knowledge, and friendship. In addition, I would also like to thank members from other labs that have helped me over the years including Sara Allen, Chenxing Niu, Siming Xu, Dr. Bong-suk Kim, Dr. Kristin Laluk, Dr. Chao-Jan Liao, and Dr. Joseph Lynch. Additional faculty I would like to express gratitude for include Dr. Bruce Cooper, Dr. Natalia Dudareva, and Dr. Charles Woloshuk for their advice and use of their equipment. Above all, I would like to thank my family for their unwavering support throughout my time at Purdue.

# TABLE OF CONTENTS

# LIST OF FIGURES

# LIST OF TABLES

# LIST OF ABBREVIATIONS

| | |
|---|---|
| APR | Adult plant resistance |
| CCR1 | *Cochliobolus carbonum* race 1 |
| DEG | Differentially expressed gene |
| ET | Ethylene |
| HAT | Histone acetyltransferase |
| HCTR | HC-toxin reductase |
| HDAC | Histone deacetylase |
| hpi | hours post inoculation |
| HST | host-selective toxin |
| JA | Jasmonic acid |
| $k_{cat}$ | catalytic rate constant; turnover number |
| $K_M$ | Michaelis constant |
| NAD(H) | Nicotinamide adenine dinucleotide |
| NADP(H) | Nicotinamide adenine dinucleotide phosphate |
| PR | Pathogenesis-related |
| ROS | Reactive oxygen species |
| SA | Salicylic acid |

# ABSTRACT

Author: Chu, Kevin Lee. Ph.D.
Institution: Purdue University
Degree received: December 2016.
Title: Dissecting the Multifaceted Relationship Between Maize and *Cochliobolus carbonum* race 1.
Major Professor: Dr. Gurmukh Johal.

The maize pathogen *Cochliobolus carbonum* race 1 (CCR1) utilizes HC-toxin, an inhibitor of histone deacetylases, as a key determinant of virulence. The maize *Hm1* gene confers complete resistance to CCR1 at all stages of development by encoding for an NADPH-dependent reductase that inactivates HC-toxin. *Hm1A*, *Hm1-SM1*, and *Hm1-SM2* are alleles of *Hm1* that exhibit an adult plant resistance (APR) phenotype, being fairly susceptible during the seedling stage and gradually increasing in resistance with development. The HM1A protein differs from HM1 by five amino acid substitutions while HM1-SM1 and HM1-SM2 have a single amino acid substitution each in the predicted NADPH binding pocket. Given that gene and protein expression of these APR alleles do not increase with age, the APR phenotype must be dictated post-translationally. In this study we characterize the biochemical basis underlying APR. We show that the pool of the NADPH cofactor is higher during the day in adult leaf tissue compared to juvenile leaves. We also demonstrate that the various APR alleles do in fact display compromised enzymatic activities, while also characterizing recombinant proteins to conclude that the superior resistance conferred by *Hm1* is unlikely to be simply due to the stronger affinity of its enzyme for the NADPH substrate.

We also investigated the role HC-toxin plays in promoting susceptibility by comparing transcriptomic and metabolic data of plants inoculated with either CCR1 or a non-HC-toxin producing strain. We found that HC-toxin is not globally downregulating defense responses as previously thought but is causing massive deregulation of numerous metabolic pathways, including downregulating the light reactions of photosynthesis and increasing protein turnover. These results indicate that HC-toxin is likely promoting

susceptibility by interfering with fundamental metabolic processes rather than by suppression of specific defense pathways.

# CHAPTER I: LITERATURE REVIEW

## Introduction

The interactions between plants and pathogens are extraordinarily complex. Plants, being generally sessile organisms, possess a wide range of elaborate defenses aimed at preventing and containing pathogen attack. Because these defenses are often metabolically costly, plants will specifically tailor their defense response to the nature of the invading pathogen. A key distinction between plant pathogens is their mode of nutrition. Biotrophic pathogens feed off of living tissue, seeking to avoid detection by the host plant and often utilizing specialized infection-related structures known as haustoria (Mendgen and Hahn, 2002), while necrotrophic pathogens actively kill host cells to feed off of dead or dying tissue (Stone, 2001). Resistance to biotroph infection is generally via a rapid, localized form of programmed cell death known as the hypersensitive response (HR) (Coll et al., 2011), mediated by dominant resistance genes (R-genes) (Bent and Mackey, 2007) and the phytohormone salicylic acid (SA). Conversely, resistance to necrotroph infection often focuses on constraining necrosis to prevent the pathogen's spread (Mengiste, 2011) and is mostly mediated by the phytohormones jasmonic acid (JA) and ethylene (ET) (Glazebrook, 2005). Much work with the model plant *Arabidopsis thaliana* has established a generally antagonistic interaction between SA- and JA/ET-dependent defense responses, though the nature of the relationships between these three phytohormones can be rather complex, often differing based on timing and relative concentrations (Mur et al., 2006; Mengiste, 2011). Necrotrophs are often further grouped into broad-host range necrotrophs and host-specific necrotrophs. Broad-host range necrotrophs such as *Botryris cinerea* and *Alternaria brassicicola* can infect a wide range of plant species, utilizing an array of phytotoxins, lytic enzymes, and other secondary metabolites as virulence factors to infect the host, colonize host tissue, and suppress host defense responses (Laluk and Mengiste, 2010). Resistance to broad-host range necrotrophs is often quantitative due to the wide variety of virulence factors employed by these pathogens. Host-specific necrotrophs, including several members of the fungal genus *Cochliobolus*, possess a very limited host range, many having been observed to infect only a single plant species in nature. These necrotrophs often utilize host-selective toxins (HSTs), substances necessary for pathogenicity or virulence

that are only toxic to the respective hosts of the pathogen. Resistance to host-specific necrotrophs is often mediated by a single gene that either inactivates the HST or confers susceptibility to the HST (Wolpert et al., 2002). In these pathosystems, the plant host is susceptible only if the pathogen is capable of producing the HST and the plant lacks the corresponding resistance gene that detoxifies the HST.

**The Cochliobolus genus**

The ascomycete fungal genus *Cochliobolus* contains many plant pathogens (reviewed by Manamgoda et al., 2011), many of which can be economically significant. In the 1940s, *Cochliobolus victoriae* caused widespread yield losses in oat varieties in America that contained the recently introduced crown rust resistance gene *Pc-2* (Meehan and Murphy, 1946). Similarly in 1970, an outbreak of Southern corn leaf blight caused by a new race of *Cochliobolus heterostrophus* (anamorph *Helminthosporium maydis*) led to the loss of over 19 million metric tons of maize, more than 15% of the U.S. maize crop (Tatum, 1971; Ullstrup, 1972). It is important to note that both disease outbreaks occurred after the introduction of a new trait into their respective crops. In the case of *C. victoriae*, it was the introduction of the *Pc-2* crown rust resistance gene (Litzenberger, 1949), while in the case of *C. heterostrophus*, it was the widespread commercial use of male-sterile plants containing Texas male sterile cytoplasm (Tcms) (Klittich and Bronson, 1986). In both cases, proteins associated with these traits were later found to be specifically targeted by toxins produced by the pathogens. The pathogenicity of *C. victoriae* was found to be dependent on the production of the toxin victorin (Wolpert et al., 1985), with sensitivity to victorin in oats being conferred by the dominant *Vb* gene. As this gene was found to be genetically inseparable from the *Pc-2* resistance gene, it was concluded that the two were the same gene (Luke et al., 1966; Rines and Luke, 1985; Mayama et al., 1995). The new race of *C. heterostrophus* responsible for the 1970 outbreak was designated “Race T” due to its high virulence on Tcms maize (Smith et al., 1970) and was found to produce a series of race-specific polyketides collectively named T-toxin (Kono and Daly, 1979). T-toxin was shown to specifically target a maternally inherited protein on the inner mitochondrial membrane in Tcms maize lines, leading to membrane permeability and blockage of host cell energy production (Braun et al., 1990; Rhoads et al., 1995), leading to widespread

necrosis (Yoder and Gracen, 1975), possibly due to apotosis (Wolpert et al., 2002). Both victorin and T-toxin have been cited as classic examples of host-selective toxins, though *Arabidopsis thaliana* mutants sensitive to victorin and *C. victoriae* infection have been found (Lorang et al., 2004). This discovery, combined with the studies of *C. carbonum*'s HC-toxin discussed below, suggests that terms such as "host-specific necrotroph" and "host-selective toxin" may be misleading and simply be due to an incomplete understanding of the pathosystem.

***Cochliobolus carbonum***

Another plant pathogen from this genus is *Cochliobolus carbonum*, previously known by its anamorph name *Bipolaris zeicola* (Shoemaker) or *Helminthosporium carbonum* (Ullstrup), the causal agent of Northern Leaf Spot (NLS) and ear mold on maize (Manamgoda et al., 2011). First reported in 1938 on the Pr inbred line of maize grown in Indiana (Ullstrup, 1941; Nelson and Ullstrup, 1964), the disease was at first thought to be caused by a race of *Helminthosporium maydis* before being characterized as a new species (Ullstrup, 1944). Race 1 of *C. carbonum* was found to be a devastatingly powerful pathogen capable of infecting all parts of the maize plant and killing susceptible plants at any stage of development (Fig. 1.1) (Ullstrup, 1941; Sindhu et al., 2008). As with other pathogenic members of *Cochliobolus*, *C. carbonum* is a filamentous fungal necrotroph that actively promotes the death of host cells for sustenance. Like *C. victoriae* and *C. heterostrophus*, *C. carbonum* race 1 (CCR1) utilizes a toxin that acts as a key determinant of disease, though this was only discovered more than twenty years after the identification of the pathogen (Scheffer and Ullstrup, 1965). The toxin, named HC-toxin after *H. carbonum*, was determined to be a cyclic tetrapeptide of the structure cyclo-(D-Pro-L-Ala-D-Ala-L-Aeo), with Aeo being 2-amino-9,10-epoxi-8-oxodecanoic acid (Fig. 1.2) (Liesch et al., 1982; Gross et al., 1982; Walton et al., 1982). Due to its ability to be soluble in water, lower alcohols, and chloroform, HC-toxin does not appear to face any significant barriers to freely move through living tissues (Walton, 2006). CCR1 was found to also produce three minor forms of HC-toxin with various substitutions that exhibited reduced potency (Rasmussen and Scheffer, 1988). In addition, three other naturally occurring races of *C. carbonum* are not capable of producing any HC-toxin and are only weakly pathogenic

to maize (Comstock and Scheffer, 1973; Jones and Dunkle, 1993; Walton et al., 1997). Exogenous application of HC-toxin, however, greatly increases the virulence of these races on susceptible maize plants. Similar to victorin and T-toxin, the production of HC-toxin was found to be controlled by a single genetic locus, TOX2 (Scheffer et al., 1967), which was later resolved into a cluster of genes (Ahn et al., 2002; Walton, 2006) , not unusual in fungal secondary metabolite biosynthesis. Interestingly, the fungus *Alternaria jesenskae* was also recently found to produce HC-toxin, with the genes for HC-toxin biosynthesis being duplicated (Wight et al., 2013). Though the genus *Alternaria* contains many plant pathogens, *A. jesenskae* itself is not known to be pathogenic. The implications of this discovery in clarifying the role of HC-toxin in pathogenesis remain ambiguous.

**Figure 1.1. The fungal pathogen *Cochliobolus carbonum* race 1 can affect every part of the maize plant** (Sindhu et al., 2008)**.**

**Mode of action of HC-toxin**

Though the biosynthesis and structure of HC-toxin have been well characterized, its mode of action continues to be unclear. Despite its name, HC-toxin is not strictly a toxin since it does not directly cause cell death; rather it appears to inhibit cell division (Walton, 2006). HC-toxin was found to inhibit the growth of several plants in root and seedling assays, with susceptible maize roots being inhibited at concentrations 100-fold lower than those required to inhibit resistant maize roots (Walton et al., 1982; Rasmussen

and Scheffer, 1988). Notably, HC-toxin was found to be a potent reversible and uncompetitive inhibitor of Rpd3/Hda1 class histone deacetylases (HDACs/KDACs) both *in vivo* and *in vitro*, not only of maize but also of all other organisms tested, including yeast, *Physarum*, and chicken (Brosch et al., 1995). In addition, HC-toxin also inhibits the plant-specific HD2 class of HDACs but not the $NAD^+$-dependent sirtuin class (Walton, 2006). In the susceptible maize inbred Pr, accumulation of hyperacetylated forms of the core (nucleosomal) H3 and H4 histones, but not H2A or H2B histones, was observed during the early stages of infection with CCR1 (Ransom and Walton, 1997). Attempts to elucidate the role histone acetylation/deacetylation plays in inducing susceptibility to CCR1 have been complicated by the presence of 14 separate HC-toxin-sensitive HDACs in maize (Gendler et al., 2008) as well as the presence of multiple lysine residues on the multiple core histones that can be reversibly acetylated (Ransom and Walton, 1997). Acetylation of lysine residues on histones by histone acetyltransferases (HATs) is typically associated with transcriptional activation via relaxation of chromatin structure, while deacetylation by HDACs is associated with transcriptional repression via the promotion of a more closed chromatin state (Chinnusamy and Zhu, 2009). The plant pathogen *Alternaria brassicicola* is also known to produce a HDAC inhibitor, depudecin, as a virulence factor, though it is not a key determinant of disease like HC-toxin (Wight et al., 2009). In *Arabidopsis thaliana*, application of HDAC inhibitors has been shown to inhibit root growth via PIN1 degradation (Nguyen et al., 2013), possibly explaining HC-toxin's inhibition of maize roots. The Arabidopsis histone deacetylase HDA19 was found to be induced by wounding, the phytohormones jasmonic acid (JA) and ethylene (ET), and the pathogen *A. brassicicola*, with *HDA19* overexpression and downregulation increasing and decreasing resistance to this pathogen, respectively (Zhou et al., 2005). HDA19 was later found to be an important regulator of defense involved in repressing salicylic acid (SA) biosynthesis and SA-mediated defense responses (Choi et al., 2012). In addition, the histone deacetylase HDA6, already shown to interact with the JA receptor COI1, was found to be recruited by JAZ proteins as a corepressor of JA- and ET-dependent responses (Zhu et al., 2011). Various other chromatin remodeling factors such as the SWI/SNF class chromatin remodeling ATPase SPLAYED (SYD), the histone methyltransferase SET DOMAIN GROUP8 (SDG8), and the RING E3 ligase HISTONE MONOUBIQUITINATION1

(HUB1) have all been demonstrated to regulate defense responses against necrotrophs in Arabidopsis, often via the JA or ET pathways (Walley et al., 2008; Berr et al., 2010; Dhawan et al., 2009).

As CCR1 is a necrotrophic pathogen, it may be theorized that HC-toxin's inhibition of HDACs interferes with the proper induction of JA/ET-mediated defense responses in the host plant to promote susceptibility. Experiments have shown that HC-toxin application shuts down expression of defense genes even when applied days after inoculation with a $Tox^-$ strain of CCR1 (Young, 2008). No disease phenotype was observed, however, upon inoculation of either JA- or SA-deficient maize mutants (Johal, unpublished) (Kolomiets, unpublished); nor was resistance strengthened upon constitutively activating defense responses of maize plants in susceptible backgrounds (Johal, unpublished). The discovery that lysine acetylation extends to multiple nonhistone proteins (Wang et al., 2010; Zhao et al., 2010), including several enzymes involved in primary metabolism, suggests that protein acetylation is a widespread regulatory mechanism analogous to phosphorylation conserved from bacteria to mammals, including plants such as Arabidopsis and rice (Shen et al., 2015; Xiong et al., 2016). Acetylation of numerous central metabolic enzymes in Arabidopsis has been demonstrated to significantly affect their activities (Finkemeier et al., 2011). Interestingly, HDAC inhibitors have emerged as an important new class of anti-cancer agents (Liu et al., 2006; Khan and La Thangue, 2012), having been shown to induce morphological reversion of oncogene-transformed mammalian cells (Yoshida and Sugita, 1992). Out of a screen of 34 HDAC inhibitors, HC-toxin was found to exhibit the most potent antitumor activity (Zhou et al., 2016). The mode of action of HC-toxin, therefore, may be more complex than previously thought, possibly via interference with the metabolic status of the plant host rather than directly repressing defense responses.

**Maize resistance to CCR1**

Unlike *C. victoriae* and *C. heterostrophus, C. carbonum* has fortunately never been associated with an epidemic due to most of the maize germplasm being resistant. Resistance to CCR1 infection was found to be conferred by a dominant gene on the long arm of chromosome 1 named *Hm1* after *Helminthosporium maydis* (Ullstrup, 1941).

Through transposon mutagenesis, the *Hm1* gene was the first disease resistance gene cloned in plants, found to consist of five exons encoding a NADPH-dependent reductase with significant sequence homology to dihydroflavonol reductase (DFR), an enzyme involved in the biosynthesis of flavonoids and anthocyanins throughout the plant kingdom (Johal and Briggs, 1992). This enzyme, called HC-toxin reductase (HCTR), acts by reducing the 8-keto group of HC-toxin's Aeo to an 8-hydroxy derivative, thus inactivating the toxin (Fig. 1.2) (Meeley and Walton, 1991; Meeley et al., 1992). Thus, the two key determinants of disease in this pathosystem are the presence of HC-toxin produced by the pathogen and the absence of the *Hm1* resistance gene that inactivates the toxin (Walton, 1996). *Hm1* confers resistance to CCR1 in all parts of the plant at all stages of development. Interestingly, *Hm1* expression has also been shown to be induced upon wounding, suggesting a link with the JA-mediated wounding response. Further genetic analysis revealed the presence of an allele of *Hm1* named *Hm1A* and a homeologue named *Hm2* found on the long arm of chromosome 9 (Nelson and Ullstrup, 1964). Both *Hm1A* and *Hm2* were found to provide a partial resistance to CCR1, conferring resistance only fully effective at maturity. This adult plant resistance (APR) phenotype is ordinarily masked by the complete resistance conferred by *Hm1* and can only be observed in its absence. Though the phenomenon of APR (also known as age-related resistance) is well-documented in many plant species, the molecular mechanisms underlying it remain poorly understood (Kus et al., 2002). Rather than abruptly manifesting in younger tissue as observed in the flag leaf of the *Lr34*-mediated APR in the wheat-*Puccinia triticina* pathosystem (Krattinger et al., 2009), *Hm1A*- and *Hm2*-mediated resistance builds up gradually with development (Fig. 1.3), with *Hm1A* providing slightly stronger resistance than *Hm2*. This gradual onset of APR with the advancement of plant age is also observed with *Xa21* in the rice-*Xanthomonas oryzae pv. oryzae* pathosystem (Song et al., 1995; Century et al., 1999) and *Yr36* in the wheat-*Puccinia striiformis* pathosystem (Fu et al., 2009). As observed with several other APR genes (McDowell et al., 2005; Krattinger et al., 2009), the transcriptional status of both *Hm1A* and *Hm2* do not appear to change with growth (Chintamanani et al., 2007; Marla, 2014). Similarly, levels of HM2 protein also did not show any significantly variation over time. Plants homozygous for *Hm2*, however, were observed to display both increased gene transcription and increased resistance to

CCR1 at most growth stages compared to heterozygous (*Hm2hm2*) plants, indicating a gene-dosage effect (Chintamanani et al., 2007).

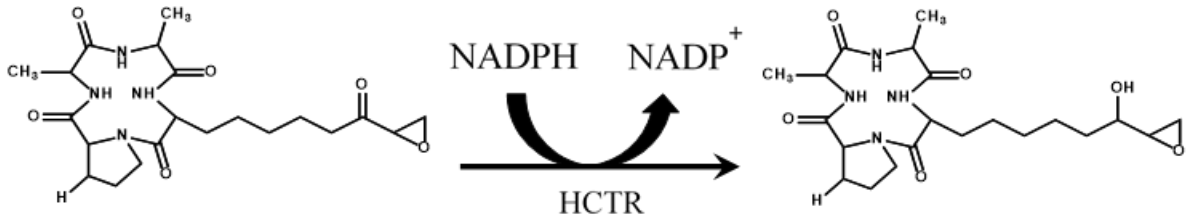


**Figure 1.2. HC-toxin reductase uses NADPH to inactivate HC-toxin by reducing an essential keto group to an alcohol.**

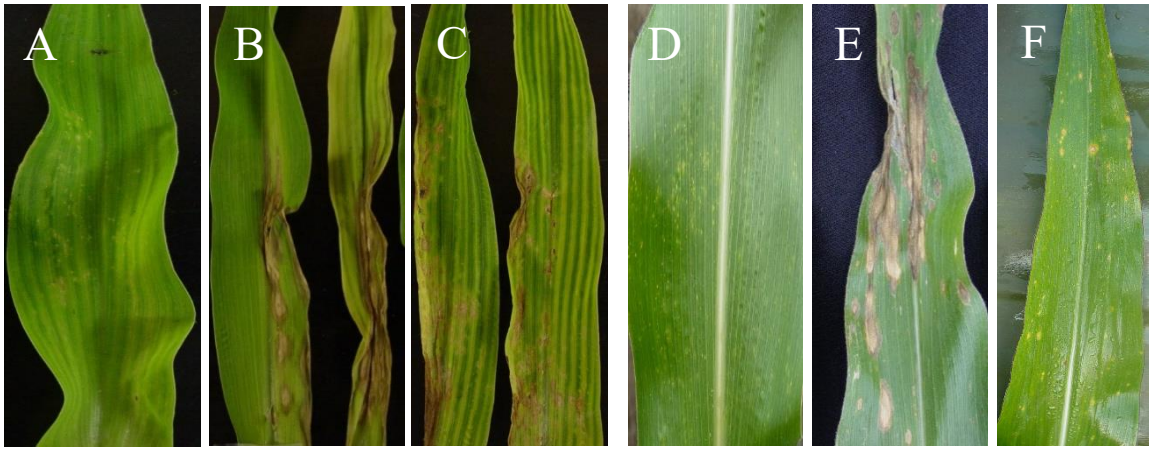


**Figure 1.3. The degree of resistance to CCR1 depends on genotype and age.** 1.3.A-F. Response of *Hm1Hm1* (A,D), *hm1hm1* (B,E), and *Hm1AHm1A* (C,F) maize leaves to CCR1 inoculation at 3 weeks (A-C) and 6 weeks (D-F) after planting (Marla, 2014).

**Adult Plant Resistance alleles of *Hm1***

Cloning of *Hm2* revealed it to encode a truncated HCTR missing the last 52 C-terminal amino acids due to the loss of the fifth exon, with the remainder displaying 89% peptide homology to the wild-type HCTR of the resistant B73 inbred (Chintamanani et al., 2007). Cloning of *Hm1A*, however, revealed that it contains five amino acid substitutions compared to *Hm1* from the resistant B73 background, only one of which is absent among

the *Hm1* genes from various resistant inbred lines (Marla, 2014). Though these changes likely adversely affect the HCTR activity of *Hm1A* and *Hm2*, precisely how this compromised enzymatic activity underlies the observed APR phenotype remains unanswered. Two new partial loss-of-function alleles generated via EMS mutagenesis, *Hm1*-SM1 (with a T90M subsitution) and *Hm1*-SM2 (with a V210M subsitution), were both also found to exhibit an APR phenotype similar to that of $Hm1^A$ and *Hm2*, though all four APR alleles confer slightly different levels of resistance (Marla, 2014). Structural modeling of the HM1 protein predicts both T90 and V210 to be localized in the binding site of the NADPH cofactor (Dehury et al., 2013). As seen for several other APR genes (Jones, 1975; Pretorius et al., 2007; Fu et al., 2009; Krattinger et al., 2009; Chen et al., 2013; Gusberti et al., 2012), the relative degree of resistance conferred by *Hm1A* and *Hm2* has been observed to be affected by environmental factors, especially photoperiod. Relatively cool and cloudy summers have led to decreased field resistance to CCR1 in both *Hm1A* and *Hm2* plants. The strength of resistance conferred by seedling *Hm1A* plants was enhanced markedly when the plants were grown under an 18 hour light: 6 hour dark photoperiod, while APR was dramatically compromised when plants were grown under a 6 hour light: 18 hour dark photoperiod (Marla, 2014). Supplementation of CCR1-inoculated seedlings kept in the dark with sucrose was further shown to prevent erosion of APR. These findings and observations strongly suggest that the plant's metabolic status and its degree of susceptibility to CCR1 are tightly linked.

**"Guardian of grasses"**

It is now understood that the Pr inbred of maize in which the Northern leaf spot disease was initially reported in 1938 had become susceptible to CCR1 due to a transposon insertion in its *Hm1* gene and a partial deletion of its *Hm2* gene (Multani et al., 1998). Mutations in these two genes have been found in all known susceptible maize inbreds. Though CCR1 has only been observed to cause significant disease on maize, homologs of the *Hm1* gene exist in all grass species, with barley, rice, and sorghum possessing true orthologs that are syntenic to the maize *Hm* genes (Han et al., 1997; Multani et al., 1998). HCTR activity has also been observed in all grasses tested (Walton, 2006), but interestingly not in any non-grass species including the model dicot *Arabidopsis thaliana*. The seeming

ubiquity of the *Hm1* gene in grasses suggested either a new unknown role for the gene or an ancient and evolutionarily-conserved need to detoxify HC-toxin. The latter was confirmed when silencing of the *Hm1* homolog in barley via virus-induced gene silencing (VIGS) led to susceptibility to CCR1 infection (Sindhu et al., 2008). Phylogenetic analysis revealed that the *Hm1* gene evolved exclusively early on in the grass lineage, with *Hm2* emerging only in the maize lineage as a result of a whole genome duplication event (Sindhu et al., 2008). As CCR1 is one of the most destructive pathogens on susceptible maize plants lacking the ability to detoxify HC-toxin, it was concluded that *Hm1* served as an important "guardian of grasses", allowing early grasses to spread and flourish by protecting them from an ancestral form of CCR1. Why CCR1 is unable to cause disease on dicots despite HC-toxin's universal ability to affect HDACs is not yet clear. Phylogenetic analysis also led to the identification of an *Hm1*-like (*Hml*) gene that also predates the radiation of the major grasses (Sindhu et al., 2008). Though resistance to CCR1 has never been mapped to its locus on the short arm of chromosome 7 in maize, *Hml*'s conservation in grasses makes it unlikely to be a pseudogene. Additionally, the *Hml* clade appears to have undergone significant expansion in the rice lineage. The role of *Hml* in grasses remains unknown and presents an intriguing area for further research.

**NADPH**

The pyridine nucleotide nicotinamide adenine dinucleotide (NAD) and its phosphorylated derivative NADP function as essential redox transfer carriers in all organisms. Oxidized $NAD^+$ functions as an universal electron acceptor, whereas NADP functions as an universal electron donor in its reduced form NADPH. By maintaining these two pyridine nucleotides in different redox states, cells can simultaneously employ them for very different roles. $NAD^+$ is utilized as an oxidizing agent for catabolic reactions that break down large molecules while NADPH often serves as a reducing agent for anabolic reactions in the biosynthesis of complex molecules (Nelson and Cox, 2005). In plant cells, NADP is mostly localized in chloroplasts in its reduced form (Heber and Santarius, 1965; Wigge et al., 1993). Here, $NADP^+$ serves as the terminal electron acceptor in the photosynthetic electron transport chain during the light-dependent reactions of photosynthesis, with the enzyme ferredoxin-NADP reductase generating the NADPH that

subsequently provides reducing power for carbon fixation in the Calvin cycle. During $C_4$ photosynthesis in maize, $NADP^+$ is produced from NADPH during the conversion of oxaloacetate into malate by $NADP^+$-malate dehydrogenase in mesophyll cells, while NADPH is generated from $NADP^+$ during the conversion of malate into $CO_2$ and pyruvate by $NADP^+$-malic enzyme in bundle sheath cells. The chloroplasts of bundle sheath cells lack stacked membranes and exhibit little PSII activity compared to the mesophyll cells (Buchanan et al., 2015). In the dark and in non-photosynthetic plastids, NADPH is primarily generated from glucose via the enzymes glucose-6-phosphate dehydrogenase (G6PDH) and 6-phosphogluconate dehydrogenase (6PGD) in the oxidative pentose phosphate pathway (OPPP). The cytosolic isoform of G6PDH produces NADPH primarily utilized for biosynthetic reactions and is strongly inhibited by the NADPH product, while plastidal G6PDH is deactivated by photoreduced thioredoxins under photosynthetic (reducing) conditions when the oxidative steps of the pentose phosphate pathway become superfluous (Nee et al., 2013). Though plants have several distinct cytosolic and plastid isoforms of 6PGD, no regulatory properties have been described thus far and their activities are most likely determined by the availability of the 6-phosphogluconate substrate (Buchanan et al., 2015). Reduced NADPH levels in the mitochondria have been shown to be highly variable with light and carbon dioxide, while NADPH levels in the cytosol remained constant (Igamberdiev and Gardeström, 2003). NADPH can be rapidly generated by several single-step enzymatic reactions including multiple $NADP^+$-dependent dehydrogenases, pyridine nucleotide transhydrogenases that transfer electrons from NADH to $NADP^+$, and NADH kinases that directly phosphorylate NADH, though most of the NADPH supply is produced via the combined action of NAD kinases and $NADP^+$-dependent dehydrogenases (Shi et al., 2009). $NADP^+$ is itself generated from NAD through ATP-dependent phosphorylation by NAD kinases. The model plant *Arabidopsis thaliana* has 3 isoforms, with NADK1 operating in the cytosol, NADK2 in chloroplasts, and NADK3 (a NADH kinase) in peroxisomes (Waller et al., 2009). Comparative genome analysis has identified four NAD kinases in maize (Li et al., 2014).

The production of cytosolic NADPH can be accomplished by multiple reactions (reviewed by Rasmusson and Wallström, 2010) including the previously mentioned G6PDH and 6PGD in the OPPP (Kruger and von Schaewen, 2003), cytosolic NADP-malic

enzyme (Schaaf et al., 1995), a cytosolic NADP–isocitrate dehydrogenase (Hodges, 2002), a nonphosphorylating NADP-glyceraldehyde-3-phosphate connected with a dihydroxyacetone 3-phosphate (DHAP)/ 3-phosphoglycerate (3-PGA) shuttle (Kelly and Gibbs, 1973; Rius et al., 2006), and the citrate valve (Igamberdiev and Gardeström, 2003), with the last two suggested to export NADPH from chloroplasts and mitochondria respectively under certain conditions as NAD(P)H cannot cross organellar membranes directly and must instead be transported using the aforementioned shuttles as well as a chloroplastic malate/oxaloacetate shuttle (Hoefnagel et al., 1998). Evidence suggests that most of these pathways can compensate each other to some extent. For example, an *Arabidopsis* mutant lacking the NADPH-generating enzyme of the triose-phosphate shuttle was actually found to have higher foliar NADPH levels than wild-type plants, mostly likely due to the increased expression of cytosolic G6PDHs (Rius et al., 2006). This (over)compensation, coupled with the observation that several of these NADPH-generating pathways appear to be active mainly under high light or photorespiratory conditions and the fact that cytosolic G6PDH is strongly inhibited by NADPH itself, highlights the major role played by the OPPP in providing NADPH in non-photosynthetic cells (Hutchings et al., 2005). In *Arabidopsis* leaves, neither the total contents nor the redox state of NADP display any trend with development, unlike either NAD or the antioxidants ascorbate and glutathione (Queval and Noctor, 2007), indicating strict homeostatic regulation of this important reductant. In *Arabidopsis* plants grown under diurnal conditions and placed under constant light, NADPH levels peaked before subjective dawn and $NADP^+$ levels peaked before subjective dusk. The NADPH/$NADP^+$ ratio was also shown to oscillate in a circadian manner, being highest during later part of subjective dusk (Zhou et al., 2015). Conversely, the NADPH/$NADP^+$ ratio was observed to increase with the onset of the light period and decrease with the onset of the dark period in maize mesophyll chloroplasts (Usuda, 1988). Though NAD kinases have not been demonstrated to be directly regulated by light, NADK2 has been shown to bind calmodulin, suggesting some degree of $Ca^{2+}$-dependent activity (Turner et al., 2004). Since $Ca^{2+}$ levels are light-regulated, an increase in NADK2 activity could explain this observed increase in the NADPH/$NADP^+$ ratio in the light, also seen with spinach stroma (Heineke et al., 1991).

**Role of NADPH in redox reactions and plant defense**

In addition to providing reducing power for numerous biosynthetic reactions, NADPH also serves as the master soluble molecule in redox signalling, providing the electrons necessary to regenerate the reduced forms of the antioxidants glutathione (GSH), ascorbate (ASC), and thioredoxins (Foyer and Noctor, 2011; Michelet et al., 2013) as well as directly powering the formation of reactive oxygen species (ROS) through NADPH oxidases (known as respiratory burst oxidase homologs (RBOH)) in the plasma membrane (reviewed by Marino et al., 2012). NADPH thus occupies a unique position as a molecule ultimately responsible for both the controlled creation and the detoxification of ROS and other oxidative stresses. ROS, such as superoxide ($O2^{\bullet -}$), hydrogen peroxide ($H_2O_2$), hydroxyl radicals ($HO^{\bullet}$), and singlet oxygen ($^1O_2$) produced by NADPH oxidases or as natural byproducts of aerobic metabolism and both abiotic and biotic stresses, are harmful free radicals that can cause oxidative damage to DNA, proteins, and lipids (Petrov and Van Breusegem, 2012). The constant regeneration of antioxidants via NADPH thus provides an important buffer against these potentially rogue oxidizing agents. The oxidized and reduced forms of ascorbate and glutathione are the main cellular redox couples, with the two antioxidants working together in the ascorbate-glutathione cycle to detoxify ROS as well as separately by directly scavenging ROS (Foyer and Noctor, 2011; Zechmann, 2014). Glutathione in particular is probably the most important antioxidant in plants, being essential for growth and development as well as being a key agent in plant responses to both abiotic and biotic stresses (Kocsy et al., 2013).

Despite their reactivity, reactive oxygen species have been shown to play an important role in responses to both abiotic and biotic stresses, both directly and indirectly as signaling molecules (Kotchoni and Gachomo, 2006). In plant-pathogen interactions, ROS can strengthen cell walls via oxidative cross-linking of cell wall glycoproteins (Bradley et al., 1992) as well as directly harm certain types of pathogens. The oxidative burst is a rapid, transient production of ROS that is a hallmark of successful pathogen recognition (Torres et al., 2006). The oxidative burst typically is biphasic, with a first non-specific phase that occurs within minutes of pathogen interaction (PAMP recognition) followed by a second prolonged phase usually leads to the establishment of effector-triggered immunity (ETI) and controlled cell death via the hypersensitive response (HR)

(Torres et al., 2005). The biphasic nature of the oxidative burst illustrates various roles ROS can play due to differential degree, timing, and duration of the ROS signal. Interestingly, the Arabidopsis NADPH oxidase gene *respiratory burst oxidase homolog D* (*RbohD*) was shown to mediate a rapid systemic ROS signal in response to various stimuli (Miller et al., 2009). This long-distance signaling capacity of ROS in association with the phytohormone salicylic acid (SA) is key in the establishment of systemic acquired resistance (SAR), an immune response that enhances broad-spectrum pathogen resistance in uninfected portions of the plant (Durrant and Dong, 2004). In addition, the transcription factor NPR1 (NON-EXPRESSOR of PATHOGENESIS-RELATED GENES 1), the master regulator of SA-responsive genes, is redox regulated (Mou et al., 2003). NPR1 exists as an oligomer in the absence of SA due to intermolecular disulfide bonds, but SA-induced changes in redox status leads to the reduction of these cysteine residues, allowing NPR1 monomers to enter the nucleus and affect transcriptional responses (Tada et al., 2008). The actual effect ROS has on disease resistance, however, often varies depending on the pathosystem as well as the timing and strength of the signal, with different signaling functions sometimes having opposing effects. While early activation of ROS signaling appears important for the proper induction of innate immune responses against necrotrophs (Asselbergh et al., 2007; L'Haridon et al., 2011; Williams et al., 2011), the cell death facilitated by sustained ROS production may actually promote susceptibility as necrotrophic pathogens derive their nutrition from dead and dying tissue (Govrin and Levine, 2000; Temme and Tudzynski, 2009). In addition, the Arabidopsis RBOHD was found to simultaneously trigger cell death in cells damaged by *Alternaria brassicicola* infection and inhibit cell death in neighboring cells by down-regulating free salicylic acid and ethylene levels (Pogány et al., 2009).

**Research objectives**

Given that HCTR requires NADPH as a cofactor for activity, one possible explanation for why weak *Hm1* alleles confer APR is that resistance is dictated by availability of this reducing agent. It has been shown that photosynthates assimilated by seedling leaves during the day are either consumed or exported to sink tissues by the first half of the night (Kalt-Torres et al., 1987). Since NADPH is produced during the light-dependent reactions of photosynthesis and several other NADPH-generating pathways are active mainly in the light (Rasmusson and Wallström, 2010), we reason that cellular NADPH levels may drop at night and fall below a threshold level required by the mutant HCTRs for maximum activity. As a result, not all of the HC-toxin will not be inactivated at night and will thus have a window of opportunity to induce disease. The wild-type HCTR is thought to be resilient enough not to be impacted by this routine dip in NADPH at night. As plants age, their ability to buffer against NADPH fluctuations probably improves, providing an explanation as to why APR builds gradually in this pathosystem. Supporting this hypothesis is the finding that the strength of resistance conferred by seedling *Hm1A* plants is enhanced markedly when the plants are grown under an 18 hour light: 6 hour dark photoperiod, while APR is dramatically compromised when plants are grown under a 6 hour light: 18 hour dark photoperiod (Marla, 2014). Moreover, supplementing CCR1-inoculated seedlings kept in the dark with sucrose prevented APR erosion. These findings and observations support strongly the hypothesis that NADPH levels underlie APR, the testing of which is the first major focus of this thesis. The second major focus involves elucidating the function of HC-toxin in promoting susceptibility to CCR1.

In this thesis, the objectives are to 1) quantify temporal and developmental fluctuations of foliar NADPH levels, 2) characterize the enzymatic activities of the wild-type and APR HCTR enzymes, and 3) investigate the role of HC-toxin in pathogenesis. Objectives 1 and 2 are covered in Chapter 2 while Objective 3 is covered in Chapter 3.

# CHAPTER 2: MOLECULAR AND BIOCHEMICAL CHARACTERIZATION OF ADULT PLANT RESISTANCE IN THE MAIZE-*COCHLIOBOLUS CARBONUM* RACE 1 PATHOSYSTEM


## Abstract

The maize *Hm1* gene encodes a NADPH-dependent reductase that inactivates HC-toxin, a key determinant of disease in the maize-*Cochliobolus carbonum* race 1 (CCR1) pathosystem, thus conferring complete protection at all stages of plant development. Two naturally occurring variants of this gene occur that display an adult plant resistance (APR) phenotype: *Hm1A*, a weak allele of *Hm1* with five amino acid substitutions compared to the wild-type B73 allele, and *Hm2*, a duplicate gene encoding a truncated protein. Resistance against CCR1 conferred by these genes is weak in seedlings but gradually increases with age until mature plants are fairly immune. Given that the transcriptional and translational levels of *Hm1A* and *Hm2* appear to be unchanged during development, their APR phenotypes are expected to be dictated post-translationally. Two new APR alleles of *Hm1* generated via targeted EMS were found to have changes in their predicted NADPH-binding sites, leading to the hypothesis that developmental fluctuations of this cofactor compromised the activity of the APR enzymes. To test this hypothesis, we quantified NADP(H) levels in juvenile and adult leaf tissue and performed *in vitro* kinetics assays to determine HC-toxin reductase (HCTR) activity. The total pool of NADP(H) was demonstrated to be higher for adult leaf tissue during the day compared to juvenile leaf tissue. The HCTR activity of crude leaf protein extracts from the different alleles of *Hm1* was found to be linearly correlated with the strength of CCR1 resistance displayed by juvenile plants, with older, more resistant APR plants still displaying this compromised HCTR activity. The importance of the $L_{116}H$ change in HM1A was investigated through the use of site-directed mutagenesis. Though the HM1A and HM2 recombinant proteins could not be effectively purified, kinetic parameters for HM1, HM1-L116H, and HM1A-H116L proteins indicated that wild-type HM1 had a higher affinity for both NADPH and HC-toxin substrates than either mutant construct but a lower turnover rate. Together, these data suggest that although there is some evidence that the APR phenotypes of *Hm1A* and

*Hm2* to CCR1 are regulated by developmental changes in the availability of the NADPH substrate, altered NADPH levels alone do not adequately explain the biochemical basis of APR.

**Introduction**

Resistance to plant pathogens can generally be classified as seedling resistance or adult plant resistance (APR). Seedling or all-stage resistance usually provides complete resistance in all parts of the plant at all stages of life. Seedling resistance is often conferred by single, often race-specific resistance (R) genes that trigger a hypersensitive response (HR) characterized by localized cell death when these R genes directly or indirectly interact with a corresponding avirulence gene product from the pathogen in a gene-for-gene fashion (Jones and Dangl, 2006). Of the over 140 R genes that have been cloned and characterized, more than 80% encode nucleotide-binding site leucine-rich repeat (NBS-LRR) proteins, which number in the hundreds in some plant genomes (Shao et al., 2016). While R gene-mediated resistance is quite strong, it is seldom very durable due to its highly specialized gene-for-gene nature. Breeders must often stack multiple R genes in order to prevent the loss of resistance that would inevitably occur when the evolving pathogen discards or mutates its avirulence protein such that it can no longer be recognized by the R gene. When a pathogen relies on a single toxin as a key determinant of disease, another form of monogenic seedling resistance occurs when a single host gene is either responsible for inactivating the toxin, as occurs with the maize *Hm1* gene encoding for a reductase that inactivates the HC-toxin necessary for successful pathogenesis of *Cochliobolus carbonum* race 1 (Johal and Briggs, 1992); or is itself the target of this toxin, as for the URF13 protein in Texas male sterile cytoplasm (Tcms) maize targeted by T-toxin produced by *Cochliobolus heterostrophus* race T (Rhoads et al., 1995). In this latter case, it is in fact the *absence* of the host target protein that provides resistance.

In contrast to seedling resistance, adult plant resistance or age-related resistance occurs only when the plant has reached a certain developmental stage and often provides only partial resistance, though this resistance is often more durable and non-specific than R gene-mediated resistance. The phenomenon of APR has been widely studied in wheat interactions with various *Puccinia* rust pathogens and has also been characterized in maize

(Chintamanani et al., 2007), rice (Century et al., 1999), tomato (Levy and Lapidot, 2007), cucumber (Ando et al., 2015), apple (Gusberti et al., 2013), Arabidopsis (Kus et al., 2002), and several other plant species (Develey-Rivière and Galiana, 2007). In some cases, APR can be effective against multiple pathogen species as with the wheat *Lr34* and *Lr67* genes which both provide broad-spectrum partial resistance to several rust and mildew pathogens (Krattinger et al., 2009; Herrera-Foessel et al., 2014). Though individual APR genes may be weak, they often interact additively such that wheat lines containing 4-5 APR genes display high resistance to rusts that is stable across different environments (Singh et al., 2011). APR can progressively increase in strength from juvenile to adult tissue as observed for the rice receptor kinase *Xa21* against rice bacterial blight caused by *Xanthomonas oryzae* pv. *oryzae* (Century et al., 1999) and the wheat kinase-START gene *Yr36* against wheat stripe rust caused by *Puccinia striiformis* f. sp. *tritici* (Fu et al., 2009). Alternatively, APR can also abruptly manifest in specific tissues as observed in mature flag leaves of wheat for the previously mentioned ABC transporter *Lr34* gene against *Puccinia triticina* (leaf rust), *P. striiformis* f.sp *tritici* (stripe rust), *P. graminis* f.sp *tritici* (stem rust) and *Blumeria graminis* (powdery mildew) (Krattinger et al., 2009). In the maize-*Puccinia sorghi* (common rust) pathosystem, resistance only manifests after the phase transition from juvenile to adult vegetative tissue has occurred in the host plant (Abedon and Tracy, 1996). The transition from juvenile to adult tissue was also found to be correlated with resistance to downy mildew in cabbage (Coelho et al., 1998).

The molecular mechanisms controlling APR remain poorly understood compared to NBS-LRR R gene-mediated resistance. Though several APR genes have been cloned, the underlying genes and mechanisms often differ greatly depending on pathosystem (Develey-Rivière and Galiana, 2007; Rinaldo et al., 2016). ARR in *Arabidopsis thaliana* against *Pseudomonas syringae* appears to be dependent on the intercellular accumulation of the phytohormone salicylic acid (SA) and potentially the SA-catabolite 2,3-dihydroxybenzoic acid (DHBA) (Carella et al., 2015). The tomato *Cf-9B* gene that provides APR against *Cladosporium fulvu* is actually a paralogous flanking gene to the *Cf-9* R gene that provides constitutive resistance (Panter et al., 2002). The later onset of *Cf-9B*-mediated resistance compared to *Cf-9* did not appear to be due to transcriptional regulation. The wheat rust APR gene *Lr67* encodes a mutated hexose transporter that

reduces glucose transport via dominant-negative interference through heterodimerization with functional transporters (Moore et al., 2015), while the wheat *Yr36* gene encodes a protein combining a kinase with START domain that hastens cell death by reducing the ability to detoxify reactive oxygen species via the phosphorylation of a thylakoid-associated ascorbate peroxidase (Gou et al., 2015). Physiological barriers such as the cuticle were found to be important for APR in strawberry and grape against powdery mildew (Peries, 1962; Ficke et al., 2002, 2003) but not for APR in apple against apple scab (Valsangiacomo and Gessler, 1988). In the effort to further understand the pathways behind APR, there have been several recent transcriptomic studies of various pathosystems that have identified many key genes and pathways underlying resistance (Ando et al., 2015; Gusberti et al., 2013; Hao et al., 2016b; Peng et al., 2015).

The maize-*Cochliobolus carbonum* race 1 (CCR1) pathosystem provides an unusual case study of the phenomena of APR. CCR1 (anamorph *Bipolaris zeicola*) is an ascomycete necrotroph that is the causal agent of Northern corn leaf spot, a potentially destructive pathogen that can kill susceptible maize lines at any stage of development (Sindhu et al., 2008). A key determinant of disease is HC-toxin, a cyclic tetrapeptide produced by CCR1 that has been shown to be an inhibitor of a broad spectrum of histone deacetylases (Comstock and Scheffer, 1973; Walton, 2006). Strains of CCR1 unable to produce HC-toxin are only weakly pathogenic and are generally unable to spread beyond the initial sites of infection, though exogenously applied HC-toxin can promote growth and colonization (Sindhu et al., 2008). Resistance to CCR1 is conferred by *Hm1*, a gene present in most of the maize germplasm that encodes HC-toxin reductase (HCTR), a NADPH-dependent reductase that targets HC-toxin for inactivation (Johal and Briggs, 1992). While *Hm1* confers seedling resistance, protecting all parts of the plant at all stages of development, there are two naturally occurring variants of *Hm1* that exhibit APR: a weak allele of *Hm1* termed *Hm1A* and a duplicate gene named *Hm2* (Nelson and Ullstrup, 1964), with *Hm1A* providing slightly stronger resistance than *Hm2*. Cloning of the *Hm1A* gene revealed that the HM1A protein differed from HM1 from the resistant B73 background by five amino acids ($S_{99}Y$, $D_{110}Y$, $L_{116}H$, $S_{191}N$, $L_{240}P$) (Marla, 2014), none of which are predicted to be directly involved in the binding of either the NADPH or the HC-toxin substrate based on structural modeling (Dehury et al., 2013). Since the Leucine at position

116 was the only of these five amino acids found to be consistently conserved in HCTRs from various resistant maize genetic backgrounds (Marla, 2014), it is hypothesized that this specific mutation may underlie the APR nature of this allele. The *Hm2* gene was found to encode a truncated HCTR missing the 52 C-terminal amino acids, with the remainder of the protein having an 89 percent peptide homology to HM1:B73 (Chintamanani et al., 2007). The APR nature of both of these genes is masked by the dominant nature of the *Hm1* gene when it is also present.

Resistance to CCR1 conferred by both *Hm1A* and *Hm2* is almost absent in young seedlings, gradually increasing in strength with development and becoming fully effective in mature plants (Chintamanani et al., 2007; Marla, 2014), a pattern shared with the aforementioned rice *Xa21* and wheat *Yr36* APR genes. Why *Hm1A* and *Hm2* display an APR phenotype is not clear. As observed with the tomato *Cf-9B* APR gene, neither the promoter activity nor the transcription levels for the two genes appears to vary significantly with age (Chintamanani et al., 2007; Marla, 2014), though both APR genes also demonstrate a dosage-dependent nature. In addition, the translational status of these two genes appears to be fairly constant with development, suggesting altered posttranslational regulation. Environmental factors have been observed to influence the strength of resistance conferred by *Hm1A* and *Hm2*, as documented with temperature (Fu et al., 2009; Krattinger et al., 2009; Chen et al., 2013) and photoperiod/light intensity (Pretorius et al., 2007; Jones, 1975) affecting resistance to wheat rust and oat powdery mildew. Greenhouse-grown plants displayed weaker resistance than field-grown plants, an observation supported by the decreased APR seen in photosynthetically-compromised backgrounds (Johal, unpublished). Extending the photoperiod of *Hm1A* plants in growth chambers also led to increased resistance in seedlings (Marla, 2014). Targeted EMS mutagenesis was used to generate two new alleles of *Hm1* that also display the APR phenotype to varying degrees. These new alleles each encode HCTRs that differ from HM1-B73 by a single amino acid change: a tyrosine to methionine change at position 90 for HM1-SM1 and a valine to methionine change at position 210 for HM1-SM2. Both of these residues are predicted to interact with the NADPH substrate in its binding site (Dehury et al., 2013). Together these data led us to suspect the NADPH cofactor as a major factor underlying APR in this pathosystem. We believe that levels of free foliar NADPH

increase with both photoperiod and development. We thus hypothesize that the observed APR phenotypes of *Hm1A* and *Hm2* are due to compromised HCTR activity caused by decreased affinity of their enzymes for the NADPH substrate such that they are unable to sufficiently inactivate HC-toxin in juvenile tissue possessing limited NADPH. The wild-type HCTRs have presumably evolved to effectively function at these lower NADPH levels. As NADPH levels increase with age and approach the threshold concentration for maximum HCTR activity, the APR enzymes also become more effective at detoxifying HC-toxin, thus revealing a direct link between metabolic status and disease resistance. Here, we report that the NADP(H) pool does increase during the day for older maize plants. We also confirm that the HCTR activities of the APR enzymes are compromised compared to wild-type and demonstrate the importance of the conserved leucine residue at position 116 for proper substrate binding. The enzymatic data, however, does not satisfactorily support NADPH as the primary factor underlying APR, suggesting a key role for an additional currently unidentified factor.

## Materials and methods

### Plant growth and maintenance

Maize plants were either grown in the field at the Purdue Agronomy Center for Research and Education (ACRE) or in Conviron PGR-15 growth chambers at 28ºC (day) 23ºC (night) on a 12 hr light/12 hr dark cycle. The *Hm1A*, *Hm1-SM1*, and *Hm1-SM2* APR alleles of *Hm1* used had previously been backcrossed using marker-assisted selection for four generations into the resistant B73 background, which lacks a functional *Hm2* gene. Segregating progeny were selected for their APR phenotype upon infection with CCR1 pathogen and self-crossed to produce the $BC_4F_3$ plants used in this study. As the *Hm2* gene had not been sufficiently backcrossed into B73 at the time of this study, we did not utilize this genotype for the *in planta* HCTR assays. A susceptible *hm1* allele derived from an EMS-mutagenized B73 population was used as a negative control after two generations of backcrossing and selection.

### Pathogen maintenance and inoculations

*Cochliobolus carbonum* race 1 fungus was cultured on carrot juice agar plates as previously described (Johal and Briggs, 1992). For leaf whorl inoculations, 200 µL of 50,000 spores/mL CCR1 conidial spore suspension in double-distilled $H_2O$ was used as inoculum. The affected leaf tissue was collected and flash-frozen in liquid nitrogen 24 hours post inoculation (hpi) for both the crude protein HCTR assays and the molecular cloning of the *Hm1*, *Hm1A*, and *Hm2* cDNAs. Disease severity scoring on a scale from 1 to 10 was performed 7 days post inoculation; therefore scoring at week 3 was for plants inoculated at week 2. As CCR1 disease had spread to all *hm1* plants in the field by week 6, we were unable to perform any tissue collection from freshly inoculated plants for the week 7 studies.

### NADP(H) quantification

At both the V3 and V12 growth stages, the youngest fully expanded leaf (leaf 3 and leaf 12, respectively) was collected from B73 plants growing in the field every 3 hours over a 24-hour period starting and ending at midnight. During the times of sample collection, sunrise was around 6 AM while sunset was around 9 PM. For each time point,

4 biological replicates of 3 leaves each were collected, pooled, flash-frozen in liquid nitrogen, and stored at -80°C. The leaf tissue was ground into a powder and roughly 50 mg aliquots were weighed out, with care taken not to thaw the tissue.

NADPH and $NADP^+$ levels were measured using a modified thiazolyl blue tetrazolium bromide (MTT) colorimetric cycling assay adapted from (Spielbauer et al., 2013). 0.75 mL of 0.1 M NaOH or HCl for NADPH or $NADP^+$, respectively, was added to the 50 mg aliquots on ice, which were then transferred to a 90º C water bath for 2 minutes. After the samples were cooled on ice, 0.75 mL HCl or NaOH was added for neutralization, and the volumes were adjusted to 5 mL with 0.1 M Tricine-NaOH (pH 8.0). 0.5 mL aliquots of each sample were then centrifuged at 15,000 x *g* for 10 minutes at 4ºC, and 15 µL of the supernatant or NADP(H) standard was used for each reaction containing 90 µL 0.1 M Tricine-NaOH and 20 µL assay mixture (40 mM EDTA (pH 8.0), 50 mM glucose-6-phosphate, 4.2 mM MTT, 16.8 mM phenazine ethosulfate). The cycling reactions were started by adding 1 µL glucose-6-phosphate dehydrogenase (Sigma G5885, 35U/ml in 0.1 M Tricine-NaOH). Reactions were incubated in the dark at 37ºC for 30 minutes, and the absorbance at 570 nm was measured.

**Crude plant protein extraction and HCTR assays**

*Hm1*, *Hm1-SM1*, *Hm1A*, *Hm1-SM2*, and *hm1* plants in the field were inoculated with CCR1 conidial spore suspension as described above into the leaf whorl at weeks 3 and 7. Four biological reps of three inoculated plants were sampled 24 hpi and stored at -80°C until further use. Total plant protein was extracted using a protocol adapted from (Hayashi et al., 2005) and desalted using a Sephadex G-50 Fine column (GE Healthcare). After determining protein concentration with a Bradford assay, 13.55 µg of protein was used to start reactions containing 25 mM Tris-HCl (pH 7.0), 160 mM NADPH, and 55 µM HC-toxin. The assays were run at 30° C in the dark for 45 minutes and then stopped by the addition of 1250 µL cold acetone. After centrifugation at 15,000 x *g* for 15 min at 4° C, 10 µL of the supernatant was injected onto an Atlantis T3 column (2.1 x 150 mm, 3 µm, 100 Å, Waters) maintained at room temperature and analyzed using an Agilent 1200 series LC instrument coupled to an Agilent 6460 triple quadrupole mass spectrometer (Agilent Technologies) at the Bindley Bioscience Center in Purdue Discovery Park. The solvent

system contained solvents A (0.1% formic acid in dd$H_2O$) and B (0.1% acetonitrile). The column was eluted with 85% A and 15% B (0 to 1 min), followed by a linear gradient from 1 to 16 min to 40% A and 60% B, 16 to 16.5 min to 40% A and 60% B. The column was then reduced from 60% B to 15% B (16.5 to 17 min) and kept isocratic at 15% B from 17 to 22 min with a flow rate of 0.3 mL/min. HC-toxin and its reduced form eluted from the column at 8.5–11.5 min under these conditions. During the analysis, the column effluent was directed to the MS/MS, with the Jetstream ESI set to positive mode with nozzle and capillary voltages at 1000 – 4000 V. The nebulizer pressure was set at 35 psi, the nitrogen drying gas was set at 325°C with a flow rate of 8 L/min, and the sheath gas was held at 250°C at a flow rate of 7 L/min. Fragmentation was achieved with 70 V for both analytes. Multiple reaction monitoring (MRM) was used to selectively detect HC-toxin and its reduced form. The first quadrupole was set to transition between the $[M-H]^+$ of the analytes, whereas the last quadrupole monitored *m/z* 411 and 409 for reduced and normal HC-toxin respectively. Each transition was monitored with a dwell time of 150 ms and a collision energy of 15 V, with ultrapure nitrogen used as the collision gas. Mass selection was achieved using the following ions: 439.3 for reduced HC-toxin and 437.3 for HC-toxin. Data was collected and analyzed via the MassHunter Workstation (version B.06.00, Agilent Technologies), and peak areas were determined by integration.

**Recombinant HCTR purification and enzyme assays**

*Hm1*, *Hm1A*, and *Hm2* plants in growth chambers were inoculated with CCR1 conidial spore suspension as described above into the leaf whorl of 10 day old plants, with the affected tissue from 3 plants per genotype collected 24 hpi, pooled, and ground using liquid nitrogen. Total RNA was extracted using a protocol modified from (Eggermont et al., 1996) and treated with DNaseI (Thermo Fisher Scientific). Reverse transcription for cDNA synthesis was performed using iScript (BioRad). The primer pair *Hm1*-IF5 (5’ – CGGGATCCATGGCCGAAAAGGAGAGCAACG – 3’) and *Hm1*-IR6 (5’ – GCCAAGCTTTTATCCTTTCTGTAGGCCGAG – 3’) was used to isolate and PCR-amplify the entire coding region of both *Hm1* and *Hm1A*, adding a 5’ *BamHI* and a 3’ *HindIII* restriction site, while the primer pair N-*Hm2*-F2 (5’ – CCGGAATTCATGAACAGCAGTAGCAGTGA – 3’) and N-*Hm2*-R2 (5’ –

CCCAAGCTTTTACGCTCTGAGGACGTCGA – 3') was used for the entire coding region of *Hm2*, adding a 5' *EcoRI* and a 3' *HindIII* restriction site. The isolated cDNAs were ligated into pGEM-T Easy (Promega) vectors and transformed into DH5α cells (Invitrogen) according to the manufacturer's instructions. After plasmid isolation using a QIAprep Spin Miniprep kit (Qiagen) and sequencing to confirm that no PCR-induced errors had been introduced, site-directed mutagenesis of the *Hm1* and *Hm1A* constructs was performed using the QuikChange II kit (Agilent). The primer pair *Hm1-t347a-Sense* (5' – GCGCGCGATCCACCGGCAATGCG – 3') and *Hm1-t347a-Antisense* (5' – CGCATTGCCGGTGGATCGCGCGC – 3') was used for converting HM1 to HM1-L116H, while the primer pair *Hm1A-a347t-Sense* (5' – CGCATTGCCGGAGGATCGCGCGC – 3') and *Hm1A-a347t-Antisense* (5' – GCGCGCGATCCTCCGGCAATGCG – 3') was used for converting HM1A to HM1A-H116L. The cDNA inserts were subcloned into the *BamHI*/*HindIII* (*EcoRI*/*HindIII* for *Hm2*) restriction sites of the pET-32a(+) and pET-44a(+) expression vectors (Novagen) containing a N-terminal hexahistadine fusion tag, and the expression constructs were then transformed into BL21(DE3)pLysS cells (Promega).

Expression, induction, and purification were performed as described in (Kaminaga et al., 2006) with some modifications. Induction with isopropyl β-D-thiogalactopyranoside (IPTG) to a final concentration of 1 mM was performed when the culture density of a 1 L culture reached $A_{600}$ = 0.5. The lysis buffer contained 20 mM sodium phosphate (pH 7.5), 100 mM NaCl, 5 mM imidazole, 10% (v/v) glycerol, and 1 mM DTT. The cells were treated with 50 mg lysozyme, 1 mg DNaseI, and 1.25 mM PMSF and incubated for 30 min on ice before being lysed by running twice through a French pressure cell press at 1000 psi. After centrifugation at 10,000 x *g* for 30 min at 4º C, the HCTR in the supernatant was purified by affinity chromatography using a nickel-nitrilotriacetic acid (Ni-NTA) agarose column (0.75 mL bed volume). The enzymes were eluted using a buffer containing 20 mM sodium phosphate (pH 7.5), 450 mM NaCl, and 100 mM imidazole, desalted using Econo-Pac® 10DG columns (Bio-Rad) into an assay buffer (20 mM Tris-HCl (pH 8.0), 1 mM EDTA (pH 8.0), 50 mM NaCl, 10% (v/v) glycerol, and 1 mM DTT), and concentrated using Amicon Ultra-15 Centrifugal Filters (Amicon). The purity of the isolated proteins, determined by Coomassie Brillant Blue staining of

SDS-PAGE gels, was found to be near 100% for HM1, 72% for HM1-L116H, and 80% for HM1A-H116L. These purities were taken into account when calculating the $k_{cat}$ values. Protein concentrations were determined using Bradford assays. For HM1A and HM2, attempts to obtain increased soluble protein included testing multiple colonies from several independent transformation events, trying both pET-32a and pET-44a vectors, growing the cells at 16ºC, harvesting cells only 1 hr after IPTG induction, and several variations on the above purification procedure.

The HCTR activity of the recombinant proteins was examined by measuring the rate of NADPH oxidation at 340 nm using a NanoDrop 2000c Spectrophotometer (Thermo Scientific), following the protocol previously described by (Trabelsi et al., 2011) with slight modifications. The assay reaction mixture containing 25 mM Tris-HCl (pH 7.0), NADPH (in 25 mM Tris-HCl (pH 8.0)) and HC-toxin (in $ddH_2O$) was incubated at 30°C for 3 min before the reaction was started by the addition of an appropriate concentration of enzyme. The $A_{340}$ was measured every 2 sec for 5 min, and the linear portion of each plot was used for calculating velocity. The kinetics data was analyzed using hyperbolic regression analysis (HYPER.EXE v1.00, 1992). As HC-toxin potentially displayed some substrate-inhibitory effect, data points that did not fit the standard hyperbolic curve of the velocity versus substrate concentration plot were removed from analysis. Since hyperbolic regression analysis yielded rather high standard error values for HC-toxin kinetic parameters, these parameters were also calculated using Eadie-Hofstee plots for comparison. Assays were performed in triplicate for each data point.

## Results

### NADPH and NADP$^+$ levels both increase with age

While developmental levels of pyridine nucleotides in Arabidopsis plants have previously been measured (Queval and Noctor, 2007), we are not aware of any equivalent studies done with field-grown maize plants. We quantified levels of NADPH and its reduced form NADP$^+$ from the youngest fully expanded leaf of both juvenile (V3) and adult (V12) field-grown B73 maize plants over a 24-hour period. While we did not find any notable differences among the juvenile samples at different time points, we did find that both NADPH and NADP$^+$ levels were significantly higher for the adult samples during the day than for adult samples during the night or for the juvenile samples overall (Fig.2.1.A and 2.1.B). In adult leaves, the entire NADP(H) pool was shown to display a diurnal fluctuation pattern, rising in the morning after dawn, peaking in the afternoon, and dropping with the sunset. Interestingly, the NADP(H) pool in adult leaves actually appears to drop below that of juvenile leaves during the night. Though the ratio of NADPH to NADP$^+$ was not found to display a clear pattern for the V12 leaf tissue, we observed two peaks at 6 AM and 6 PM for the V3 leaf tissue (Fig.2.1.C). The ratios also indicate that juvenile leaves generally have a higher proportion of the NADP(H) pool kept in the reduced form (NADPH) compared to the adult leaves. Assuming most of the leaf tissue fresh weight is water, the measured values for NADP(H) roughly correspond to μM concentrations.

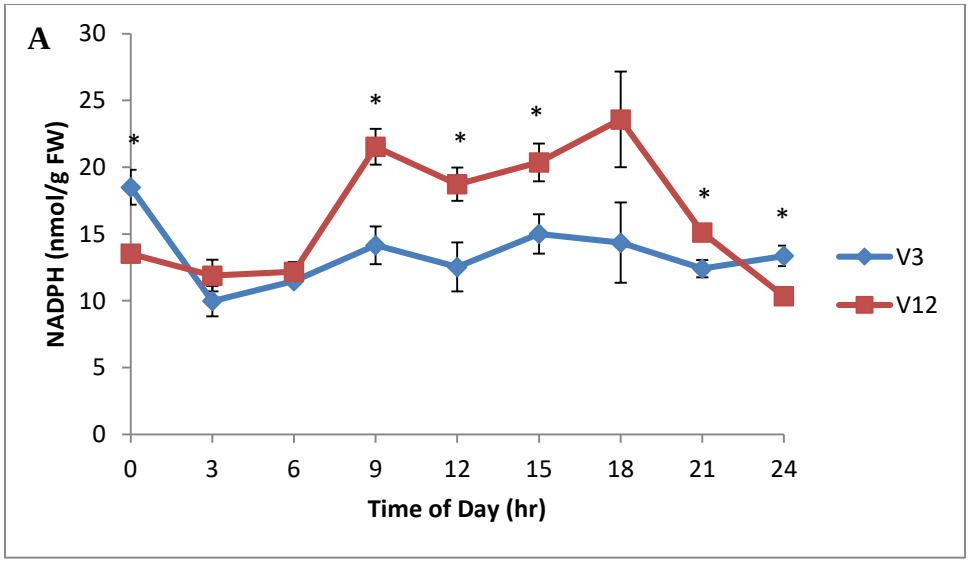

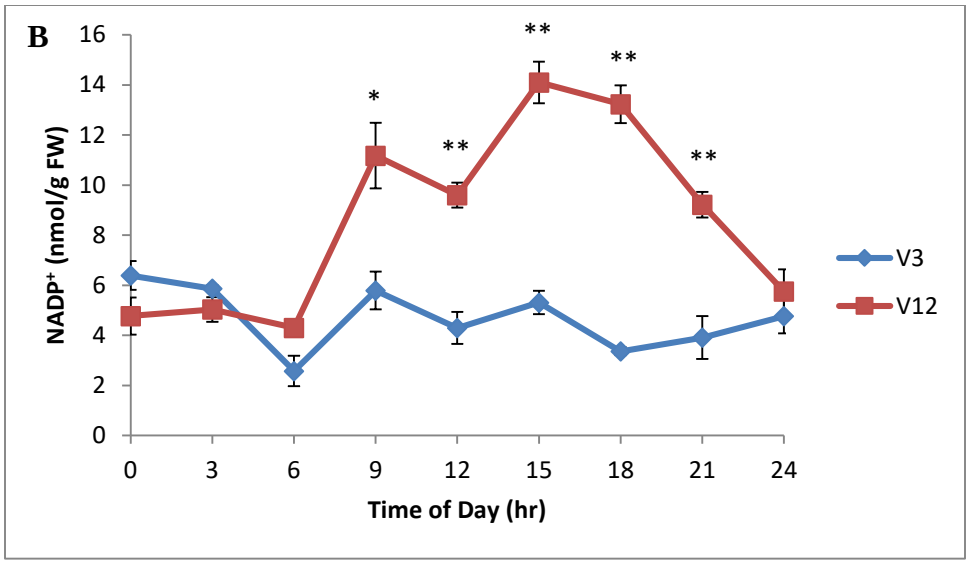


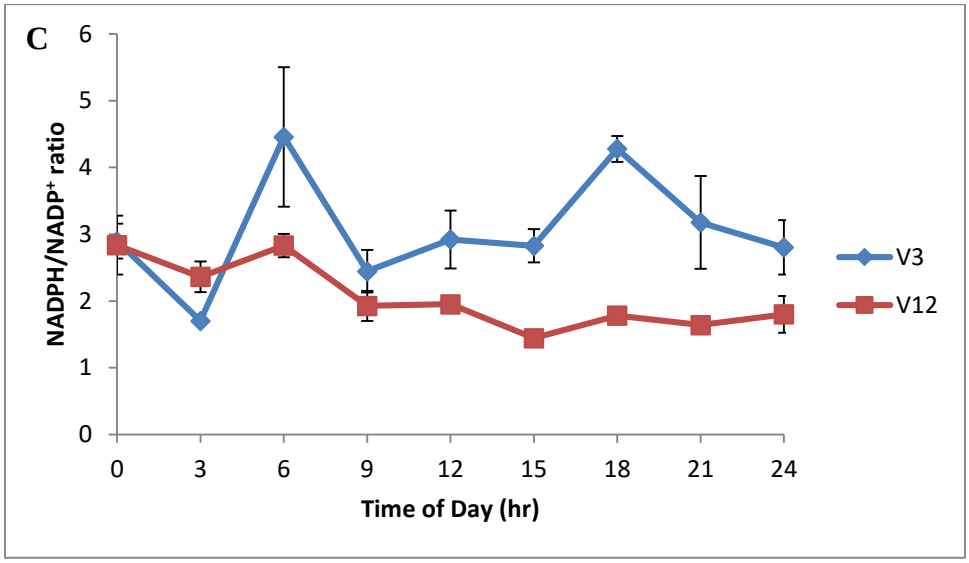


**Figure 2.1. NADPH and NADP$^+$ levels display diurnal fluctuations in adult leaf tissue.** 2.1.A. NADPH levels of the youngest fully expanded leaf at V3 and V12. 2.1.B. NADP$^+$ levels of the youngest fully expanded leaf at V3 and V12. 2.1.C. The ratio of NADPH to NADP$^+$. Data are means ± SE (n=4).

**HCTR activity is compromised for the APR alleles of *Hm1***

Previous studies have demonstrated that susceptibility to CCR1 was directly correlated with the inability of the maize plant to inactivate HC-toxin (Meeley and Walton,

1991; Johal and Briggs, 1992). Genetic and molecular characterization of *Hm1A* and *Hm2* suggest that they encode HCTRs with compromised activity. The generation of *Hm1-SM1* and *Hm1-SM2*, two new partial loss-of function alleles of *Hm1* that exhibit APR, by targeted EMS mutagenesis confirmed that the APR phenotype is due to altered HCTR enzymes. To further characterize the APR alleles biochemically, we decided to test the HC-toxin reductase activity of several APR alleles of *Hm1* displaying a range of resistances (in order of strength: *Hm1-SM1*, *Hm1A*, *Hm1-SM2*, with *Hm1* and *hm1* serving as resistant and susceptible controls, respectively). Crude protein was extracted from plants infected with CCR1 to induce HCTR expression at an age where the APR plants were still fairly susceptible (week 3) and at a later stage when they had become fairly resistant (week 7). We found that the APR alleles of *Hm1* do indeed display compromised HCTR activity (Fig.2.2.A), with more susceptible alleles showing less inactivation of HC-toxin. Surprisingly, the susceptible allele *hm1-K114* also exhibited some HCTR activity. The compromised HCTR activity of the APR alleles was not observed to be significantly higher in older, more resistant plants except for *Hm1-SM1*. Comparison of these enzymatic activities with the disease severity rating assigned to CCR1-inoculated plants in the field at weeks 3 and 7 (Fig. 2.2.B) revealed that the observed HCTR activity was linearly correlated with the degree of susceptibility displayed by the different *Hm1* alleles at week 3 but not week 7 (Fig.2.2.C).

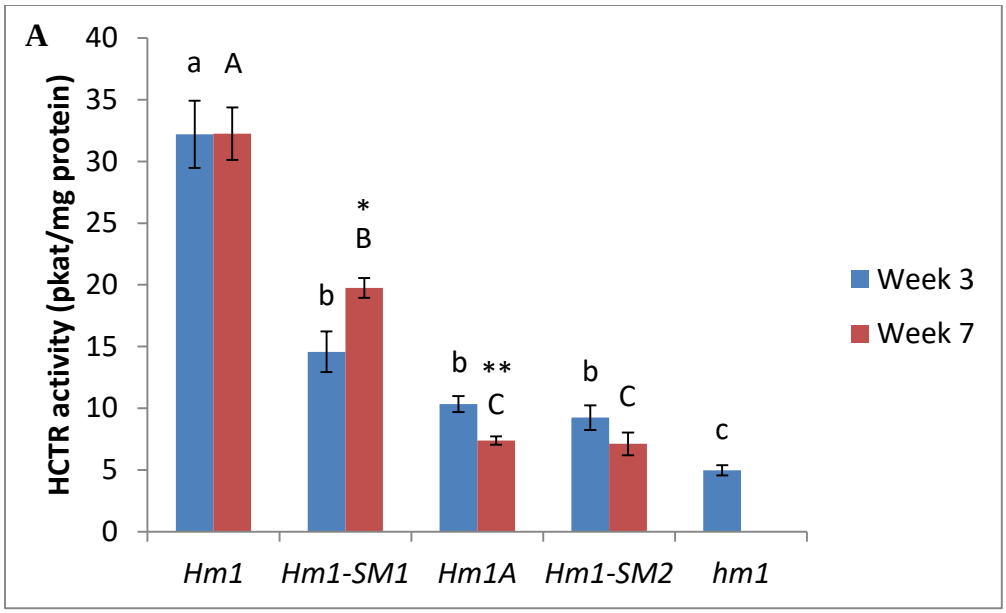
A
HCTR activity (pkat/mg protein)
40
35
30
25
20
15
10
5
0
a A
b
*
B
b **
C
b
C
c
Hm1
Hm1-SM1
Hm1A
Hm1-SM2
hm1
Week 3
Week 7

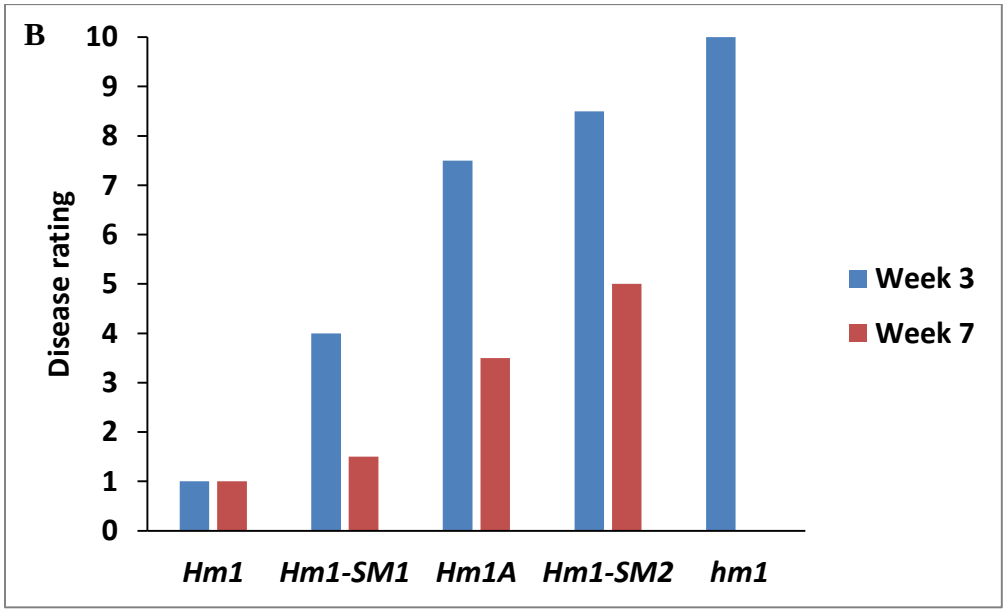
B
Disease rating
10
9
8
7
6
5
4
3
2
1
0
Hm1
Hm1-SM1
Hm1A
Hm1-SM2
hm1
Week 3
Week 7

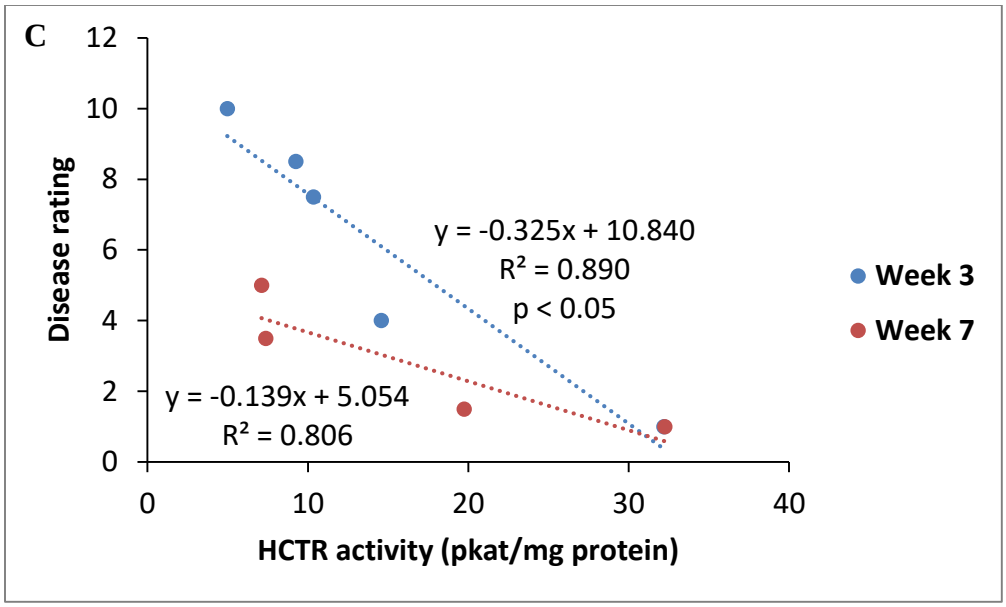


**Figure 2.2. HCTR activity is compromised for alleles of *Hm1* displaying an APR phenotype.** Figure 2.2.A. HCTR activity as measured by reduction of HC-toxin of crude leaf protein extract from week 3 and week 7 *Hm1* (resistant), *Hm1-SM1*, *Hm1A*, *Hm1-SM2*, and *hm1* (susceptible) plants 24 hpi. Letters represent whether differences among each age group were significant ($p_{adj} < 0.05$), with lowercase letters used for week 3 and uppercase letters used for week 7. Asterisks represent whether differences between week 3 and week 7 values were significant (p < 0.01:**, < 0.05:*). Figure 2.2.B. Disease rating scores of *Hm1-SM1*, *Hm1A*, and *Hm1-SM2* plants at weeks 3 and 7, 7 days post inoculation. Figure 2.2.C. Linear correlation of HCTR activity with disease rating with both weeks 3 and 7.

**Kinetic studies with recombinant HCTRs**

To further characterize the biochemical activity of the APR enzymes, we cloned the *Hm1*, *Hm1A*, and *Hm2* cDNAs and expressed them in bacteria to isolate recombinant protein for kinetics analysis. We also expressed the HM1-L116H and HM1A-H116L constructs created via site-directed mutagenesis to study the importance of this conserved residue. We were unable to effectively purify either the HM1A or HM2 recombinant proteins. Though Western blotting was able to detect some soluble protein that did display weakened HCTR activity upon assaying, little protein was visible upon SDS-PAGE analysis for purity as the majority of both the HM1A and HM2 proteins were found in the insoluble fractions after post-lysis centrifugation. We tested several colonies from

independent transformation events and cell batches, different growth and induction conditions, modifications to the purification procedure, and a second expression vector (pET-44a) to no avail. We were able to satisfactorily purify HM1 and the HM1-L116H and HM1A-H116L mutant proteins and determine their kinetic parameters for both the NADPH and HC-toxin substrates. Though HCTR shows close homology to the well-characterized dihydroflavonol 4-reductase (DFR), a NADPH-dependent reductase involved in the biosynthesis of flavonoids that displays substrate inhibition with its dihydroquercetin substrate (Trabelsi et al., 2011), we did not consistently observe a clear inhibition of enzymatic activity at the higher concentrations of HC-toxin tested. We nevertheless utilized only those concentrations of HC-toxin that fit the standard hyperbolic curve of velocity versus substrate concentration. We did not observe any substrate inhibition with NADPH at the concentrations tested.

Our kinetics data revealed that HM1 had the lowest $K_M$ values for both NADPH and HC-toxin substrates of the three enzymes tested (Tables 2.1 and 2.2). As the Michaelis constant is an (indirect) inverse measure of an enzyme's affinity for the substrate, these values indicate that the HM1 enzyme has the highest affinity for both substrates. The $K_M$ values for NADPH are all in the low μM range, below our measured foliar NADPH concentrations. Surprisingly, HM1-L116H was found to have a higher turnover number ($k_{cat}$) than HM1 for both substrates, with the $k_{cat}$ values for HM1A-L116H between those for HM1 and HM1-L116H for both substrates. While the turnover number reflects the rate of product formation at saturating substrate concentrations, the specificity constant $k_{cat}/K_M$ is usually used instead to compare the catalytic efficiencies of different enzymes. HM1-L116H was again found to have the highest specificity constant of the three enzymes, appearing to be more efficient at binding NADPH and HC-toxin and catalyzing HC-toxin reduction than HM1 and HM1A-H116L, though the difference between $k_{cat}/K_M$ values is not statistically significant (Tables 2.1 and 2.2). Although HM1A-H116L displayed higher $k_{cat}$ values than HM1 for both substrates, its $k_{cat}/K_M$ values were found to be similar, indicating little increase in actual catalytic efficiency compared to the wild-type enzyme.

**Table 2.1. Kinetic parameters for the NADPH substrate.**

| Enzyme | $K_M$ (μM) | $V_{max}$ (nkat per mg protein) | $k_{cat}$ ($s^{-1}$) | $k_{cat}/K_M$ ($s^{-1}\mu M^{-1}$) |
|---|---|---|---|---|
| HM1 | 2.26 ± 1.118 | 267.8 ± 25.45 | 15.012 ± 1.427 | 6.643 ± 3.917 |
| HM1-L116H | 4.759 ± 1.424 | 727.4 ± 50.82 | 40.793 ± 2.85 | 8.572 ± 3.164 |
| HM1A-H116L | 4.403 ± 0.759 | 538.7 ± 17.98 | 30.271 ± 1.01 | 6.875 ± 1.415 |

All values represent means ± SE (n = 3). $K_M$: Michaelis constant, $V_{max}$: maximal velocity, $k_{cat}$: turnover number.

**Table 2.2. Kinetic parameters for the HC-toxin substrate.**

Hyperbolic regression analysis

| Enzyme | $K_M$ (μM) | $V_{max}$ (nkat per mg protein) | $k_{cat}$ ($s^{-1}$) | $k_{cat}/K_M$ ($s^{-1}\mu M^{-1}$) |
|---|---|---|---|---|
| HM1 | 4.567 ± 4.572 | 427.5 ± 148.2 | 23.964 ± 8.308 | 5.247 ± 7.072 |
| HM1-L116H | 8.275 ± 4.187 | 1282 ± 236 | 71.896 ± 13.235 | 8.688 ± 5.996 |
| HM1A-H116L | 7.519 ± 4.933 | 742.2 ± 224.9 | 41.706 ± 12.638 | 5.547 ± 5.320 |

All values represent means ± SE (n = 3). $K_M$: Michaelis constant, $V_{max}$: maximal velocity, $k_{cat}$: turnover number.

Eadie-Hofstee plot

| Enzyme | $K_M$ (μM) | $V_{max}$ (nkat per mg protein) | $k_{cat}$ ($s^{-1}$) | $k_{cat}/K_M$ ($s^{-1}\mu M^{-1}$) |
|---|---|---|---|---|
| HM1 | 4.063 | 408.4 | 22.894 | 5.635 |
| HM1-L116H | 7.6 | 1195 | 67.017 | 8.818 |
| HM1A-H116L | 7.59 | 737.6 | 41.447 | 5.461 |

All values represent means (n = 3). $K_M$: Michaelis constant, $V_{max}$: maximal velocity, $k_{cat}$: turnover number.

**Discussion**

The molecular mechanisms underlying the phenomena of adult plant resistance have not been as well characterized as R gene-mediated resistance. Though several APR genes have been cloned and characterized, most of these studies have identified different factors for each pathosystem. In this study, we characterize the biochemistry behind APR in the maize-CCR1 pathosystem. This pathosystem offers a unique link between plant immunity and plant metabolic status due to the HCTR resistance gene utilizing the reducing metabolite NADPH as a cofactor for its activity. NADPH plays a fundamental role in redox reactions, being involved in both the generation of reactive oxygen species (ROS) as well as the regeneration of ROS-managing antioxidants (Noctor, 2006), in addition to its role as a reducing agent for anabolic reactions. We showed that levels of both NADPH and its oxidized form $NADP^+$ are higher in adult leaf tissue during the day than in juvenile leaf tissue, indicating a diurnal increase in the overall pool of NADP(H) in adult tissue. This fluctuation was surprising as we had expected to observe greater NADP(H) fluctuation in the juvenile leaves which presumably have a lessened ability to buffer energetic demands. A possible explanation for this temporary increase is the greater demand for the use of these NADP(H) cofactors during photosynthesis. Since photosynthesis can only occur during the day, mature plants may be able to generate more NADP(H) metabolites during those times to maximize photosynthetic efficiency and/or minimize the resultant formation of potentially harmful ROS by-products. It is interesting that this diurnal fluctuation of NADP(H) is clearly observed in adult leaf tissue only. Perhaps since young maize plants are rapidly growing and have less source tissue, the smaller juvenile leaves presumably do not possess significant energy reserves nor generate sufficient ROS to justify the need for a temporarily increased NADP(H) pool. It must also be kept in mind that although our results suggest an increase in the pool of free NADPH in mature leaf tissue during the day, we could not capture any organelle-specific differences in NADP(H) levels since we utilized homogenized whole leaf tissue for our assays. Previous studies have shown significant intracellular differences in NADP(H) distribution across various organelles (Wigge et al., 1993), with chloroplasts containing the majority of the NADP(H) pool as expected. Localization studies of the HCTR enzyme (predicted to

be cytoplasmic) during various stages of infection are needed to establish which subcellular NADP(H) pool is actually free for use by the enzyme.

There have been multiple studies reviewing the roles the pyridine nucleotides NAD(H) and NADP(H) play in plant immunity (Pétriacq et al., 2013, 2016; Wang et al., 2016). A common factor is the relationship between these redox molecules, ROS, and the defense phytohormone salicylic acid (SA), likely through the redox-sensitivity of the master immune regulator NPR1 (Zhou et al., 2015). Many of these studies involved biotrophic pathogens that are mainly countered by SA-mediated defenses. As SA-mediated signaling can act antagonistically to defense responses against necrotrophic pathogens mediated by jasmonic acid (JA) and ethylene (ET) signaling (Glazebrook, 2005), the role NADP(H) may play in necrotroph defense responses is less clear. NADP application was not found to induce JA/ET-mediated defense responses nor have any effect on the disease severity of the necrotroph *Botrytis cinerea* on Arabidopsis leaves (Wang et al., 2016). The maize-CCR1 pathosystem offers a more direct connection to NADPH through HCTR activity being directly correlated with the disease resistance phenotype. We establish that the APR alleles of *Hm1* all display reduced HCTR activity consistent with their relative degree of observed resistance to CCR1 in the field, with lines exhibiting stronger resistance showing greater HC-toxin reduction. We have thus provided biochemical verification that the increased susceptibility of the APR plants is due to compromised HCTR activity reducing the plants' ability to inactivate HC-toxin. Since the HCTR activity was not shown to be higher in adult leaf tissue compared to juvenile leaf tissue for most of the APR alleles, it is unlikely that the increase in resistance with development is due to a concurrent accumulation of HCTR enzymes with age. As the reactions were run using equal concentrations of crude leaf protein extract, our findings support previous findings that APR does not appear to be due to altered transcriptional or translational regulation with plant age, though we cannot completely rule out posttranslational modifications. *In silico* analysis of the HM1A amino acid sequence did not find any differences in predicted phosphorylation sites that were not also present in other HM1 proteins from resistant maize backgrounds (Marla, 2014). The mechanism underlying the manifestation of the APR phenotype is thus very likely another factor that somehow alters the stability or activity of the APR enzymes.

While we were able to purify recombinant HM1 and mutants generated via site-directed mutagenesis, we were unable to effectively purify the HM1A and HM2 recombinant proteins so the kinetic parameters of these APR enzymes remain unknown. Our inability to extract soluble recombinant HM1A protein was surprising given that we did not have trouble purifying the HM1A-H116L protein generated by site-directed mutagenesis of the HM1A cloning construct. The fact that we were also able to purify the HM1-L116H mutant protein suggests that this particular mutation alone is not sufficient to explain the insolubility of the recombinant protein. Expression of the APR proteins in a eukaryotic system such as yeast instead of bacteria may be necessary for their successful purification. There is the possibility that the HM1A and HM2 enzymes are inherently less soluble or stable than the wild-type HCTRs, especially given that HM2 is a truncated protein, despite *in silico* analyses predicting low instability indexes and high solubility for all of the recombinant proteins. Though this could explain the reduced HCTR activity observed in both juvenile and mature tissues, how this altered enzyme solubility/stability is related to increased resistance with development is not clear. One possibility is that there is simply more of the mutant enzyme present in mature plants. Since our evidence against this hypothesis is only based on semi-quantitative PCR and Western blotting, performing qPCR and a quantitative ELISA or fluorescence Western blot may capture variations in expression not detectable with the earlier techniques. Protein localization studies at different disease stages using either a HM1-specific antibody against separated subcellular fractions or GFP-tagged HCTRs transformed into a grass system would allow us to definitively show whether the APR enzymes are in fact less soluble and/or stable than their wild-type counterparts or have altered localization dynamics during disease progression.

We were able to study the importance of the conserved Leucine residue at position 116 due to successful purification of HM1 as well as the HM1-L116H and HM1A-H116L mutants generated via site-directed mutagenesis. Our kinetics studies demonstrated that the wild-type HM1 had the highest affinities for both the NADPH and HC-toxin substrates, indicating that it can function at maximal activity at lower substrate concentrations than either of the mutated enzymes. Though the $K_M$ values for the NADPH substrate are lower than the observed NADPH concentrations in both juvenile and adult leaf tissue, subcellular variations in the NADP(H) pool must be considered in order for direct comparisons to be

meaningful. It is possible that this increased substrate affinity plays a role in allowing the wild-type HM1 to confer complete resistance at all stages of development since HM1 did not appear to possess any increased catalytic efficiency. The single L116H change was shown to increase the $K_M$ values for both substrates, indicating the importance of this residue for proper substrate affinity. The combined effect of the other 4 HM1A amino acid changes, however, had a similar effect for HM1A-H116L, indicating that the mutation of this Leucine residue to Histidine was sufficient but not necessary for decreasing substrate affinity. Since the effects of these amino acid changes are likely additive, the HM1A enzyme is expected to possess an even lower substrate affinity than the two mutant recombinant enzymes. Though none of the five altered amino acids in HM1A are predicted to directly interact with either the NADPH or HC-toxin substrates, they may be important for the proper structural orientation of essential interacting residues in the substrate binding pockets. A significant reduction in affinity for NADPH combined with the lower concentrations of free NADPH in juvenile plants compared to adult plants would very clearly explain the nature of *Hm1A*'s APR phenotype. The observed deficiency in HCTR activity of the *Hm1A* plant crude protein extracts run at presumably saturating NADPH substrate concentrations, however, suggests that altered NADPH binding alone is insufficient to explain APR. It is possible that the amino acid substitutions could also increase the promiscuity of the HCTR enzyme for other substrates in addition to decreasing affinity for the normal NADPH and HC-toxin substrates, as such an effect would not have been observable with our controlled *in vitro* reactions. For example, the related pyridine nucleotide NADH has been demonstrated to function approximately 30% as effective as NADPH a substrate for the HCTR reaction (Meeley and Walton, 1991). The amino acid changes in the HM1A enzyme could greatly increase its affinity for NADH such that intracellular NADH becomes a potent competitor of the normal NADPH substrate. Testing both crude plant extracts and the recombinant proteins using NADH as a substrate would allow us to determine whether altered affinity for NADH may play an important role in causing APR. Again, subcellular quantification of localized NAD(H) and NADP(H) pools would be essential in providing a physiological basis for this hypothesis.

Unexpectedly, HM1 did not appear to have the highest turnover number of those tested, having a lower $k_{cat}$ than both HM1-L116H and HM1A-H116L for both substrates.

These $k_{cat}$ values suggest that both the L116H change and the combined effect of the other four HM1A changes greatly increase the maximum enzymatic rate. Though it may seem unusual for these mutant enzymes to catalyze the HC-toxin reduction reaction faster than the wild-type HM1 enzyme, these faster rates are only achievable under saturating substrate conditions, an unlikely physiological scenario. When substrate affinity is considered, the differences among the $k_{cat}/K_M$ values for both substrates are not statistically significant, indicating that the actual catalytic efficiencies of the three enzymes are likely similar. Although the $L_{116}H$ amino acid change alone appears to increase the turnover rate sufficiently to marginally increase its catalytic efficiency, this increase could potentially be cancelled out by the presence of the other 4 amino acid changes in the actual HM1A enzyme. As discussed above, the combined effect of all five amino acid changes in the HM1A enzyme may fundamentally alter enzyme stability/solubility as well as further decrease affinity for the proper substrates. In any case, the kinetic properties of HM1 are sufficient for it to inactivate enough HC-toxin to provide complete resistance to the plant at all stages of development. Since we did not transform either of our mutated alleles into susceptible maize plants, we cannot directly correlate any of these differences *in vitro* kinetic parameters with altered disease phenotypes. An interesting experiment would be to create multiple *Hm1* constructs containing differing combinations of these 5 amino acid changes and determine the kinetic parameters for each. The constructs showing the most promise could then be transformed into a susceptible grass species and the disease phenotype assayed with development to definitively locate the causal mutation(s) and the corresponding affected kinetic parameters, if APR is indeed due to altered enzyme kinetics.

While this study yielded biochemical validation that adult plant resistance in the maize-CCR1 pathosystem is due to compromised HCTR activity, we were unable to conclusively demonstrate that the APR phenotype is caused by increased susceptibility of the APR enzymes to developmental changes in the NADPH pool. Though we show here that NADPH levels are higher during the day in adult leaf tissue and that the wild-type HM1 enzyme has a higher NADPH substrate affinity than the HM1A-H116L and HM1-L116H mutants, we also observed decreased HCTR activity of the APR alleles even at saturating NADPH concentrations, and a significantly increased turnover rate for HM1A-H116L and HM1-L116H compared to HM1 enzyme. Overall, the data suggests that an

additional factor besides NADPH plays an important role in determining the APR phenotype of HM1A. When determining kinetic parameters for the actual APR enzymes HM1A and HM2, the potentially competitive role of the alternate substrate NADH needs to be carefully considered. Combining kinetics data demonstrating altered substrate affinity with subcellular localization studies of both the HCTR enzymes and the NAD(P)H pool would allow us to definitively link disease phenotype with the bioenergetics status of the plant. Evidence of such a connection would potentially allow us to use the expressed degree of disease phenotype in the APR plants as markers for the general metabolic status of the plant, facilitating further research in the dynamic interplay between plant metabolism and defense.

# CHAPTER 3: HC-TOXIN CAUSES MASSIVE TRANSCRIPTIONAL AND METABOLIC CHANGES IN MAIZE DURING *COCHLIOBOLUS CARBONUM* RACE 1 INFECTION


## Abstract

The maize pathogen *Cochliobolus carbonum* race 1 (CCR1) utilizes the cyclic tetrapeptide HC-toxin as a key determinant of virulence, with strains of CCR1 unable to produce HC-toxin not able to spread beyond the initial point of infection unless HC-toxin is provided exogenously. Despite its name, HC-toxin is not cytotoxic but has been demonstrated to inhibit a broad spectrum of histone deacetylases. Previous experiments have suggested that HC-toxin is somehow shutting down defense gene expression during infection. To further clarify the role HC-toxin is playing in pathogenesis, we performed a RNA-seq study to observe and compare changes in the transcriptomes of $Tox^-$ and $Tox^+$ CCR1-inoculated maize leaf tissue. We show here that HC-toxin actually leads to the increased expression of most defense genes during infection. Examination of the biosynthesis and signaling pathways of various defense hormones revealed increased upregulation in the $Tox^+$ CCR1 interaction, suggesting that HC-toxin does not repress immune pathways. Amino acid extraction and quantification revealed large-scale metabolic perturbations indicative of increased protein turnover and cellular stress. We also showed the deregulation of multiple primary and secondary metabolic pathways, notably the consistent upregulation of the shikimate pathway and downregulation of the light reactions of photosynthesis by the $Tox^+$ CCR1 interaction. These findings suggest that HC-toxin may be inducing susceptibility by inhibiting photosynthesis and deregulating metabolism, thus rapidly inducing a starvation response similar to that induced by darkness-induced loss of immunity.


## Introduction

A successful plant defense response against pathogen invasion requires the fine-tuned activation and regulation of numerous immune responses, often at the expense of plant growth due to limited resources (Huot et al., 2014). These immune responses involve

the induction of certain phytohormone signaling pathways, the production of antimicrobial proteins and metabolites, the formation of histological barriers, the generation and regulation of reactive oxygen species, and even host cell death during the hypersensitive response (Mengiste, 2011). The proper timing, localization, intensity, duration, and interaction of these responses are crucial to prevent pathogen spread. Not surprisingly, effective transcriptional reprogramming and regulation play an important role in immune responses. A wide range of transcription factor families such as WRKYs, MYBs, and ERFs have been demonstrated to play important roles as transcriptional activators, suppressors, and/or regulators in the various types of defense signaling (Mengiste, 2011; Moore et al., 2011). The activation of the appropriate defense pathways often depends on proper recognition of the lifestyle of the invading pathogen. For example, biotrophic pathogens that attempt to surreptitiously feed off of living host tissue are countered by salicylic acid (SA)-mediated responses that often culminate in the rapid cell death of the hypersensitive response, while necrotrophic pathogens that actively destroy host tissue for nutrition are more effectively countered by defense pathways mediated by jasmonic acid (JA) and ethylene (ET) (Pieterse et al., 2009). The two different defense pathways often act antagonistically, though their actual interaction is rather more complex (Mur et al., 2006; Mengiste, 2011)

Epigenetic changes through DNA methylation and chromatin remodeling allow the regulation of gene expression without altering the underlying nucleotide sequence. The basic unit of chromatin structure is the nucleosome, which consists of DNA wrapped around an octamer of two copies of each of the core histones H2A, H2B, H3, and H4 (Luger et al., 1997). The tails of these histone proteins can undergo a diverse range of post-translational modifications (PTMs) such as acetylation, methylation, phosphorylation, ubiquitination, sumoylation, carbonylation, and glycosylation, most of which serve to regulate the transcription of the underlying genes (Kouzarides, 2007; Zhang et al., 2007a). Histone acetyltransferases (HATs) add acetyl groups to histone lysine residues, thereby neutralizing their positive charges and weakening their interaction with the negatively charged DNA backbone. This more relaxed chromatin conformation is usually correlated with increased gene transcription (Eberharter and Becker, 2002). Another class of enzymes known as histone deacetylases (HDACs) performs the reverse reaction, removing acetyl

groups and promoting a more closed chromatin conformation associated with transcriptional repression. The specific residues targeted by these PTMs can play an important role in determining the type of regulation conferred. For example, histone lysine trimethylation at H3K4 and H3K36 and monobiquitination of H2B is generally associated with active gene expression (Shilatifard, 2006; Xu et al., 2008; Zhang et al., 2009), while trimethylation at H3K27 is associated with gene repression (Zhang et al., 2007b). Histone modifications thus permit a fine-tuned regulatory mechanism that has been demonstrated to play an important role in proper gene expression for many developmental processes such as flowering time, seed development, and cell differentiation, as well as for stress responses (Lagacé et al., 2003; Liu et al., 2007; Servet et al., 2010; Chen and Zhou, 2013; Ma et al., 2013; Liu et al., 2016).

It is not surprising that chromatin modifications have also been demonstrated to play important roles in plant immunity, not only in the regulation of energy-intensive defense responses, but also for keeping those defense genes primed in anticipation of further pathogen infection (Ding and Wang, 2015). Enrichment of H3K9ac, H3K14ac, H3K4me2, and H3K4me3 at the promoters of defense genes serve as markers of priming (Zhu et al., 2015). For example, treatment of Arabidopsis plants with the salicylic acid analog acibenzolar *S*-methyl led to the increase of H3K4me2, H3K4me3, H3K9ac, H4K5ac, H4K8ac, and H4K12ac markers at the promoters of the defense related transcription factors WRKY6, WRKY29, and WRKY53, though there was little or no actual induction of these genes. Stress treatment 72 hours after priming led to enhanced gene expression compared to unprimed plants (Jaskiewicz et al., 2010). Defense gene priming and long distance signaling are key for the establishment of systemic acquired resistance (SAR) and induced systemic resistance (ISR) whereby local pathogen infection or rhizobacteria interaction, respectively, leads to an extended broad-spectrum resistance to multiple pathogens in distal tissues (Reimer-Michalski and Conrath, 2016). There is even evidence that epigenetic defense gene priming can be inherited transgenerationally (Luna et al., 2012; Slaughter et al., 2012), though these findings are not without debate (Gutzat and Mittelsten Scheid, 2012; Pecinka and Mittelsten Scheid, 2012).

There have been several documented cases of histone deacetylases playing important roles in plant defense (Song and Walley, 2016). Overexpression of the histone

deacetylase701 (HDT701) in rice led to enhanced susceptibility to the pathogens *Magnaporthe oryzae* and *Xanthomonas oryzae* pv. *oryzae*, while silencing HDT701 enhanced resistance, likely due to elevated defense gene transcription associated with pattern-triggered immunity (Ding et al., 2012). The Arabidopsis RPD3-type histone deacetylase HDA6 is important in regulating JA- and ET-signaling responses via recruitment by JASMONATE-ZIM DOMAIN (JAZ) proteins as a corepressor to suppress EIN3/EIL1-dependent transcription and JA signaling important in necrotrophic defense responses (Zhu et al., 2011). The similar HDA19 has been demonstrated to repress both SA biosynthesis and SA-mediated defenses against biotrophs (Choi et al., 2012), while promoting JA/ET-mediated responses against necrotrophs (Zhou et al., 2005). Interestingly, acetylation has been shown to act as a regulatory mechanism on a wide variety of non-histone proteins including several key metabolic enzymes in bacteria (Wang et al., 2010), mammals (Zhao et al., 2010), rice (Xiong et al., 2016), and wheat (Zhang et al., 2016). The large number of processes and interactions modulated by protein acetylation suggests acetylation may rival phosphorylation in regulating diverse cellular functions (Norvell and McMahon, 2010). Furthermore, HATs and HDACs are expected to play important roles in coordinating metabolism and gene expression as sensors of cellular metabolite levels through their acetyl-CoA and $NAD^+$ substrates (for sirtuin class HDACs), respectively (Shen et al., 2015, 2016). Acetylation/deacetylation has been demonstrated to directly affect the activities of certain key plant enzymes including kinases (Hao et al., 2016a) and RuBisCO (Gao et al., 2016). In addition, certain pathogen-produced effector proteins have been found to possess acetyltransferase activity, acetylating various host proteins to promote virulence by manipulating host defenses (Song and Walley, 2016).

The fungal ascomycete *Cochliobolus carbonum* race 1 (CCR1) is an aggressive pathogen capable of rapidly destroying susceptible maize plants at any stage of development. CCR1 (anamorph *Bipolaris zeicola*) can infect any part of the plant, capable of causing lethal leaf blight, stem rot, and ear mold on susceptible lines (Sindhu et al., 2008). A key determinant of virulence is the ability of the pathogen to produce the cyclic tetrapeptide HC-toxin (Scheffer and Ullstrup, 1965). Strains of CCR1 unable to produce HC-toxin ($Tox^-$) do not spread beyond their initial penetration sites, although they can

further colonize host tissue if HC-toxin is provided exogenously (Comstock and Scheffer, 1973). The pathogen is so potentially devastating that almost all grasses have evolved a NADPH-dependent HC-toxin reductase (HCTR) gene seemingly for the sole purpose of detoxifying HC-toxin (Sindhu et al., 2008). Disruption or inactivation of the HCTR gene, called *Hm1* in maize, leads to susceptibility to $Tox^+$ CCR1.

What HC-toxin actually does to promote susceptibility is not entirely clear. Despite its name, HC-toxin is not cytotoxic but rather cytostatic in that it inhibits growth and cell division (Walton, 2006). The structure and properties of HC-toxin are such that it is soluble yet can move freely through living tissues. During CCR1 infection of the susceptible maize inbred Pr, HC-toxin led to the accumulation of hyperacetylated H3 and H4 histones, but not H2A or H2B histones (Ransom and Walton, 1997). HC-toxin has been demonstrated to inhibit RPD3, HDA1, and the plant specific HD2 class histone deacetylases, but not the $NAD^+$-dependent sirtuin class (Walton, 2006). HC-toxin-induced HDAC inhibition was observed both *in vitro* and *in vivo* across a wide range of species, including yeast, *Physarum*, chicken, and maize (Brosch et al., 1995). Pathogenic use of a HDAC inhibitor as a virulence factor is also seen with depudecin from *Alternaria brassicicola*, though depudecin does not appear to be a key determinant of disease like HC-toxin (Wight et al., 2009). Previous findings seem to suggest that the presence of HC-toxin during CCR1 infection leads to the shutdown of defense genes by 48 hpi (Fig.3.1) (Young, 2008). Though this may seem counter-intuitive with the observed increased histone acetylation, increased expression of a strong negative regulator of defense responses remains a possibility. In this study, we performed transcriptomic and targeted metabolite analysis of $Tox^-$ and $Tox^+$ CCR1-inoculated *hm1* maize plants to further investigate the role of HC-toxin in promoting virulence. Our data reveals that HC-toxin is causing massive changes in gene expression and metabolism. Instead of causing a global shutdown of defense genes as previously hypothesized, the presence of HC-toxin during CCR1 infection actually upregulated most components of various defense pathways, though the presence of downregulated components within the same pathway suggests a complex situation. Our study suggests that HC-toxin is acting as an agent of chaos, completely deregulating proper cellular function to prevent the plant from mounting an effective resistance response.

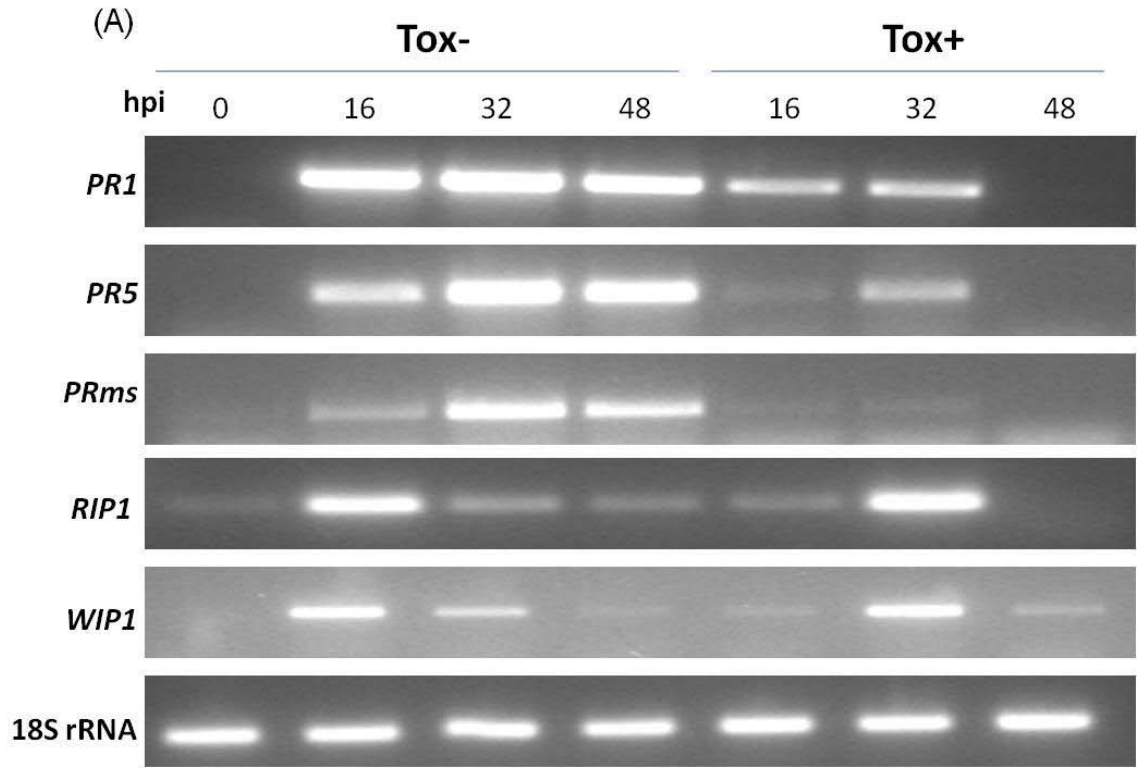


**Figure 3.1. Expression analyses of selected maize defense genes during infection with either Tox$^-$ or Tox$^+$ CCR1 using RT-PCR.** (Young, 2008)

## Materials and Methods

### Plant growth and maintenance

Susceptible *hm1*-K114 maize plants in the B73 background were grown on Sunshine MVP Propagation Mix (Sungro Horticulture) in Conviron PGR-15 growth chambers at 28º C (day) 23ºC (night) on a 12 hr light/12 hr dark cycle.

### Pathogen maintenance and inoculations

*Cochliobolus carbonum* race 1 fungus was cultured on carrot juice agar plates as previously described (Johal and Briggs, 1992). For leaf inoculations, 2 mL of ~160,000 spores/mL of either $Tox^-$ or $Tox^+$ CCR1 conidial spore suspension in double-distilled $H_2O$ with 0.1% Tween-20 was used as inoculum, with $H_2O$ and 0.1% Tween-20 serving as mock. The spore suspensions were sprayed onto the first leaf of 7-day-old plants, and the plants were covered with a clear plastic dome and placed in a humidity chamber set at 70% for 16 hr. The plants were then transferred back into the growth chambers and the first leaf collected and flash-frozen in liquid nitrogen 44 hr post inoculation. Three biological replicates of 36 leaves each were sampled for each treatment.

### Transcriptome analyses

Total RNA was extracted using a protocol modified from (Eggermont et al., 1996) and treated with DNaseI (Thermo Fisher Scientific). After verifying concentrations with a Nanodrop 2000c Spectrophotometer (Thermo Scientific), the RNA was sent to the Purdue Genomics Core Facility for sequencing on an Illumina HiSeq2500. All reads were trimmed to remove adapters using FASTQ/A Trimmer. FASTQ files with trimmed reads were aligned to the B73_RefGenV3.30 file (plants.ensembl.org) using Bowtie 2 (Langmead and Salzberg, 2012). Sorted SAM files with aligned reads were used to make counts tables using HTSeq (Anders et al., 2015) for input into DESeq2 (Love et al., 2014) for determining differential expression between Mock, $Tox^-$ CCR1, and $Tox^+$ CCR1 samples. A Benjamini-Hochberg adjusted p-value for multiple test correction was calculated for each gene in the output. Maize genes were identified via a blastp analysis against an Arabidopsis protein database with an E-value score cutoff of “1e-05” and annotated using the Arabidopsis TAIR10 annotation file (Arabidopsis.org). Differentially expressed genes

analyzed in this study were defined as genes whose $p_{adj} < 0.05$ and $|\log_2$ fold change$| \geq 1$. Venn diagrams were constructed using Venny 2.1 (Oliveros, 2015). The MapMan software (Usadel et al., 2005) was utilized for visualizing overviews of metabolism and photosynthesis using the Zm_B73_5b_FGS_cds_2012 mapping file (mapman.gabipd.org).

**Amino acid analyses**

For amino acid extraction, 100 mg of powdered leaf tissue was extracted in 5 mL methanol in the dark for 24 hr, after which 2.5 mL each of chloroform and water were added and allowed to settle in the dark at 4ºC for 20 min. The upper aqueous phase was then transferred into a glass vial, dried under a stream of air overnight, and stored at -20ºC until use. After resuspending the samples in double-distilled $H_2O$, amino acids were purified by running the samples on a previously protonated Dowex 50W X8 (Sigma) column and eluting with 6 N ammonium hydroxide. The samples were again dried under a stream of air overnight and stored at -20ºC until derivatization. For derivatization with heptafluorobutyric acid anhydride (HFBA), the dried samples were resuspended in 200 µL 5:1 (v/v) isobutanol:acetyl chloride, heated at 120ºC for 20 min, cooled and dried under a stream of air, resuspended in 100 µL HFBA, heated at 120ºC for 10 min, cooled and dried under a stream of air, and resuspended in 50 µL 1:1 (v/v) ethyl acetate:acetic anhydride. The derivatized samples were analyzed using GC-MS (5975 inert XL EI/CI mass spectrometer detector combined with a 6890N GC system (Agilent Technologies)) with an Agilent 19091S-433 HP-5MS capillary column (30 m x 0.25 mm; film thickness 0.25 µm). A 100-250ºC oven temperature range, increasing 6ºC per minute, was used for each sample. Objects were scanned in the 200-400 mass range. Peak identification and integration was performed using the Wsearch32 software (wsearch.com.au).

## Results

### The presence of HC-toxin during CCR1 infection greatly increases the number of differentially regulated genes

Our transcriptomic analysis revealed that 4662 genes were differentially regulated in the $Tox^-$ CCR1 vs Mock comparison (Fig. 3.2A.), representing genes whose expressions change during a resistant immune response. Of these differentially regulated genes (DEGs), 1324 were downregulated and 3338 were upregulated. The induced genes presumably include defense genes necessary for preventing the CCR1 pathogen from spreading beyond its initial sites of infection. A total of 14107 genes were differentially regulated in the $Tox^+$ CCR1 vs Mock comparison, representing genes whose expressions change during a susceptible immune response. These DEGs, of which 5835 were downregulated and 8272 upregulated, represent genes whose expression has been either directly altered by HC-toxin or is responding to the increased cell death caused by the spreading pathogen. The number of DEGs in the $Tox^+$ CCR1 vs $Tox^+$ CCR1 comparison is close to that observed in the $Tox^+$ CCR1 vs Mock comparison, further emphasizing the large-scale transcriptional changes induced by $Tox^+$ CCR1 infection. A surprisingly small number of DEGs displayed contrasting expression patterns, with only 124 genes downregulated in the resistant interaction being upregulated by the susceptible interaction and 146 genes upregulated in the susceptible interaction being downregulated by the susceptible interaction (Fig. 3.2B.). It is in this latter gene set that we would expect to observe any defense gene repression caused by HC-toxin.

**A**

| | Down | Up | Total |
|---|---|---|---|
| $Tox^-$ VS Mock | 1324 | 3338 | 4662 |
| $Tox^+$ VS Mock | 5835 | 8272 | 14107 |
| $Tox^+$ VS $Tox^-$ | 4789 | 7101 | 11890 |

**B**

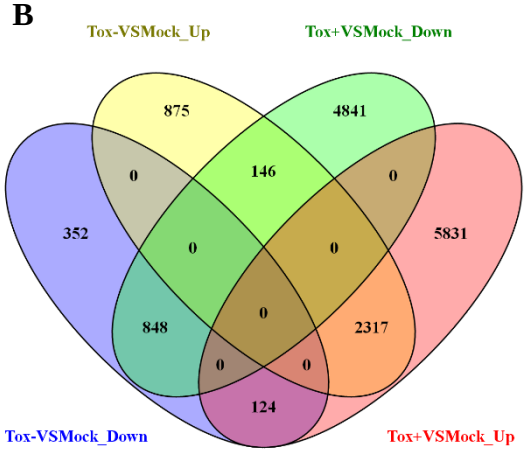


**Figure 3.2. $Tox^+$ CCR1 infection leads to more DEGs than $Tox^-$ CCR1.** 3.2.A. Total number of down- and upregulated DEGs in the $Tox^-$ CCR1 vs Mock, $Tox^+$ CCR1 vs Mock, and $Tox^+$ CCR1 vs $Tox^-$ CCR1 comparisons. 3.2.B. Venn diagram demonstrating numbers of unique and shared down- and upregulated DEGs between $Tox^-$ CCR1 vs Mock and $Tox^+$ CCR1 vs Mock.

### HC-toxin is not repressing defense pathways

After observing that the previous set of defense genes analyzed by RT-PCR displayed a similar pattern in our RNA-seq data, we developed a greatly expanded list of defense genes that includes additional pathogenesis-related (PR) genes, chitinases (Hawkins et al., 2015), and various other defense genes from Arabidopsis and maize literature (Laluk and Mengiste, 2010; Huffaker et al., 2011). We found that the presence of HC-toxin during CCR1 infection actually appears to be upregulating the majority of the defense genes analyzed (Table 3.1), contrary to previous expectations.

**Table 3.1. Defense gene expression is mostly upregulated by Tox$^+$ CCR1 infection.**

| GeneID | Gene Name | Tox$^-$ vs Mock log$_2$FC | | Tox$^+$ vs Mock log$_2$FC | | Tox$^+$ vs Tox$^-$ log$_2$FC | |
|---|---|---|---|---|---|---|---|
| **Previous gene list** | | | | | | | |
| GRMZM2G465226 | PR1 | 5.793 | *** | 2.688 | *** | -3.074 | *** |
| GRMZM2G402631 | PR5 | 4.358 | *** | 4.023 | *** | -0.308 | |
| AC205274.3_FG001 | PRms | 11.123 | *** | 5.789 | *** | -5.318 | *** |
| GRMZM2G063536 | RIP1 | 2.042 | | -0.904 | | -3.037 | * |
| GRMZM2G156632 | WIP1 | 6.672 | *** | 10.968 | *** | 4.333 | *** |
| **Other defense genes** | | | | | | | |
| GRMZM2G065585 | PRM6b | 7.632 | *** | 5.578 | *** | -2.024 | *** |
| GRMZM2G117971 | PR4b | 5.941 | *** | 5.362 | *** | -0.547 | * |
| GRMZM2G112488 | PR10 | 4.916 | *** | 9.166 | *** | 4.284 | *** |
| GRMZM2G075283 | PR10 putative | 8.098 | *** | 7.285 | *** | -0.757 | ** |
| GRMZM2G112524 | PR10 putative | 3.087 | *** | 7.898 | *** | 4.843 | *** |
| GRMZM2G112538 | PR10 putative | 3.226 | *** | 8.516 | *** | 5.327 | *** |
| GRMZM2G099454 | Basic endochitinase C | 2.122 | *** | -0.383 | | -2.478 | *** |
| GRMZM2G162505 | Chitinase 2 | 4.352 | *** | 6.403 | *** | 2.082 | *** |
| GRMZM2G057093 | Chitinase 2 | 2.554 | *** | 2.247 | *** | -0.280 | |
| GRMZM2G051921 | Putative uncharacterized protein | 9.048 | *** | 8.911 | *** | -0.109 | |
| GRMZM2G051943 | Endochitinase A | 8.935 | *** | 8.201 | *** | -0.719 | * |
| GRMZM5G837822 | Hevamine-A | 0.222 | | 4.441 | *** | 4.255 | *** |
| GRMZM2G430942 | Chitinase A | 0.077 | | 5.352 | *** | 5.462 | *** |
| GRMZM2G453805 | PRm3 | 4.524 | *** | 6.787 | *** | 2.296 | *** |
| GRMZM2G133781 | Putative uncharacterized protein | 4.155 | * | 7.097 | *** | 3.033 | *** |
| GRMZM2G358153 | Chitinase 1 | 6.314 | *** | 6.231 | *** | -0.050 | |
| GRMZM2G129189 | Endochitinase PR4 | 3.678 | *** | 4.458 | *** | 0.804 | * |
| GRMZM2G145461 | Acidic class I chitinase | 4.977 | *** | 4.330 | *** | -0.614 | * |
| GRMZM2G447795 | Xylanase inhibitor protein 1 | 5.624 | *** | 8.214 | *** | 2.614 | *** |
| GRMZM2G162359 | Uncharacterized protein | 5.568 | *** | 7.500 | *** | 1.973 | *** |
| GRMZM2G062974 | Basic Endochitinase A | 2.396 | *** | 5.484 | *** | 3.127 | *** |
| GRMZM2G037694 | Hydrolase, hydrolyzing O-glycosyl compound | 0.093 | | -1.487 | * | -1.560 | *** |
| GRMZM2G117405 | Beta-hexosaminidase | -0.701 | | 1.360 | | 2.095 | * |
| GRMZM2G090441 | Uncharacterized protein | -4.235 | | 1.988 | | 6.406 | * |
| GRMZM2G005633 | Endochitinase B | 8.701 | *** | 9.773 | *** | 1.130 | *** |
| GRMZM2G474575 | KTI1 | 2.269 | | 8.397 | *** | 6.100 | *** |
| GRMZM5G865319 | SerPIN | 0.631 | | 4.680 | *** | 4.084 | *** |
| GRMZM2G028393 | MPI | 1.621 | *** | 1.815 | *** | 0.223 | |
| GRMZM5G899080 | PROPEP1 | -1.575 | *** | -2.151 | *** | -0.561 | |

| | | | | | | | |
|---|---|---|---|---|---|---|---|
| GRMZM5G834697 | MKK5 | 0.678 | ** | 1.809 | *** | 1.163 | *** |
| GRMZM2G017792 | MPK3 | 1.546 | *** | 2.196 | *** | 0.682 | * |
| GRMZM2G148087 | WRKY33 | 3.094 | *** | 5.053 | *** | 1.991 | *** |

Asterisks denote whether the difference in gene expression was significant (FDR < 0.001:***, < 0.01:**, < 0.05*).

We next examined the effects of HC-toxin on the biosynthesis and signaling response pathways of the three major plant defense hormones: jasmonic acid (JA), ethylene (ET), and salicylic acid (SA). We also observed the biosynthetic pathways of other related oxylipins, including the death acids formed by 9-lipoxygenase pathways parallel to the 13-lipoxygenase pathway that leads to JA production (Christensen et al., 2015). The genes involved in the biosynthesis of JA and other oxylipins were generally found to be upregulated by both $Tox^-$ and $Tox^+$ CCR1 infection, but more strongly in the presence of HC-toxin (Table 3.2). Of the few genes that were downregulated by $Tox^+$ CCR1 infection, *OPR8* stands out due to its important role in JA biosynthesis (along with its paralog *OPR7*) and its contrasting expression pattern suggesting that HC-toxin is downregulating a key gene normally induced by CCR1 infection. The various JA signaling and responsive genes, assembled from both database and literature searches (Christensen et al., 2015; Yang et al., 2015), were also observed to be generally further upregulated in the susceptible response (Table 3.3). The biosynthetic and signaling pathways for ET and SA were similarly observed to display increased upregulation during $Tox^+$ CCR1 infection (Tables 3.4 and 3.5), indicating that neither immune pathway appears to be repressed.

**Table 3.2. Jasmonic acid and oxylipin biosynthesis genes are mostly upregulated by Tox$^+$ CCR1 infection.**

| GeneID | Gene Name | Tox$^-$ vs Mock log$_2$FC | | Tox$^+$ vs Mock log$_2$FC | | Tox$^+$ vs Tox$^-$ log$_2$FC | |
|---|---|---|---|---|---|---|---|
| **JA biosynthesis** | | | | | | | |
| GRMZM2G067225 | AOS1 | 4.107 | *** | 4.394 | *** | 0.321 | |
| GRMZM2G002178 | AOS2 | -0.606 | | 7.879 | *** | 8.496 | *** |
| GRMZM2G376661 | AOS3 | 3.097 | * | 3.968 | *** | 0.893 | |
| GRMZM2G072653 | AOS4 | -0.717 | | -3.806 | * | -3.050 | |
| GRMZM2G033098 | AOS | 2.413 | *** | 5.267 | *** | 2.889 | *** |
| GRMZM2G077316 | AOC | 1.949 | *** | 2.309 | *** | 0.393 | |
| GRMZM2G104843 | LOX8 | 0.597 | * | 3.389 | *** | 2.828 | *** |
| GRMZM2G148281 | OPR7 | 0.179 | | 0.487 | * | 0.338 | |
| GRMZM2G082087 | **OPR8** | 1.024 | *** | -1.279 | *** | -2.274 | *** |
| GRMZM2G091276 | JAR1a | 0.081 | | 2.017 | *** | 1.968 | *** |
| GRMZM2G162413 | JAR1b | -0.175 | | 1.853 | *** | 2.062 | *** |
| GRMZM2G136857 | JA carboxyl methyltransferase | -2.698 | *** | -3.296 | *** | -0.584 | |
| **Oxylipin biosynthesis** | | | | | | | |
| GRMZM2G156861 | LOX1 | 0.454 | | 1.710 | *** | 1.287 | *** |
| GRMZM2G109130 | LOX3 | 3.863 | *** | 7.444 | *** | 3.619 | *** |
| GRMZM2G109056 | LOX4 | 2.214 | *** | 4.290 | *** | 2.110 | *** |
| GRMZM2G102760 | LOX5 | 1.680 | *** | 4.061 | | 2.415 | *** |
| GRMZM2G040095 | LOX6 | -1.708 | *** | -1.854 | *** | -0.127 | |
| GRMZM2G017616 | LOX9 | 1.653 | *** | 2.246 | *** | 0.628 | * |
| GRMZM2G015419 | LOX10 | -1.241 | *** | -1.798 | ** | -0.539 | |
| GRMZM2G009479 | LOX11 | -0.639 | *** | 0.615 | * | 1.285 | *** |
| GRMZM2G106748 | LOX12 | -0.750 | ** | -2.086 | *** | -1.312 | ** |
| GRMZM5G822593 | LOX13 | 3.694 | *** | 5.325 | NA | 1.669 | *** |
| GRMZM2G106303 | OPR1 | 4.423 | | 8.484 | *** | 4.095 | *** |
| GRMZM2G000236 | OPR2 | 4.338 | *** | 8.427 | *** | 4.126 | *** |
| GRMZM2G156712 | OPR3 | 3.190 | *** | 4.274 | *** | 1.116 | ** |
| GRMZM2G087192 | OPR5 | 0.950 | *** | 2.724 | *** | 1.808 | *** |
| GRMZM2G068947 | OPR6 | -1.536 | *** | -2.726 | * | -1.176 | |
| GRMZM6G986387 | HPL | -0.543 | | -2.011 | *** | -1.450 | ** |

Asterisks denote whether the difference in gene expression was significant (FDR < 0.001:***, < 0.01:**, < 0.05*).

**Table 3.3. JA signaling and response genes are mostly upregulated by Tox$^+$ CCR1 infection.**

| GeneID | Gene Name | Tox$^-$ vs Mock log$_2$FC | | Tox$^+$ vs Mock log$_2$FC | | Tox$^+$ vs Tox$^-$ log$_2$FC | |
|---|---|---|---|---|---|---|---|
| **JA signaling** | | | | | | | |
| GRMZM2G343157 | JAZ1 | 4.045 | *** | 2.347 | ** | -1.689 | ** |
| GRMZM2G445634 | JAZ2 | 1.404 | *** | 4.675 | *** | 3.303 | |
| GRMZM2G117513 | JAZ3 | -0.396 | ** | 0.665 | ** | 1.093 | *** |
| GRMZM2G145412 | JAZ5 | 1.717 | *** | 6.300 | *** | 4.617 | *** |
| GRMZM2G145458 | JAZ6 | 1.995 | | 4.723 | *** | 2.643 | *** |
| GRMZM2G086920 | JAZ8 | -0.229 | | 0.815 | *** | 1.075 | *** |
| GRMZM2G145407 | JAZ9 | 3.983 | | 6.558 | *** | 2.551 | *** |
| GRMZM2G005954 | JAZ11 | -1.203 | *** | -0.151 | | 1.081 | *** |
| GRMZM2G101769 | JAZ12 | -0.027 | | 0.961 | *** | 1.018 | *** |
| GRMZM2G173596 | JAZ15 | 5.412 | *** | 10.188 | *** | 4.818 | *** |
| GRMZM2G116614 | JAZ18 | -2.315 | *** | 0.659 | * | 3.006 | *** |
| GRMZM2G089736 | JAZ20 | 1.199 | *** | 3.485 | *** | 2.318 | *** |
| GRMZM2G036351 | JAZ21 | 2.894 | *** | 7.029 | *** | 4.182 | *** |
| GRMZM2G036288 | JAZ22 | 6.457 | | 9.083 | *** | 2.642 | ** |
| GRMZM2G143402 | JAZ23 | -0.013 | | 2.445 | *** | 2.491 | *** |
| GRMZM2G065896 | ZML1 | -0.245 | | -2.232 | *** | -1.967 | ** |
| GRMZM2G080509 | ZML3 | -0.159 | | -1.545 | *** | -1.358 | *** |
| GRMZM2G001930 | MYC7 | -0.151 | | 0.949 | *** | 1.134 | *** |
| GRMZM2G049229 | MYC2-like | 1.493 | *** | 3.134 | *** | 1.672 | *** |
| GRMZM2G129860 | CYP11 | 0.158 | | 1.080 | *** | 0.953 | *** |
| GRMZM2G042992 | TRP1 | 1.109 | *** | 2.877 | *** | 2.877 | *** |
| GRMZM2G043764 | NINJA | 0.055 | | -1.055 | *** | -1.085 | *** |
| **JA response** | | | | | | | |
| GRMZM2G179092 | TPS10 | 4.476 | *** | 4.991 | *** | 0.549 | |
| GRMZM2G156632 | BBTI12 | 6.672 | *** | 10.968 | *** | 4.333 | *** |
| GRMZM2G053669 | ASN1 | 5.169 | *** | 7.895 | *** | 2.766 | *** |
| GRMZM2G312997 | DOX | -1.538 | *** | 3.714 | *** | 5.287 | *** |
| AC208221.3_FG002 | BBTI2 | -3.323 | | 0.581 | | 3.879 | |
| GRMZM2G493395 | DXS | 4.651 | *** | 5.458 | *** | 0.850 | ** |
| GRMZM2G096680 | CI-1B | 1.080 | | 1.632 | | 0.564 | |
| GRMZM2G011523 | BBTI11 | 2.947 | *** | 7.339 | *** | 4.425 | *** |
| GRMZM2G007928 | BBTI13 | -0.859 | *** | -1.010 | | -0.134 | |
| GRMZM5G836222 | A20/AN1 | -0.242 | | 0.789 | *** | 1.062 | *** |
| AC206425.3_FG002 | jasmonate-induced protein | -1.97796 | *** | -3.550 | *** | -1.612 | |
| GRMZM2G030790 | jasmonate-induced protein | 2.627 | | -2.682 | | -5.131 | |

| | | | | | | | |
|---|---|---|---|---|---|---|---|
| GRMZM2G020423 | jasmonate-induced protein | -1.756 | *** | -5.559 | *** | -3.773 | *** |
| AC225718.2_FG006 | CCD1 | 2.802 | *** | 3.881 | *** | 1.107 | *** |
| GRMZM2G132093 | GST2 | 1.848 | *** | 6.244 | *** | 4.428 | *** |
| GRMZM2G159477 | HYD | 0.959 | *** | 3.823 | *** | 2.894 | *** |
| GRMZM2G020631 | OXR | 2.376 | *** | 6.178 | *** | 3.837 | *** |
| AC196110.4_FG004 | CC9 | -1.150 | * | -1.717 | * | -0.549 | |

Asterisks denote whether the difference in gene expression was significant (FDR < 0.001:***, < 0.01:**, < 0.05*).

**Table 3.4. Ethylene biosynthesis and signaling genes are mostly upregulated by Tox$^+$ CCR1 infection.**

| GeneID | Gene Name | Tox$^-$ vs Mock log$_2$FC | | Tox$^+$ vs Mock log$_2$FC | | Tox$^+$ vs Tox$^-$ log$_2$FC | |
|---|---|---|---|---|---|---|---|
| **Ethylene biosynthesis** | | | | | | | |
| GRMZM2G054123 | MAT | 2.634 | *** | 5.507 | *** | 2.909 | *** |
| AC199526.5_FG002 | MAT | 1.695 | *** | 4.646 | *** | 2.986 | *** |
| GRMZM2G164405 | ACS2 | 5.780 | *** | 9.752 | *** | 3.967 | *** |
| GRMZM2G018006 | ACS3 | -0.485 | ** | -1.610 | *** | -1.098 | *** |
| GRMZM2G054361 | ACS6 | 0.560 | | 6.724 | *** | 6.543 | *** |
| GRMZM5G894619 | ACS7 | 2.353 | *** | 8.390 | *** | 6.054 | *** |
| GRMZM2G166639 | ACO15 | 1.038 | *** | 1.071 | *** | 0.066 | |
| GRMZM2G126732 | ACO20 | 0.706 | ** | 2.410 | *** | 1.735 | *** |
| GRMZM2G072529 | ACO31 | 1.621 | *** | 3.994 | *** | 2.408 | *** |
| GRMZM2G052422 | ACO35 | -0.556 | ** | 2.620 | *** | 3.207 | *** |
| **Ethylene signaling** | | | | | | | |
| GRMZM2G068217 | EIN2 | -0.398 | * | -1.374 | *** | -0.950 | *** |
| GRMZM2G033570 | EIN3 | -0.475 | ** | 0.089 | | 0.595 | * |
| GRMZM2G317584 | EIL1 | -0.105 | | -1.069 | *** | -0.938 | ** |
| GRMZM2G053503 | ERF1 | 1.742 | *** | 3.754 | *** | 2.048 | *** |
| GRMZM2G381441 | EREB58 | 3.260 | * | 6.779 | *** | 3.552 | *** |
| GRMZM5G805505 | EREB87 | 2.435 | | 6.179 | *** | 3.725 | *** |
| GRMZM2G057386 | EREB107 | 0.920 | * | 3.078 | *** | 2.190 | *** |

Asterisks denote whether the difference in gene expression was significant (FDR < 0.001:***, < 0.01:**, < 0.05*).

**Table 3.5. Shikimate pathway and salicylic acid signaling genes are mostly upregulated by Tox$^+$ CCR1 infection.**

| GeneID | Gene Name | Tox$^-$ vs Mock log$_2$FC | | Tox$^+$ vs Mock log$_2$FC | | Tox$^+$ vs Tox$^-$ log$_2$FC | |
|---|---|---|---|---|---|---|---|
| **Shikimate pathway** | | | | | | | |
| GRMZM2G365160 | DAHPS | 3.556 | *** | 7.479 | *** | 3.954 | *** |
| GRMZM2G117707 | DAHPS | 3.452 | *** | 8.286 | *** | 4.873 | *** |
| GRMZM2G022837 | ICS | -0.489 | * | -0.536 | | -0.025 | |
| GRMZM2G437912 | PDT | 2.084 | *** | 4.590 | | 2.539 | *** |
| GRMZM2G074604 | PAL1 | 2.995 | *** | 5.828 | *** | 2.868 | *** |
| GRMZM2G441347 | PAL2 | -0.910 | | 5.770 | *** | 6.716 | *** |
| GRMZM2G160541 | PAL3 | 1.761 | *** | 7.921 | *** | 6.196 | *** |
| GRMZM2G118345 | PAL4 | 2.454 | *** | 7.245 | *** | 4.828 | *** |
| GRMZM2G063917 | PAL5 | 3.944 | *** | 8.270 | *** | 4.359 | *** |
| GRMZM2G081582 | PAL6 | 4.270 | *** | 6.843 | *** | 2.608 | *** |
| GRMZM2G170692 | PAL7 | 3.085 | *** | 7.071 | *** | 4.025 | *** |
| GRMZM2G334660 | PAL8 | 3.614 | *** | 7.589 | *** | 4.016 | *** |
| GRMZM2G029048 | PAL9 | 2.775 | *** | 4.072 | *** | 1.331 | *** |
| GRMZM2G147245 | C4H | 3.887 | *** | 8.252 | | 4.411 | *** |
| GRMZM2G139874 | C4H | 2.338 | *** | 6.141 | *** | 3.838 | *** |
| GRMZM2G138382 | AS | -0.070 | | 2.667 | *** | 2.768 | *** |
| GRMZM2G325131 | ANS1 | -0.287 | | 0.921 | *** | 1.238 | *** |
| GRMZM2G051219 | PAT | 2.248 | *** | 4.744 | *** | 2.529 | *** |
| GRMZM2G106950 | IGPS | -0.905 | *** | 0.461 | | 1.395 | *** |
| GRMZM2G046191 | IGL | -0.326 | | 1.024 | *** | 1.380 | *** |
| GRMZM2G171383 | ANS2 | -0.396 | | 3.906 | *** | 4.328 | *** |
| GRMZM2G127948 | OMT1 | 2.487 | *** | 3.619 | *** | 1.165 | *** |
| GRMZM2G155329 | CHI1 | 0.863 | *** | 1.716 | *** | 0.886 | ** |
| GRMZM5G877500 | EPS1 | 2.174 | *** | 5.207 | *** | 3.067 | *** |
| **SA signaling** | | | | | | | |
| GRMZM2G065154 | EDS5 | 0.557 | | 1.903 | *** | 1.380 | *** |
| GRMZM2G152739 | PAD4 | 1.575 | *** | 3.093 | *** | 1.551 | *** |
| GRMZM2G126749 | SARD1 | 2.423 | *** | 3.738 | *** | 1.347 | *** |
| GRMZM2G077197 | NPR1 | 0.796 | *** | 0.686 | ** | -0.079 | |
| GRMZM2G076450 | NPR3/NPR4-like | 0.024 | | -0.912 | *** | -0.909 | *** |
| GRMZM2G115162 | NPR3/NPR4-like | -0.185 | | -1.674 | *** | -1.465 | *** |

Asterisks denote whether the difference in gene expression was significant (FDR < 0.001:***, < 0.01:**, < 0.05*).

**HC-toxin leads to significant metabolic perturbations during CCR1 infection**

Besides salicylic acid, the shikimate pathway also leads to the production of several other metabolites including aromatic amino acids, auxin, lignin, phenylpropanoids, and the defense related benzoxazinoids (Tzin and Galili, 2010; Vogt, 2010). Though the shikimate pathway itself is strongly upregulated by $Tox^+$ CCR1 infection (Table 3.5), the core benzoxazinoid biosynthesis pathway leading up to DIMBOA-Glc appears to be weakly downregulated by both $Tox^-$ and $Tox^+$ CCR1 interactions (Table 3.6). To further analyze the metabolic perturbations induced by HC-toxin, we extracted and quantified amino acids from the same leaf tissue samples used for the RNA-seq analysis. We observed that $Tox^+$ CCR1 infection led to significantly increased accumulation of α-aminobutyric acid, valine, threonine, serine, leucine, isoleucine, 5-hydroxynorvaline, tyramine, aspartic acid, phenylalanine, lysine and tyrosine, α-aminoadipic acid, arginine, histidine, and cysteine levels compared to both $Tox^-$ CCR1 infection and mock treatment (Table 3.7). Levels of alanine, glycine, γ-aminobutyric acid, pipecolic acid, and glutamic acid were also shown to accumulate during $Tox^+$ CCR1 infection though not at levels significantly different from those induced by $Tox^-$ CCR1.

**Table 3.6. Core benzoxazinoid biosynthesis genes are generally weakly downregulated by Tox$^+$ CCR1 infection.**

| GeneID | Gene Name | Tox$^-$ vs Mock log$_2$FC | | Tox$^+$ vs Mock log$_2$FC | | Tox$^+$ vs Tox$^-$ log$_2$FC | |
|---|---|---|---|---|---|---|---|
| **Benzoxazinoid biosynthesis** | | | | | | | |
| GRMZM2G085381 | BX1 | -2.137 | *** | -3.263 | *** | -1.110 | |
| GRMZM2G085661 | BX2 | -1.089 | *** | -0.712 | | 0.397 | |
| GRMZM2G167549 | BX3 | -1.094 | *** | 0.126 | | 1.245 | *** |
| GRMZM2G172491 | BX4 | -1.016 | *** | -1.688 | ** | -0.655 | |
| GRMZM2G063756 | BX5 | -1.092 | *** | -1.764 | ** | -0.656 | |
| GRMZM2G085054 | BX8 | 0.323 | | -0.719 | ** | -1.015 | *** |
| GRMZM2G161335 | BX9 | -0.010 | | -0.591 | * | -0.554 | ** |
| GRMZM6G617209 | BX6 | -0.872 | *** | -1.793 | *** | -0.901 | * |
| GRMZM2G441753 | BX7 | -1.853 | *** | -1.427 | *** | 0.449 | |
| GRMZM2G311036 | BX10 | 6.502 | *** | 11.675 | *** | 5.203 | *** |
| GRMZM2G336824 | BX11 | 6.178 | *** | 9.909 | *** | 3.770 | *** |
| GRMZM2G023325 | BX12 | 4.875 | | 11.067 | *** | 6.207 | *** |
| AC148152.3_FG005 | BX13 | 0.555 | | 3.532 | *** | 2.983 | *** |
| GRMZM2G127418 | BX14 | 9.176 | *** | 6.767 | *** | -2.377 | *** |
| GRMZM2G016890 | GLU1 | 3.502 | *** | 5.359 | *** | 1.889 | *** |

Asterisks denote whether the difference in gene expression was significant (FDR < 0.001:***, < 0.01:**, < 0.05*).

**Table 3.7. Changes in free amino acid levels caused by CCR1 infection.**

| | Mock | Tox$^-$ | Tox$^+$ |
|---|---|---|---|
| **Alanine** | 1387.357 ± 92.592 $^A$ | 2382.155 ± 32.932 $^B$ | 2811.717 ± 162.932 $^B$ |
| **Glycine** | 192.487 ± 10.935 $^A$ | 320.44 ± 85.117 $^{AC}$ | 792.57 ± 115.442 $^{BC}$ |
| **AABA** | 0 $^A$ | 4.656 ± 2.688 $^B$ | 76.872 ± 44.382 $^C$ |
| **Valine** | 74.757 ± 9.036 $^A$ | 291.926 ± 47.489 $^B$ | 2041.309 ± 310.428 $^C$ |
| **Threonine** | 142.038 ± 13.323 $^A$ | 298.982 ± 34.783 $^B$ | 2230.255 ± 276.792 $^C$ |
| **Serine** | 417.178 ± 23.402 $^A$ | 879.634 ± 78.083 $^B$ | 2360.028 ± 210.674 $^C$ |
| **Leucine** | 17.889 ± 1.977 $^A$ | 79.544 ± 15.966 $^B$ | 641.943 ± 112.170 $^C$ |
| **Isoleucine** | 26.457 ± 5.315 $^A$ | 149.167 ± 48.217 $^A$ | 1219.468 ± 171.323 $^B$ |
| **ACC** | 123.876 ± 26.293 $^A$ | 191.125 ± 116.343 $^A$ | 150.918 ± 33.075 $^A$ |
| **GABA** | 43.083 ± 15.483 $^A$ | 230.424 ± 25.159 $^B$ | 340.142 ± 52.068 $^B$ |
| **Proline** | 31.115 ± 3.742 $^A$ | 71.259 ± 8.865 $^B$ | 109.095 ± 14.194 $^B$ |
| **Pipecolic acid** | 0 $^A$ | 215.737 ± 53.706 $^B$ | 83.442 ± 14.461 $^B$ |
| **5-Hydroxynorvaline** | 0 $^A$ | 0 $^A$ | 267.995 ± 45.304 $^B$ |
| **Pyroglutamic acid** | 59.459 ± 7.586 $^A$ | 65.457 ± 38.358 $^A$ | 103.313 ± 18.544 $^A$ |
| **Tyramine** | 84.214 ± 7.208 $^A$ | 215.112 ± 20.328 $^B$ | 1423.878 ± 178.051 $^C$ |
| **Aspartic acid** | 252.981 ± 56.138 $^A$ | 606.563 ± 113.684 $^B$ | 2065.629 ± 133.213 $^C$ |
| **Phenylalanine** | 32.693 ± 6.930 $^A$ | 148.686 ± 20.866 $^B$ | 1482.475 ± 199.963 $^C$ |
| **Ornithine** | 3.616 ± 0.146 $^A$ | 6.27 ± 3.188 $^A$ | 284.72 ± 87.520 $^A$ |
| **Glutamic acid** | 1132.924 ± 52.837 $^A$ | 2166.769 ± 241.288 $^B$ | 3072.164 ± 267.499 $^B$ |

| | | | |
|---|---|---|---|
| **Lysine + Tyrosine** | 30.196 ± 3.781 $^{A}$ | 122.151 ± 20.447 $^{B}$ | 385.888 ± 53.701 $^{C}$ |
| **AADA** | 0 $^{A}$ | 18.075 ± 3.608 $^{B}$ | 69.696 ± 12.767 $^{C}$ |
| **Arginine** | 17.048 ± 1.862 $^{A}$ | 48.961 ± 14.877 $^{A}$ | 179.578 ± 25.480 $^{B}$ |
| **Histidine** | 75.213 ± 10.224 $^{A}$ | 146.258 ± 35.907 $^{A}$ | 745.111 ± 144.587 $^{B}$ |
| **Cystine** | 0 $^{A}$ | 0 $^{A}$ | 101.192 ± 25.874 $^{B}$ |

Different letters indicate the values are significantly different from each other ($p_{adj} < 0.05$).

**HC-toxin may be downregulating key genes in the light reactions of photosynthesis**

The MapMan tool was utilized to provide a metabolic overview of the changes occurring in both the $Tox^-$ CCR1 versus Mock and the $Tox^+$ CCR1 versus Mock comparisons (Usadel et al., 2009). We observed a large increase in DEGs for nearly every primary and secondary metabolic pathway when comparing the $Tox^+$ CCR1 interaction to the $Tox^-$ CCR1 interaction (Figures 3.4 and 3.5). Though most of these changes suggested increased upregulation, we noticed a fairly consistent downregulation of genes in the light reactions of photosynthesis, prompting us to investigate photosynthesis more closely (Figures 3.6 and 3.7). We observed a weak downregulation of several components involved in photosystems I and II as well as ATP and NADPH synthesis in the $Tox^-$ CCR1 interaction. This downregulation becomes stronger and more widespread in the $Tox^+$ CCR1 interaction. Analysis of these components reveals a consistent downregulation of genes encoding subunits of the protein complexes making up photosystems I and II, as well as the downregulation of several reductases involved in photosynthetic electron transport (Table 3.8). Several components of the regeneration phase of the Calvin cycle also exhibited increased downregulation during $Tox^+$ CCR1 infection, though not with the strength or consistency of the light reactions. As the ATP and NADPH produced by the light reactions are required to power the Calvin cycle, inhibition of the light reactions alone would presumably suffice to essentially shutdown photosynthesis.

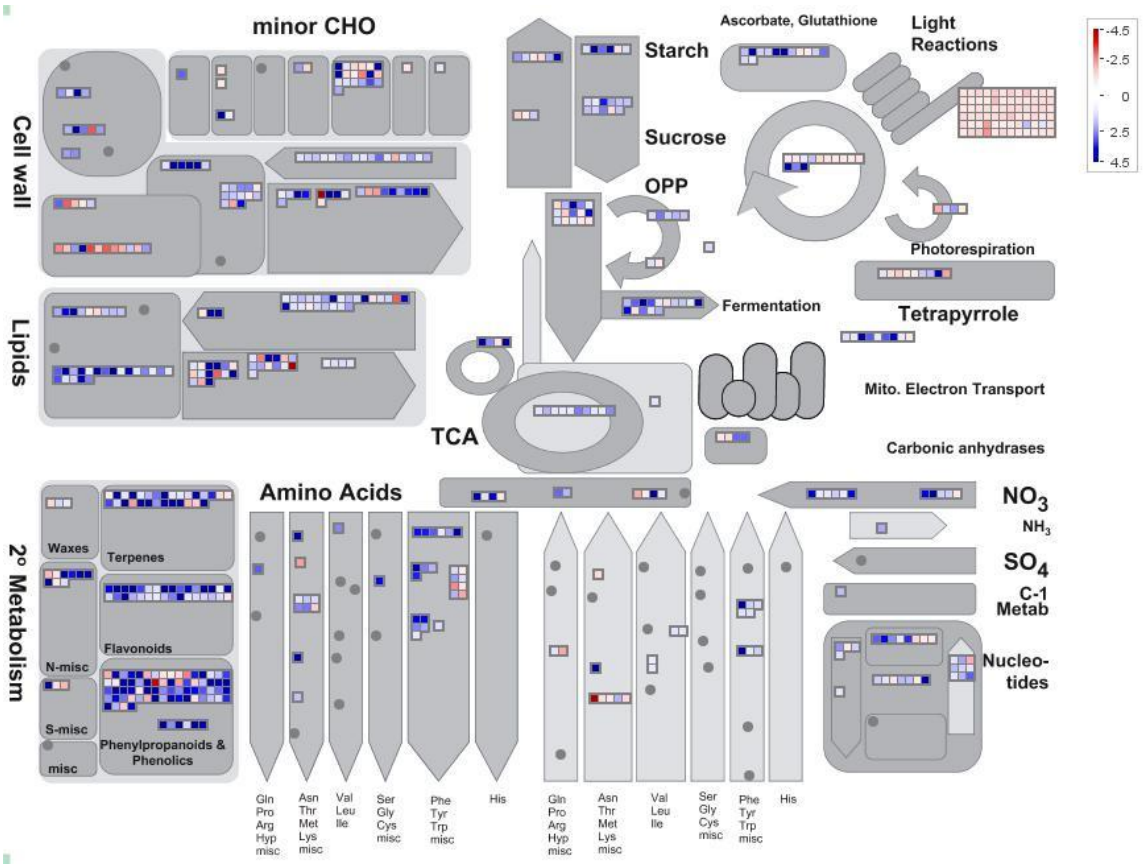


**Figure 3.3. Metabolic overview of the Tox$^-$ CCR1 vs Mock interaction.** The $\log_2$ fold change values of DEGs were analyzed using MapMan. Downregulated genes are indicated in red and upregulated genes in blue.

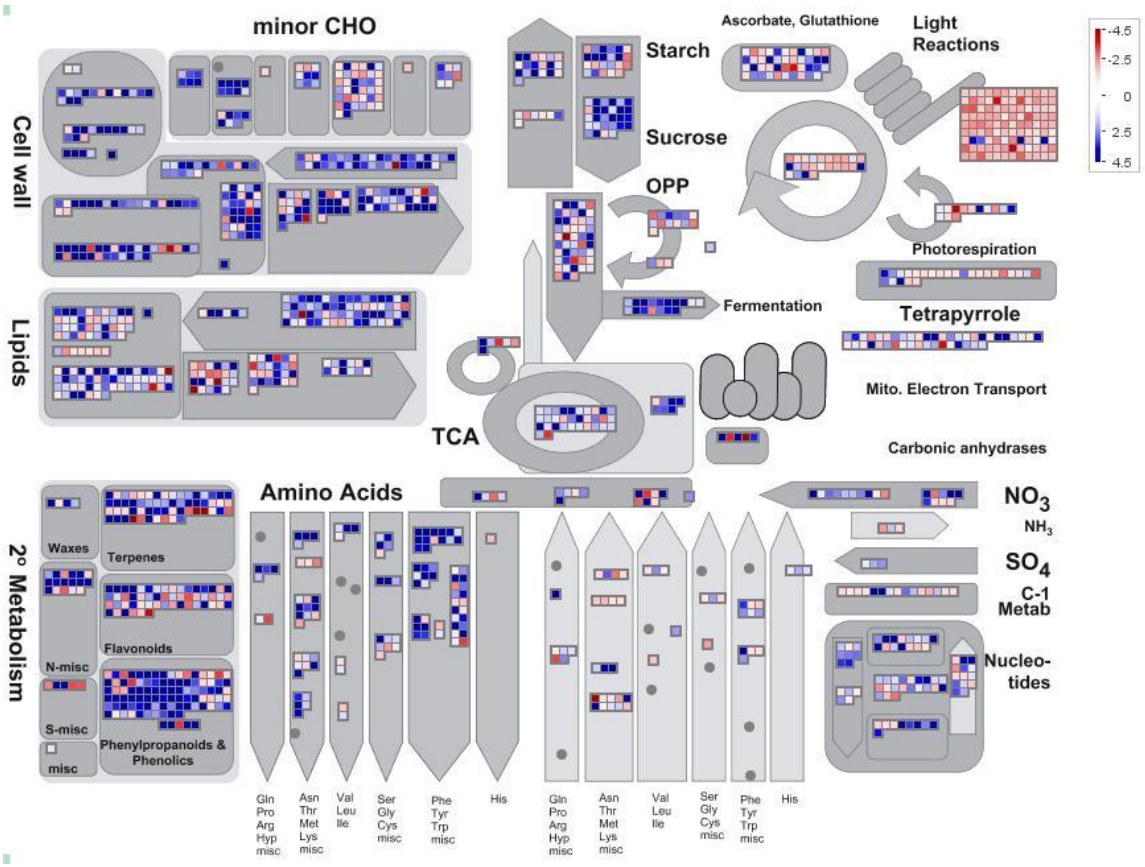


**Figure 3.4. Metabolic overview of the Tox$^+$ CCR1 vs Mock interaction.** The $\log_2$ fold change values of DEGs were analyzed using MapMan. Downregulated genes are indicated in red and upregulated genes in blue.

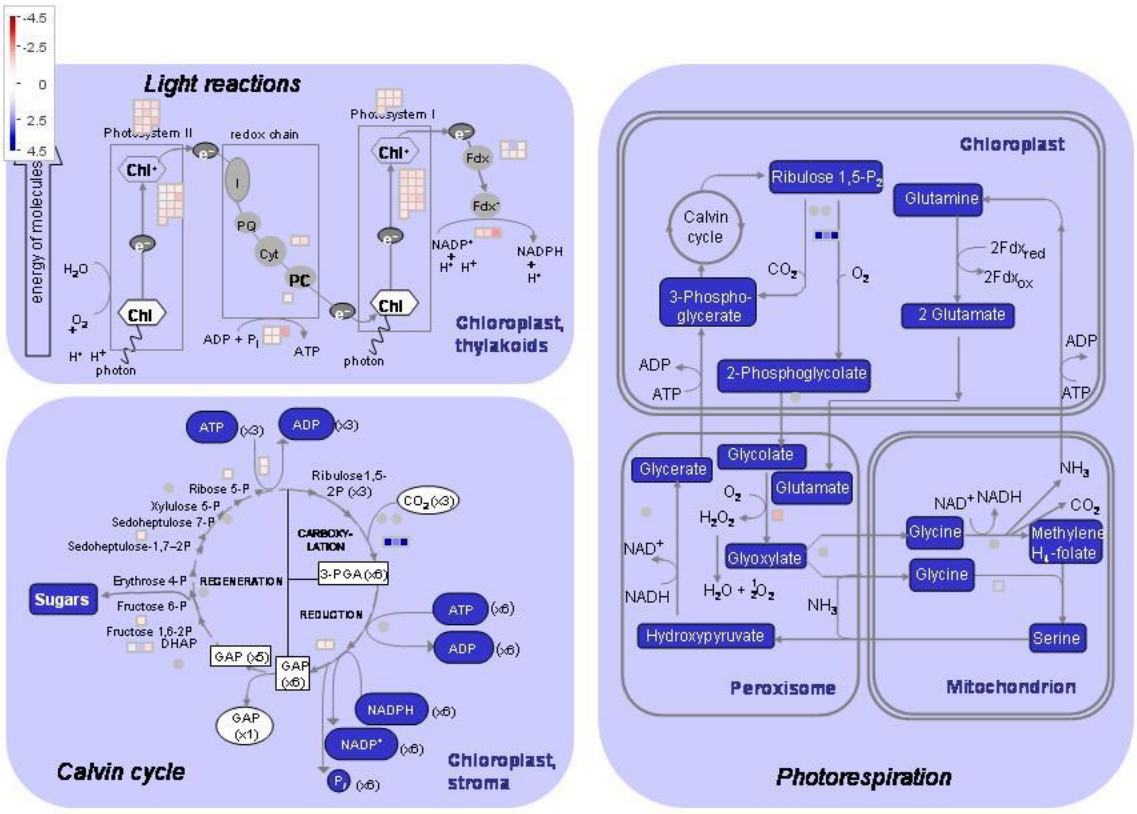


**Figure 3.5. Overview of photosynthesis in the Tox$^-$ CCR1 vs Mock interaction.** The log2 fold change values of DEGs were analyzed using MapMan.

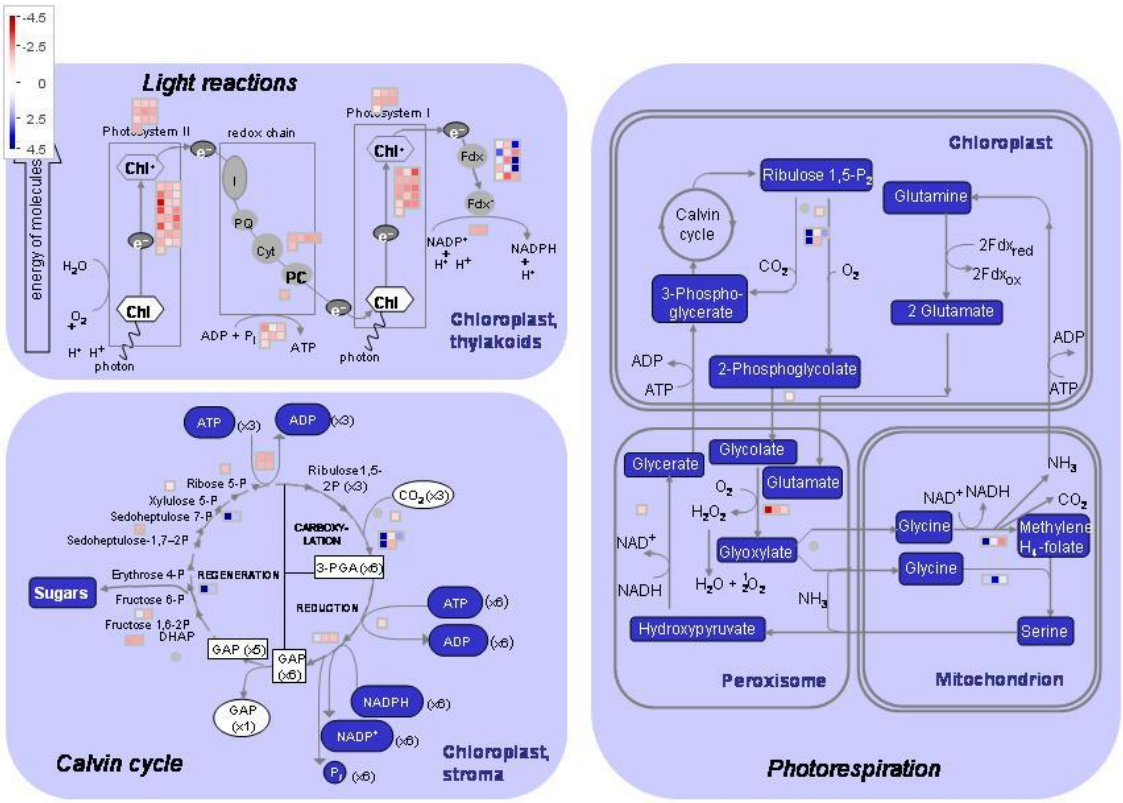


**Figure 3.6. Overview of photosynthesis in the Tox$^{+}$ CCR1 vs Mock interaction.** The log2 fold change values of DEGs were analyzed using MapMan.

**Table 3.8. Photosynthesis light reaction genes are generally downregulated by Tox$^+$ CCR1 infection.**

| GeneID | Gene Name | Tox$^-$ vs Mock log$_2$FC | | Tox$^+$ vs Mock log$_2$FC | | Tox$^+$ vs Tox$^-$ log$_2$FC | |
|---|---|---|---|---|---|---|---|
| **Light reactions of photosynthesis** | | | | | | | |
| GRMZM2G128935 | Chloroplastic quinone-oxidoreductase | -1.113 | *** | -3.059 | ** | -1.932 | |
| GRMZM2G126285 | Chloroplastic quinone-oxidoreductase | 2.243 | | 3.991 | | 1.687 | |
| GRMZM2G164558 | Plastoquinol-plastocyanin reductase | -1.141 | | -1.928 | *** | -0.769 | |
| GRMZM5G800780 | Cytochrome b6 | -3.667 | | 0.151 | | 3.879 | |
| GRMZM2G463640 | Cytochrome b6 | -0.874 | | -1.820 | * | -0.917 | |
| GRMZM2G448174 | Cytochrome f | -3.667 | | 1.413 | | 5.144 | |
| GRMZM2G162748 | Ubiquinol cytochrome c reductase | -1.387 | *** | -2.137 | *** | -0.730 | |
| GRMZM2G038365 | Ubiquinol cytochrome c reductase | -1.236 | *** | -2.211 | *** | -0.957 | |
| GRMZM2G094224 | PS I reaction center subunit XI | -1.220 | *** | -2.523 | *** | -1.286 | * |
| GRMZM2G009048 | PS I reaction center subunit N | -1.330 | *** | -2.664 | * | -1.321 | |
| GRMZM2G026015 | PS I reaction center subunit XI | -1.321 | *** | -2.248 | ** | -0.912 | |
| GRMZM2G016622 | PS I reaction center subunit IV | -1.335 | * | -2.108 | NA | -0.759 | |
| GRMZM2G080107 | PS I reaction center subunit N | -1.264 | *** | -2.182 | *** | -0.902 | |
| GRMZM2G451224 | PS I reaction center subunit VI | -1.414 | *** | -2.440 | ** | -1.011 | |
| GRMZM2G016066 | PS I reaction center subunit IV A | -1.319 | ** | -2.449 | *** | -1.115 | |
| GRMZM2G096792 | PS reaction center subunit | -2.504 | | -5.045 | | -2.495 | |
| GRMZM2G320305 | PS II reaction center protein H | -1.857 | ** | -3.166 | *** | -1.261 | |
| GRMZM2G168143 | PS II reaction center protein Z | -0.578 | | -3.901 | * | -3.273 | |
| GRMZM2G059191 | PS II reaction center protein Z | -0.972 | | -2.904 | *** | -1.897 | |
| GRMZM2G011858 | PS II reaction center W protein | -1.321 | ** | -2.232 | *** | -0.895 | |
| GRMZM2G059083 | Ferredoxin-NADP(+) reductase | -2.371 | * | -0.744 | | 1.615 | |
| GRMZM2G058760 | Ferredoxin-NADP(+) reductase | -0.884 | *** | -2.107 | *** | -1.206 | * |
| GRMZM5G831399 | Ferredoxin-NADP(+) reductase | -1.438 | *** | -1.549 | | -0.088 | |
| GRMZM2G394732 | Ferredoxin-NADP(+) reductase | 1.345 | *** | 0.786 | ** | -0.525 | |

| | | | | | | | |
|---|---|---|---|---|---|---|---|
| GRMZM2G414660 | Ferredoxin-NADP(+) reductase | -1.563 | *** | -2.057 | *** | -0.475 | |
| AC190623.3_FG001 | Ferredoxin-NADP(+) reductase | 0.856 | ** | 1.648 | *** | 0.823 | ** |

Asterisks denote whether the difference in gene expression was significant (FDR < 0.001:***, < 0.01:**, < 0.05*).

**Discussion**

Though there have been several previous transcriptomic and metabolomic studies of plant-pathogen interactions, our study of the maize-CCR1 pathosystem is unique in that the key determinant of virulence is a HDAC inhibitor. As HDAC inhibition leads to the accumulation of hyperacetylated histones associated with active gene expression, it is no surprise that the presence of HC-toxin during infection leads to the massive induction of thousands of genes. Gene Ontology (GO) and MapMan analysis of the differentially expressed genes during CCR1 infection revealed an enormous number of biological processes are affected by HC-toxin. Interestingly, KEGG pathway analysis revealed "metabolic pathways" and "biosynthesis of secondary metabolites" to be the most enriched terms for both down- and upregulated DEGs in both the $Tox^-$ CCR1 vs Mock and $Tox^+$ CCR1 vs Mock gene sets, suggesting significant metabolic changes in both the resistant and susceptible interactions.

Analysis of defense genes reveals that although certain key defense genes are downregulated during $Tox^+$ CCR1 infection compared to $Tox^-$ CCR1 infection, the majority of defense response and signaling genes examined are in fact upregulated when HC-toxin is present, clearly disproving the previously-held hypothesis that HC-toxin is globally shutting down defense responses. Upon expanding our analysis to cover additional characterized immune pathways, we found similar trends in that most components were upregulated by $Tox^+$ CCR1 infection. Although many jasmonic acid biosynthesis, signaling, and response genes were weakly upregulated in the resistant interaction, their increased upregulation in the susceptible interaction was surprising as we expected this key necrotroph defense pathway to be suppressed. Interestingly, the oxo-phytodienoate reductase *OPR8* gene actually displays contrasting expression levels in the two interactions (Table 3.2). Since *OPR8*, a key late gene in JA biosynthesis (Yan et al., 2012), is upregulated in the resistant interaction and downregulated in the susceptible interaction, it appears that HC-toxin may be repressing JA biosynthesis to promote susceptibility to the CCR1. However, we did not observe any significantly increased susceptibility to CCR1 when an *opr7opr8* double mutant severely deficient in JA levels but possessing functional *Hm1* was inoculated with the $Tox^+$ strain (Kolomiets, personal communication). This finding suggests that JA does not play an essential role in defense

against CCR1, despite the general upregulation of most JA signaling and response genes in the $Tox^+$ interaction. These results were surprising considering that disruption of proper JA biosynthesis in the *opr7opr8* mutant led to those plants being extremely susceptible to root-rotting *Pythium* necrotrophs in non-sterile soil (Yan et al., 2012). As $Tox^+$ infection also led to upregulation of several genes associated with 9-lipoxygenase-derived defense metabolites (Christensen et al., 2015), it is unlikely that production of these alternative oxylipins are important determinants of resistance to CCR1.

Analysis of ethylene biosynthesis and signaling, thought to work synergistically with JA in mediating necrotroph defense responses, and salicylic acid biosynthesis and signaling, important for mediating defense responses against biotrophs, similarly revealed the upregulation of most genes during the $Tox^+$ interaction. Since SA-mediated defenses and JA/ET-mediated defenses are often mutually antagonistic, the fact that neither immune pathway appears to be clearly repressed is unusual. CCR1 does not appear to be utilizing HC-toxin to repress any specific immune pathway, though there are several cases of pathogen effectors suppressing defense responses by manipulating the host into activating inappropriate responses instead. For example, the pathogen *Pseudomonas syringae* suppresses SA-mediated defenses by producing coronatine, a structural and functional mimic of JA-Ile, in order to misdirect the plant into promoting JA-mediated defense responses (Uppalapati et al., 2007). The role of HC-toxin in promoting virulence, however, appears to be more complex than repression of proper immune responses.

The shikimate pathway, responsible for the production of aromatic amino acids, auxin, salicylic acid, lignin, phenylpropanoids, and other secondary metabolites (Tzin and Galili, 2010; Vogt, 2010), was found to be mostly upregulated more strongly in the $Tox^+$ CCR1 interaction, suggesting increased flux into secondary metabolic pathways. Interestingly, the biosynthetic pathway of benzoxazinoids, metabolites important in defense against insect herbivory and fungal pathogens (Ahmad et al., 2011), generally showed weak downregulation of the core steps leading to DIMBOA-Glc and strong upregulation of the *O*-methyltransferases forming HDMBOA-Glc (and other derivatives) as well as one of the glucosidases responsible for cleaving off the glucose moiety to generate bioactive forms (Handrick et al., 2016). As HDMBOA-Glc often rapidly accumulates in response to biotic stress (Oikawa et al., 2004), the upregulation of these

later steps during $Tox^+$ CCR1 infection was not surprising. Again, inoculation of a *bx1* mutant plant possessing functional *Hm1* with $Tox^+$ CCR1 did not result in increased susceptibility (Johal, unpublished), suggesting that benzoxazinoids also do not play an essential role in CCR1 defense.

Though $Tox^+$ CCR1 infection was found to greatly affect the transcriptional regulation of multiple metabolic pathways, a potentially significant finding was the downregulation of many genes encoding components of the light reactions of photosynthesis. This pattern suggests that HC-toxin may be fundamentally disrupting primary metabolism by interfering with the ability to utilize light energy to power carbon fixation. Interestingly, we previously observed a similar phenomenon with darkness-induced loss of immunity (DILI). Both incubation of maize plants in the dark for an extended period of time and treatment with the photosystem II inhibitor DCMU (3-(3,4-dichlorophenyl)-1,1-dimethylurea) allows $Tox^-$ CCR1 to successfully colonize even normally resistant *Hm1* plants (Marla, 2014). The involvement of photosynthesis in the CCR1 interaction is notable since the light reactions provide a significant source of NADPH, an essential cofactor for the HCTR enzyme responsible for inactivating HC-toxin. This obvious loss of a NADPH source, however, does not completely explain susceptibility since the maize line utilized in this study lacked a functional HCTR and resistance in DCMU-treated plants could be restored by sucrose supplementation. The loss of resistance in these cases is thus likely due to a general lack of energy resulting from inhibition of photosynthesis rather than a specific side effect of inhibition of light reaction components. Though HC-toxin's effects on gene regulation may not be affecting photosynthesis as directly as darkness and DCMU treatment, it must be remembered that HC-toxin's inhibition of HDACs affects the acetylation of multiple nonhistone proteins, including several key metabolic enzymes. Since acetylation can directly alter the catalytic properties of these proteins, it is clear that our observed transcriptional changes provide only a partial picture of the metabolic perturbation induced by HC-toxin. Comparison of the acetylome of $Tox^-$ CCR1 infected plants and $Tox^-$ CCR1 infected plants would shed more light on the nature of metabolic processes affected by HC-toxin. To further investigate the linkage between photosynthesis and CCR1 susceptibility, transcriptomic

and metabolite studies of both dark-incubated and DCMU-treated plants infected with CCR1 should be compared with the results of the current study.

As plant cells undergo a starvation response due to exhaustion of carbohydrate reserves, they will turn to degrading proteins for energy, resulting in the release of free amino acids. The accumulation of valine, leucine, isoleucine, threonine, lysine, tyrosine, phenylalanine, and histidine in response to $Tox^+$ CCR1 infection is indicative of increased protein turnover (Rhodes et al., 1986). The accumulation of α-aminoadipic acid, an intermediate in the lysine catabolic pathway (Miron et al., 2000), offers further evidence for protein degradation. Analysis of the transcriptomic data, however, does not present an obvious general upregulation of protein degradation pathways but instead suggests a complex metabolic situation. Though we found that $Tox^+$ CCR1 infection significantly increases the number of differentially expressed genes involved in ubiquitin-mediated degradation, we observed both down- and upregulation of its various components and the TOR genes, while autophagy gene expression was not found to change much in either the resistant or susceptible interaction. Of the other non-protein amino acids detected, 5-hydroxynorvaline, previously shown to accumulate in maize leaves in response to abiotic stresses and insect herbivory, was observed here to accumulate in response to $Tox^+$ CCR1 infection even though infection with the related maize pathogen *Cochliobolus heterostrophus* had not led to a similar increase (Yan et al., 2015). The non-protein amino acids α-aminobutyric acid (AABA) and β-aminobutyric acid (BABA) have been shown to act as primers for enhanced defense responses (Lotan and Fluhr, 1990; Huang et al., 2011), while γ-aminobutyric acid (GABA), which acts as a neurotransmitter in animals, accumulates rapidly in response to insect feeding, abiotic stresses, and mechanical wounding, due to perturbations of $Ca^{2+}$ levels and cytosolic pH (Huang et al., 2011). It is not surprising that we see their accumulation here during both $Tox^-$ and $Tox^+$ CCR1 infection as many non-protein amino acids have been demonstrated have roles as defense metabolites, either by priming defense responses or by directly inhibiting biosynthetic pathways in pathogens and herbivores upon uptake, sometimes by mis-substituting for proper amino acids during protein synthesis (Huang et al., 2011; Yan et al., 2015). Further experiments quantifying amino acids in maize leaves treated with HC-toxin alone without pathogen are needed to establish that the increased amino acid levels observed in this study

were not simply due to amino acids from the spreading CCR1 pathogen. An untargeted metabolomics analysis would also give us a clearer view of the numerous metabolic perturbations induced by $Tox^+$ CCR1 infection.

We here clearly reveal that rather than promoting virulence by repressing defense responses, HC-toxin causes myriad complex changes in the transcriptional and metabolic status of CCR1-infected tissue. It is still unclear, however, whether or how HC-toxin is targeting specific pathways, and untangling the changes directly wrought by HC-toxin from changes due to the increased biotic stress and cell death of infection may prove challenging. Investigating the effects of HC-toxin treatment without the presence of the CCR1 pathogen may be informative though it is essential to perform a comparative study to determine which of those effects actually assist the pathogenesis of CCR1. Since CCR1 has been demonstrated to be resistant to other HDAC inhibitors chemically unrelated to HC-toxin (Brosch et al., 2001; Baidyaroy et al., 2002), establishing whether these other HDAC inhibitors could also promote virulence to $Tox^-$ CCR1 would provide a better understanding of the actual role of HC-toxin. A discovery that other HDAC inhibitors could indeed induce susceptibility to $Tox^-$ CCR1 would clearly demonstrate that inhibition of host lysine deacetylation leads to a susceptible interaction. Comparative transcriptome, acetylome, and metabolome analysis uncovering common pathway targets may hopefully further clarify HC-toxin's complex roles in the maize-CCR1 pathosystem.

# FUTURE DIRECTIONS

Though our findings offer some additional evidence in support of the hypothesis that compromised HC-toxin reductase activity and developmental changes in the NADPH pool underlie the adult plant resistance phenotype in maize to the pathogen *Cochliobolus carbonum race 1*, they also suggest that NADPH may not be the sole factor behind APR. Since the wild-type HM1 enzyme can utilize NADH as a substrate at a much reduced effectiveness, it would definitely be worthwhile to test whether the APR enzymes displayed any altered affinity for this alternate substrate. In addition, localization studies of both the HCTR enzyme and NADH/NADPH during infection are necessary in order to determine whether differences in kinetic parameters are physiologically relevant. As subcellular NADH and NADPH concentrations within plant cells can be highly compartmentalized, it is vital to know exactly how much NADH/NADPH is actually available for HCTR use. *In planta* localization studies will also answer questions concerning the solubility and stability of the HM1A and HM2 enzymes raised in this study, allowing us to determine whether altered enzyme solubility plays any role in APR. Calculation of the kinetic parameters of the APR enzymes will reveal if their compromised HCTR activities are due to reduced affinity for the NADPH substrate and/or increased affinity for NADH.

While our transcriptomic and metabolic studies of the effects of HC-toxin have shed much light on its mode of action, they also raise some interesting questions. Though we have ruled out the previous hypothesis that HC-toxin acting through repression of defense pathways and have demonstrated the dispensability of jasmonic acid in resistance, further studies involving biosynthetic mutants and/or chemical inhibitors are needed to definitively rule out a key role for the ethylene and salicylic acid pathogen defense pathways. An untargeted metabolite analysis may provide further information on the nature of the metabolic pathways being targeted by HC-toxin as well as identify key defense metabolites. Since $Tox^+$ CCR1 infection appears to downregulate the light reactions of photosynthesis more strongly than $Tox^-$ CCR1 infection, it will be interesting to further investigate the related phenomenon of darkness-induced loss of immunity to CCR1 for transcriptional and metabolic parallels to HC-toxin. Since HC-toxin's inhibition

of HDACs is also expected to affect the acetylation status (and thus catalytic activity) of multiple enzymes involved in primary metabolism, an analysis of the acetylome during disease may uncover additional key metabolic pathways targeted by HC-toxin. Determining whether chemically unrelated HDAC inhibitors can mimic the role of HC-toxin in promoting virulence to $Tox^-$ strains of CCR1 will allow us to definitively conclude that it is HC-toxin's inhibition of lysine deacetylases that leads to disease as well as highlight any specific pathways that HC-toxin may target.

# REFERENCES

Abedon, B.G. and Tracy, W.F. (1996). Corngrass 1 of Maize (Zea mays L.) Delays Development of Adult Plant Resistance to Common Rust (Puccinia sorghi Schw.) and European Corn Borer (Ostrinia nubilalis Hubner). J. Hered. 87: 219–223.

Ahmad, S., Veyrat, N., Gordon-Weeks, R., Zhang, Y., Martin, J., Smart, L., Glauser, G., Erb, M., Flors, V., Frey, M., and Ton, J. (2011). Benzoxazinoid Metabolites Regulate Innate Immunity against Aphids and Fungi in Maize. Plant Physiol. 157: 317–327.

Ahn, J.-H., Cheng, Y.-Q., and Walton, J.D. (2002). An Extended Physical Map of the TOX2 Locus of Cochliobolus carbonum Required for Biosynthesis of HC-Toxin. Fungal Genet. Biol. 35: 31–38.

Anders, S., Pyl, P.T., and Huber, W. (2015). HTSeq - A Python framework to work with high-throughput sequencing data. Bioinformatics 31.

Ando, K., Carr, K.M., Colle, M., Mansfeld, B.N., and Grumet, R. (2015). Exocarp Properties and Transcriptomic Analysis of Cucumber (*Cucumis sativus*) Fruit Expressing Age-Related Resistance to *Phytophthora capsici*. PLoS One 10: e0142133.

Asselbergh, B., Curvers, K., França, S.C., Audenaert, K., Vuylsteke, M., Van Breusegem, F., and Höfte, M. (2007). Resistance to Botrytis cinerea in sitiens, an Abscisic Acid-Deficient Tomato Mutant, Involves Timely Production of Hydrogen Peroxide and Cell Wall Modifications in the Epidermis. Plant Physiol. 144: 1863–1877.

Baidyaroy, D., Brosch, G., Graessle, S., Trojer, P., and Walton, J.D. (2002). Characterization of Inhibitor-Resistant Histone Deacetylase Activity in Plant-Pathogenic Fungi. Eukaryot. Cell 1: 538–547.

Bent, A.F. and Mackey, D. (2007). Elicitors, effectors, and R genes: the new paradigm and a lifetime supply of questions. Annu. Rev. Phytopathol. 45: 399–436.

Berr, A., McCallum, E.J., Alioua, A., Heintz, D., Heitz, T., and Shen, W.-H. (2010). Arabidopsis Histone Methyltransferase SET DOMAIN GROUP8 Mediates Induction of the Jasmonate/Ethylene Pathway Genes in Plant Defense Response to Necrotrophic Fungi. Plant Physiol. 154: 1403–1414.

Bradley, D.J., Kjellbom, P., and Lamb, C.J. (1992). Elicitor- and wound-induced oxidative cross-linking of a proline-rich plant cell wall protein: A novel, rapid defense response. Cell 70: 21–30.

Braun, C.J., Siedow, J.N., and Levings, C.S. (1990). Fungal toxins bind to the URF13 protein in maize mitochondria and Escherichia coli. Plant Cell 2: 153–161.

Brosch, G., Dangl, M., Graessle, S., Loidl, A., Trojer, P., Brandtner, E.-M., Mair, K., Walton, J.D., Baidyaroy, D., and Loidl, P. (2001). An Inhibitor-Resistant Histone Deacetylase in the Plant Pathogenic Fungus Cochliobolus carbonum. Biochemistry 40: 12855–12863.

Brosch, G., Ransom, R., Lechner, T., Walton, J.D., and Loidl, P. (1995). Inhibition of maize histone deacetylases by HC toxin, the host-selective toxin of Cochliobolus carbonum. Plant Cell 7: 1941–1950.

Buchanan, B., Gruissem, W., and Jones, R. eds (2015). Biochemistry and Molecular Biology of Plants 2nd ed. (Wiley).

Carella, P., Wilson, D.C., and Cameron, R.K. (2015). Some things get better with age: differences in salicylic acid accumulation and defense signaling in young and mature Arabidopsis . Front. Plant Sci. 5: 775.

Century, K.S., Lagman, R.A., Adkisson, M., Morlan, J., Tobias, R., Schwartz, K., Smith, A., Love, J., Ronald, P.C., and Whalen, M.C. (1999). Developmental control of Xa21-mediated disease resistance in rice. Plant J. 20: 231–236.

Chen, X., Coram, T., Huang, X., Wang, M., and Dolezal, A. (2013). Understanding Molecular Mechanisms of Durable and Non-durable Resistance to Stripe Rust in Wheat Using a Transcriptomics Approach. Curr. Genomics 14: 111–126.

Chen, X. and Zhou, D.-X. (2013). Rice epigenomics and epigenetics: challenges and opportunities. Curr. Opin. Plant Biol. 16: 164–169.

Chinnusamy, V. and Zhu, J.-K. (2009). Epigenetic regulation of stress responses in plants. Curr. Opin. Plant Biol. 12: 133–139.

Chintamanani, S., Multani, D.S., Ruess, H., and Johal, G.S. (2007). Distinct Mechanisms Govern the Dosage-Dependent and Developmentally Regulated Resistance Conferred by the Maize Hm2 Gene. Mol. Plant-Microbe Interact. 21: 79–86.

Choi, S.-M., Song, H.-R., Han, S.-K., Han, M., Kim, C.-Y., Park, J., Lee, Y.-H., Jeon, J.-S., Noh, Y.-S., and Noh, B. (2012). HDA19 is required for the repression of salicylic acid biosynthesis and salicylic acid-mediated defense responses in Arabidopsis. Plant J. 71: 135–146.

Christensen, S.A. et al. (2015). Maize death acids, 9-lipoxygenase–derived cyclopente(a)nones, display activity as cytotoxic phytoalexins and transcriptional mediators. Proc. Natl. Acad. Sci. 112: 11407–11412.

Coelho, P., Leckie, D., Astley, D., Crute, I.R., Bahcevandziev, K., Valerio, L., Monteiro, A., and Boukema, I. (1998). The relationship between cotyledon and adult plant resistance to downy mildew (Peronospora parasitica) in brassica oleracea. Acta Hortic. 459: 335–342.

Coll, N.S., Epple, P., and Dangl, J.L. (2011). Programmed cell death in the plant immune system. Cell Death Differ. 18: 1247–56.

Comstock, J. and Scheffer, R. (1973). Role of host-selective toxin in colonization of corn leaves by Helminthosporium carbonum. Phytopathology 63: 24–29.

Dehury, B., Sahu, M., Patra, M.C., Sarma, K., Sahu, J., Sen, P., Modi, M.K., Choudhury, M.D., and Barooah, M. (2013). Insights into the structure–function relationship of disease resistance protein HCTR in maize (Zea mays L.): A computational structural biology approach. J. Mol. Graph. Model. 45: 50–64.

Develey-Rivière, M.-P. and Galiana, E. (2007). Resistance to pathogens and host developmental stage: a multifaceted relationship within the plant kingdom. New Phytol. 175: 405–416.

Dhawan, R., Luo, H., Foerster, A.M., AbuQamar, S., Du, H.-N., Briggs, S.D., Scheid, O.M., and Mengiste, T. (2009). HISTONE MONOUBIQUITINATION1 Interacts with a Subunit of the Mediator Complex and Regulates Defense against Necrotrophic Fungal Pathogens in Arabidopsis. Plant Cell 21: 1000–1019.

Ding, B., Bellizzi, M. del R., Ning, Y., Meyers, B.C., and Wang, G.-L. (2012). HDT701, a Histone H4 Deacetylase, Negatively Regulates Plant Innate Immunity by Modulating Histone H4 Acetylation of Defense-Related Genes in Rice. Plant Cell 24: 3783–3794.

Ding, B. and Wang, G.-L. (2015). Chromatin versus pathogens: the function of epigenetics in plant immunity . Front. Plant Sci. 6: 675.

Durrant, W.E. and Dong, X. (2004). Systemic Acquired Resistance. Phytopathology 42: 185–209.

Eberharter, A. and Becker, P.B. (2002). Histone acetylation: a switch between repressive and permissive chromatin. EMBO Rep. 3: 224 LP-229.

Eggermont, K., Goderis, I.J., and Broekaert, W.F. (1996). High-throughput RNA extraction from plant samples based on homogenisation by reciprocal shaking in the presence of a mixture of sand and glass beads. Plant Mol. Biol. Report. 14: 273–279.

Ficke, A., Gadoury, D.M., and Seem, R.C. (2002). Ontogenic Resistance and Plant Disease Management: A Case Study of Grape Powdery Mildew. Phytopathology 92: 671–675.

Ficke, A., Gadoury, D.M., Seem, R.C., and Dry, I.B. (2003). Effects of Ontogenic Resistance upon Establishment and Growth of Uncinula necator on Grape Berries. Phytopathology 93: 556–563.

Finkemeier, I., Laxa, M., Miguet, L., Howden, A.J.M., and Sweetlove, L.J. (2011). Proteins of Diverse Function and Subcellular Location Are Lysine Acetylated in Arabidopsis. Plant Physiol. 155: 1779–1790.

Foyer, C.H. and Noctor, G. (2011). Ascorbate and Glutathione: The Heart of the Redox Hub. Plant Physiol. 155: 2–18.

Fu, D., Uauy, C., Distelfeld, A., Blechl, A., Epstein, L., Chen, X., Sela, H., Fahima, T., and Dubcovsky, J. (2009). A Kinase-START Gene Confers Temperature-Dependent Resistance to Wheat Stripe Rust. Science (80-. ). 323: 1357 LP-1360.

Gao, X., Hong, H., Li, W.-C., Yang, L., Huang, J., Xiao, Y.-L., Chen, X.-Y., and Chen, G.-Y. (2016). Downregulation of Rubisco Activity by Non-enzymatic Acetylation of RbcL. Mol. Plant 9: 1018–1027.

Gendler, K., Paulsen, T., and Napoli, C. (2008). ChromDB: The Chromatin Database. Nucleic Acids Res. 36: D298–D302.

Glazebrook, J. (2005). Contrasting Mechanisms of Defense Against Biotrophic and Necrotrophic Pathogens. Annu. Rev. Phytopathol. 43: 205–227.

Gou, J.-Y. et al. (2015). Wheat Stripe Rust Resistance Protein WKS1 Reduces the Ability of the Thylakoid-Associated Ascorbate Peroxidase to Detoxify Reactive Oxygen Species. Plant Cell 27: 1755–1770.

Govrin, E.M. and Levine, A. (2000). The hypersensitive response facilitates plant infection by the necrotrophic pathogen Botrytis cinerea. Curr. Biol. 10: 751–757.

Gross, M.L., McCrery, D., Crow, F., Tomer, K.B., Pope, M.R., Ciuffetti, L.M., Knoche, H.W., Daly, J.M., and Dunkle, L.D. (1982). The structure of the toxin from Helminthosporium carbonum. Tetrahedron Lett. 23: 5381–5384.

Gusberti, M., Gessler, C., and Broggini, G.A.L. (2013). RNA-Seq Analysis Reveals Candidate Genes for Ontogenic Resistance in *Malus venturia*. Pathosystem. PLoS One 8: e78457.

Gusberti, M., Patocchi, A., Gessler, C., and Broggini, G.A.L. (2012). Quantification of Venturia inaequalis Growth in Malus × domestica with Quantitative Real-Time Polymerase Chain Reaction. Plant Dis. 96: 1791–1797.

Gutzat, R. and Mittelsten Scheid, O. (2012). Epigenetic responses to stress: triple defense? Curr. Opin. Plant Biol. 15: 568–573.

Han, F., Kleinhofs, A., Kilian, A., and Ullrich, S.E. (1997). Cloning and Mapping of a Putative Barley NADPH-Dependent HC-Toxin Reductase. Mol. Plant-Microbe Interact. 10: 234–239.

Handrick, V. et al. (2016). Biosynthesis of 8-O-Methylated Benzoxazinoid Defense Compounds in Maize. Plant Cell 28: 1682–1700.

Hao, Y., Wang, H., Qiao, S., Leng, L., and Wang, X. (2016a). Histone deacetylase HDA6 enhances brassinosteroid signaling by inhibiting the BIN2 kinase. Proc. Natl. Acad. Sci. 113: 10418–10423.

Hao, Y., Wang, T., Wang, K., Wang, X., Fu, Y., Huang, L., and Kang, Z. (2016b). Transcriptome Analysis Provides Insights into the Mechanisms Underlying Wheat Plant Resistance to Stripe Rust at the Adult Plant Stage. PLoS One 11: e0150717.

Hawkins, L.K., Mylroie, J.E., Oliveira, D.A., Smith, J.S., Ozkan, S., Windham, G.L., Williams, W.P., and Warburton, M.L. (2015). Characterization of the Maize Chitinase Genes and Their Effect on *Aspergillus flavus* and Aflatoxin Accumulation Resistance. PLoS One 10: e0126185.

Hayashi, M., Takahashi, H., Tamura, K., Huang, J., Yu, L.-H., Kawai-Yamada, M., Tezuka, T., and Uchimiya, H. (2005). Enhanced dihydroflavonol-4-reductase activity and NAD homeostasis leading to cell death tolerance in transgenic rice. Proc. Natl. Acad. Sci. United States Am. 102: 7020–7025.

Heber, U. and Santarius, K. (1965). Compartmentation and reduction of pyridine nucleotides in relation to photosynthesis. Biochim. Biophys. Acta - Bioenerg. 109: 390–408.

Heineke, D., Riens, B., Grosse, H., Hoferichter, P., Peter, U., Flügge, U.-I., and Heldt, H.W. (1991). Redox Transfer across the Inner Chloroplast Envelope Membrane. Plant Physiol. 95: 1131–1137.

Herrera-Foessel, S.A., Singh, R.P., Lillemo, M., Huerta-Espino, J., Bhavani, S., Singh, S., Lan, C., Calvo-Salazar, V., and Lagudah, E.S. (2014). Lr67/Yr46 confers adult plant resistance to stem rust and powdery mildew in wheat. Theor. Appl. Genet. 127: 781–789.

Hodges, M. (2002). Enzyme redundancy and the importance of 2-oxoglutarate in plant ammonium assimilation. J. Exp. Bot. 53: 905–916.

Hoefnagel, M.H.N., Atkin, O.K., and Wiskich, J.T. (1998). Interdependence between chloroplasts and mitochondria in the light and the dark. Biochim. Biophys. Acta - Bioenerg. 1366: 235–255.

Huang, T., Jander, G., and de Vos, M. (2011). Non-protein amino acids in plant defense against insect herbivores: Representative cases and opportunities for further functional analysis. Phytochemistry 72: 1531–1537.

Huffaker, A., Dafoe, N.J., and Schmelz, E.A. (2011). ZmPep1, an Ortholog of Arabidopsis Elicitor Peptide 1, Regulates Maize Innate Immunity and Enhances Disease Resistance. Plant Physiol. 155: 1325–1338.

Huot, B., Yao, J., Montgomery, B.L., and He, S.Y. (2014). Growth-Defense Tradeoffs in Plants: A Balancing Act to Optimize Fitness. Mol. Plant 7: 1267–1287.

Hutchings, D., Rawsthorne, S., and Emes, M.J. (2005). Fatty acid synthesis and the oxidative pentose phosphate pathway in developing embryos of oilseed rape (Brassica napus L.). J. Exp. Bot. 56: 577–585.

Igamberdiev, A.U. and Gardeström, P. (2003). Regulation of NAD- and NADP-dependent isocitrate dehydrogenases by reduction levels of pyridine nucleotides in mitochondria and cytosol of pea leaves. Biochim. Biophys. Acta - Bioenerg. 1606: 117–125.

Jaskiewicz, M., Conrath, U., and Peterhänsel, C. (2010). Chromatin modification acts as a memory for systemic acquired resistance in the plant stress response. EMBO Rep. 12: 50 LP-55.

Johal, G.S. and Briggs, S.P. (1992). Reductase activity encoded by the HM1 disease resistance gene in maize. Science (80-. ). 258: 985 LP-987.

Jones, I. (1975). The preconditioning effect of day-length and light intensity on adult plant resistance to powdery mildew in oats. Ann. Appl. Biol. 80: 301–309.

Jones, J.D.G. and Dangl, J.L. (2006). The plant immune system. Nature 444: 323–329.

Jones, M. and Dunkle, L. (1993). Analysis of Cochliobolus carbonum Races by PCR Amplification with Arbitrary and Gene-Specific Primers. Mol. Plant Pathol. 83: 366–370.

Kalt-Torres, W., Kerr, P.S., Usuda, H., and Huber, S.C. (1987). Diurnal Changes in Maize Leaf Photosynthesis: I. Carbon Exchange Rate, Assimilate Export Rate, and Enzyme Activities . Plant Physiol. 83: 283–288.

Kaminaga, Y. et al. (2006). Plant Phenylacetaldehyde Synthase Is a Bifunctional Homotetrameric Enzyme That Catalyzes Phenylalanine Decarboxylation and Oxidation. J. Biol. Chem. 281: 23357–23366.

Kelly, G.J. and Gibbs, M. (1973). A Mechanism for the Indirect Transfer of Photosynthetically Reduced Nicotinamide Adenine Dinucleotide Phosphate from Chloroplasts to the Cytoplasm. Plant Physiol. 52: 674–676.

Khan, O. and La Thangue, N.B. (2012). HDAC inhibitors in cancer biology: emerging mechanisms and clinical applications. Immunol Cell Biol 90: 85–94.

Klittich, C. and Bronson, C. (1986). Reduced fitness associated with TOX1 of Cochliobolus heterostrophus. Phytopathology 76: 1294–1298.

Kocsy, G., Tari, I., Vanková, R., Zechmann, B., Gulyás, Z., Poór, P., and Galiba, G. (2013). Redox control of plant growth and development. Plant Sci. 211: 77–91.

Kono, Y. and Daly, J.M. (1979). Characterization of the host-specific pathotoxin produced by Helminthosporium maydis, race T, affecting corn with Texas male sterile cytoplasm. Bioorg. Chem. 8: 391–397.

Kotchoni, S.O. and Gachomo, E.W. (2006). The reactive oxygen species network pathways: an essential prerequisite for perception of pathogen attack and the acquired disease resistance in plants. J. Biosci. 31: 389–404.

Kouzarides, T. (2007). Chromatin Modifications and Their Function. Cell 128: 693–705.

Krattinger, S.G., Lagudah, E.S., Spielmeyer, W., Singh, R.P., Huerta-Espino, J., McFadden, H., Bossolini, E., Selter, L.L., and Keller, B. (2009). A Putative ABC Transporter Confers Durable Resistance to Multiple Fungal Pathogens in Wheat. Science (80-. ). 323: 1360 LP-1363.

Kruger, N.J. and von Schaewen, A. (2003). The oxidative pentose phosphate pathway: structure and organisation. Curr. Opin. Plant Biol. 6: 236–246.

Kus, J. V, Zaton, K., Sarkar, R., and Cameron, R.K. (2002). Age-Related Resistance in Arabidopsis Is a Developmentally Regulated Defense Response to Pseudomonas syringae. Plant Cell 14: 479–490.

L'Haridon, F., Besson-Bard, A., Binda, M., Serrano, M., Abou-Mansour, E., Balet, F., Schoonbeek, H.-J., Hess, S., Mir, R., Léon, J., Lamotte, O., and Métraux, J.-P. (2011). A Permeable Cuticle Is Associated with the Release of Reactive Oxygen Species and Induction of Innate Immunity. PLoS Pathog 7: e1002148.

Lagacé, M., Chantha, S.-C., Major, G., and Matton, D.P. (2003). Fertilization induces strong accumulation of a histone deacetylase (HD2) and of other chromatin-remodeling proteins in restricted areas of the ovules. Plant Mol. Biol. 53: 759–769.

Laluk, K. and Mengiste, T. (2010). Necrotroph Attacks on Plants: Wanton Destruction or Covert Extortion? Arabidopsis Book 8: e0136.

Langmead, B. and Salzberg, S.L. (2012). Fast gapped-read alignment with Bowtie 2. Nat Meth 9: 357–359.

Levy, D. and Lapidot, M. (2007). Effect of plant age at inoculation on expression of genetic resistance to tomato yellow leaf curl virus. Arch. Virol. 153: 171–179.

Li, W.-Y., Wang, X., Li, R., Li, W.-Q., and Chen, K.-M. (2014). Genome-Wide Analysis of the NADK Gene Family in Plants. PLoS One 9: e101051.

Liesch, J.M., Sweeley, C.C., Staffeld, G.D., Anderson, M.S., Weber, D.J., and Scheffer, R.P. (1982). Structure of HC-toxin, a cyclic tetrapeptide from Helminthosporium carbonum. Tetrahedron 38: 45–48.

Litzenberger, S. (1949). Nature of susceptibility to Helminthosporium victoriae and resistance to Puccinia coronata in Victoria oats. Phytopathology 300: 300–318.

Liu, B., Berr, A., Chang, C., Liu, C., Shen, W.-H., and Ruan, Y. (2016). Interplay of the histone methyltransferases SDG8 and SDG26 in the regulation of transcription and plant flowering and development. Biochim. Biophys. Acta - Gene Regul. Mech. 1859: 581–590.

Liu, T., Kuljaca, S., Tee, A., and Marshall, G.M. (2006). Histone deacetylase inhibitors: Multifunctional anticancer agents. Cancer Treat. Rev. 32: 157–165.

Liu, Y., Koornneef, M., and Soppe, W.J.J. (2007). The Absence of Histone H2B Monoubiquitination in the Arabidopsis hub1 (rdo4) Mutant Reveals a Role for Chromatin Remodeling in Seed Dormancy. Plant Cell 19: 433–444.

Lorang, J.M., Carkaci-Salli, N., and Wolpert, T.J. (2004). Identification and Characterization of Victorin Sensitivity in Arabidopsis thaliana. Mol. Plant-Microbe Interact. 17: 577–582.

Lotan, T. and Fluhr, R. (1990). Xylanase, a Novel Elicitor of Pathogenesis-Related Proteins in Tobacco, Uses a Non-Ethylene Pathway for Induction. Plant Physiol. 93: 811–817.

Love, M.I., Huber, W., and Anders, S. (2014). Moderated estimation of fold change and dispersion for RNA-seq data with DESeq2. Genome Biol. 15: 550.

Luger, K., Mader, A.W., Richmond, R.K., Sargent, D.F., and Richmond, T.J. (1997). Crystal structure of the nucleosome core particle at 2.8 A resolution. Nature 389: 251–260.

Luke, H., Murphy, H., and Petr, F. (1966). Inheritance of spontaneous mutations of the Victoria locus in oats. Phytopathology 56: 210–212.

Luna, E., Bruce, T.J.A., Roberts, M.R., Flors, V., and Ton, J. (2012). Next-Generation Systemic Acquired Resistance. Plant Physiol. 158: 844–853.

Ma, X., Lv, S., Zhang, C., and Yang, C. (2013). Histone deacetylases and their functions in plants. Plant Cell Rep. 32: 465–478.

Manamgoda, D.S., Cai, L., Bahkali, A.H., Chukeatirote, E., and Hyde, K.D. (2011). Cochliobolus: an overview and current status of species. Fungal Divers. 51: 3–42.

Marino, D., Dunand, C., Puppo, A., and Pauly, N. (2012). A burst of plant NADPH oxidases. Trends Plant Sci. 17: 9–15.

Marla, S. (2014). Characterization of adult plant resistance in the maize-Cochliobolus carbonum race 1 pathosystem revealed a close connection between plant immunity and metabolism. ProQuest Diss. Publ.

Mayama, S., Bordin, A.P.A., Morikawa, T., Tanpo, H., and Kato, H. (1995). Association of avenalumin accumulation with co-segregation of victorin sensitivity and crown rust resistance in oat lines carrying the Pc-2 gene. Physiol. Mol. Plant Pathol. 46: 263–274.

McDowell, J.M., Williams, S.G., Funderburg, N.T., Eulgem, T., and Dangl, J.L. (2005). Genetic Analysis of Developmentally Regulated Resistance to Downy Mildew (Hyaloperonospora parasitica) in Arabidopsis thaliana. Mol. Plant-Microbe Interact. 18: 1226–1234.

Meehan, F. and Murphy, H.C. (1946). A New Helminthosporium Blight of Oats. Science (80-. ). 104: 413.

Meeley, R.B., Johal, G.S., Briggs, S.P., and Walton, J.D. (1992). A Biochemical Phenotype for a Disease Resistance Gene of Maize. Plant Cell 4: 71–77.

Meeley, R.B. and Walton, J.D. (1991). Enzymatic Detoxification of HC-toxin, the Host-Selective Cyclic Peptide from Cochliobolus carbonum . Plant Physiol. 97: 1080–1086.

Mendgen, K. and Hahn, M. (2002). Plant infection and the establishment of fungal biotrophy. Trends Plant Sci. 7: 352–356.

Mengiste, T. (2011). Plant Immunity to Necrotrophs. Annu. Rev. Phytopathol. 50: 267–294.

Michelet, L., Zaffagnini, M., Morisse, S., Sparla, F., Pérez-Pérez, M.E., Francia, F., Danon, A., Marchand, C., Fermani, S., Trost, P., and Lemaire, S. (2013). Redox regulation of the Calvin–Benson cycle: something old, something new . Front. Plant Sci. 4: 470.

Miller, G., Schlauch, K., Tam, R., Cortes, D., Torres, M.A., Shulaev, V., Dangl, J.L., and Mittler, R. (2009). The Plant NADPH Oxidase RBOHD Mediates Rapid Systemic Signaling in Response to Diverse Stimuli. Sci. Signal. 2: ra45 LP-ra45.

Miron, D., Ben-Yaacov, S., Reches, D., Schupper, A., and Galili, G. (2000). Purification and Characterization of Bifunctional Lysine-Ketoglutarate Reductase/Saccharopine Dehydrogenase from Developing Soybean Seeds. Plant Physiol. 123: 655–664.

Moore, J.W. et al. (2015). A recently evolved hexose transporter variant confers resistance to multiple pathogens in wheat. Nat Genet 47: 1494–1498.

Moore, J.W., Loake, G.J., and Spoel, S.H. (2011). Transcription Dynamics in Plant Immunity. Plant Cell 23: 2809–2820.

Mou, Z., Fan, W., and Dong, X. (2003). Inducers of Plant Systemic Acquired Resistance Regulate NPR1 Function through Redox Changes. Cell 113: 935–944.

Multani, D.S., Meeley, R.B., Paterson, A.H., Gray, J., Briggs, S.P., and Johal, G.S. (1998). Plant–pathogen microevolution: Molecular basis for the origin of a fungal disease in maize. Proc. Natl. Acad. Sci. 95: 1686–1691.

Mur, L.A.J., Kenton, P., Atzorn, R., Miersch, O., and Wasternack, C. (2006). The Outcomes of Concentration-Specific Interactions between Salicylate and Jasmonate Signaling Include Synergy, Antagonism, and Oxidative Stress Leading to Cell Death. Plant Physiol. 140: 249–262.

Nee, G., Aumont-Nicaise, M., Zaffagnini, M., Nessler, S., Valerio-Lepiniec, M., and Issakidis-Bourguet, E. (2013). Redox regulation of chloroplastic G6PDH activity by TRX occurs through structural changes modifying substrate accessibility and co-factor binding. Biochem J 125: 117–125.

Nelson, D. and Cox, M. (2005). Lehninger Principles of Biochemistry 4th ed. (W. H. Freeman: New York).

Nelson, O. and Ullstrup, A. (1964). Resistance to leaf spot in maize: Genetic control of resistance to race I of Helminthosporium carbonum. J. Hered. 55: 195–200.

Nguyen, H.N., Kim, J.H., Jeong, C.Y., Hong, S.-W., and Lee, H. (2013). Inhibition of histone deacetylation alters Arabidopsis root growth in response to auxin via PIN1 degradation. Plant Cell Rep. 32: 1625–1636.

Noctor, G. (2006). Metabolic signalling in defence and stress: the central roles of soluble redox couples. Plant. Cell Environ. 29: 409–425.

Norvell, A. and McMahon, S.B. (2010). Rise of the Rival. Science (80-. ). 327: 964 LP-965.

Oikawa, A., Ishihara, A., Tanaka, C., Mori, N., Tsuda, M., and Iwamura, H. (2004). Accumulation of HDMBOA-Glc is induced by biotic stresses prior to the release of MBOA in maize leaves. Phytochemistry 65: 2995–3001.

Oliveros, J.C. (2015). Venny: An interactive tool for comparing lists with Venn diagrams.

Panter, S.N., Hammond-Kosack, K.E., Harrison, K., Jones, J.D.G., and Jones, D.A. (2002). Developmental Control of Promoter Activity Is Not Responsible for Mature Onset of Cf-9B-Mediated Resistance to Leaf Mold in Tomato. Mol. Plant-Microbe Interact. 15: 1099–1107.

Pecinka, A. and Mittelsten Scheid, O. (2012). Stress-Induced Chromatin Changes: A Critical View on Their Heritability. Plant Cell Physiol. 53: 801–808.

Peng, H., Chen, Z., Fang, Z., Zhou, J., Xia, Z., Gao, L., Chen, L., Li, L., Li, T., Zhai, W., and Zhang, W. (2015). Rice Xa21 primed genes and pathways that are critical for combating bacterial blight infection. Sci. Rep. 5: 12165.

Peries, O. (1962). Studies on strawberry mildew, caused by Sphaerotheca macularis (Wallr. ex Fries) Jaczewski - II. Host-parasite relationships on foliage of strawberry varieties. Ann. Appl. Biol. 50: 225–233.

Pétriacq, P., de Bont, L., Tcherkez, G., and Gakière, B. (2013). NAD: Not just a pawn on the board of plant-pathogen interactions. Plant Signal. Behav. 8: e22477.

Pétriacq, P., Ton, J., Patrit, O., tcherkez, guillaume g. b., and GAKIERE, B. (2016). NAD acts as an integral regulator of multiple defense layers. Plant Physiol. .

Petrov, V.D. and Van Breusegem, F. (2012). Hydrogen peroxide—a central hub for information flow in plant cells. AoB Plants 2012.

Pieterse, C.M.J., Leon-Reyes, A., Van der Ent, S., and Van Wees, S.C.M. (2009). Networking by small-molecule hormones in plant immunity. Nat Chem Biol 5: 308–316.

Pogány, M., von Rad, U., Grün, S., Dongó, A., Pintye, A., Simoneau, P., Bahnweg, G., Kiss, L., Barna, B., and Durner, J. (2009). Dual Roles of Reactive Oxygen Species and NADPH Oxidase RBOHD in an Arabidopsis-Alternaria Pathosystem. Plant Physiol. 151: 1459–1475.

Pretorius, Z.A., PienaarA, L., and Prins, R. (2007). Greenhouse and field assessment of adult plant resistance in wheat to Puccinia striiformis f. sp. tritici. Australas. Plant Pathol. 36: 552–559.

Queval, G. and Noctor, G. (2007). A plate reader method for the measurement of NAD, NADP, glutathione, and ascorbate in tissue extracts: Application to redox profiling during Arabidopsis rosette development. Anal. Biochem. 363: 58–69.

Ransom, R.F. and Walton, J.D. (1997). Histone Hyperacetylation in Maize in Response to Treatment with HC-Toxin or Infection by the Filamentous Fungus Cochliobolus carbonum. Plant Physiol. 115: 1021–1027.

Rasmussen, J.B. and Scheffer, R.P. (1988). Isolation and Biological Activities of Four Selective Toxins from Helminthosporium carbonum. Plant Physiol. 86: 187–191.

Rasmusson, A.G. and Wallström, S.V. (2010). Involvement of mitochondria in the control of plant cell NAD(P)H reduction levels. Biochem. Soc. Trans. 38: 661 LP-666.

Reimer-Michalski, E.-M. and Conrath, U. (2016). Innate immune memory in plants. Semin. Immunol. 28: 319–327.

Rhoads, D., Levings, C. 3rd, and Siedow, J. (1995). URF13, a ligand-gated, pore-forming receptor for T-toxin in the inner membrane of cms-T mitochondria. J. Bioenerg. Biomembr. 27: 437–445.

Rhodes, D., Deal, L., Haworth, P., Jamieson, G.C., Reuter, C.C., and Ericson, M.C. (1986). Amino Acid Metabolism of Lemna minor L.: I. Responses to Methionine Sulfoximine . Plant Physiol. 82: 1057–1062.

Rinaldo, A., Gilbert, B., Boni, R., Krattinger, S.G., Singh, D., Park, R.F., Lagudah, E., and Ayliffe, M. (2016). The Lr34 adult plant rust resistance gene provides seedling resistance in durum wheat without senescence. Plant Biotechnol. J.: n/a-n/a.

Rines, H. and Luke, H. (1985). Selection and regeneration of toxin-insensitive plants from tissue cultures of oats (Avena sativa) susceptible to Helminthosporium victoriae. Theor. Appl. Genet. 71: 16.

Rius, S.P., Casati, P., Iglesias, A.A., and Gomez-Casati, D.F. (2006). Characterization of an Arabidopsis thaliana mutant lacking a cytosolic non-phosphorylating glyceraldehyde-3-phosphate dehydrogenase. Plant Mol. Biol. 61: 945–957.

Schaaf, J., Walter, M.H., and Hess, D. (1995). Primary Metabolism in Plant Defense (Regulation of a Bean Malic Enzyme Gene Promoter in Transgenic Tobacco by Developmental and Environmental Cues). Plant Physiol. 108: 949–960.

Scheffer, R., Nelson, R., and Ullstrup, A. (1967). Inheritance of toxin production and pathogenicity in Cochliobolus carbonum and Cochliobolus victoriae. Phytopathology 57: 1288–1291.

Scheffer, R. and Ullstrup, A. (1965). Host-specific toxic metabolite from Helminthosporium carbonum. Phytopathology 55: 1037–1038.

Servet, C., Conde e Silva, N., and Zhou, D.-X. (2010). Histone Acetyltransferase AtGCN5/HAG1 Is a Versatile Regulator of Developmental and Inducible Gene Expression in Arabidopsis. Mol. Plant 3: 670–677.

Shao, Z.-Q., Xue, J.-Y., Wu, P., Zhang, Y.-M., Wu, Y., Hang, Y.-Y., Wang, B., and Chen, J.-Q. (2016). Large-Scale Analyses of Angiosperm Nucleotide-Binding Site-Leucine-Rich Repeat Genes Reveal Three Anciently Diverged Classes with Distinct Evolutionary Patterns. Plant Physiol. 170: 2095–2109.

Shen, Y., Issakidis-Bourguet, E., and Zhou, D.-X. (2016). Perspectives on the interactions between metabolism, redox, and epigenetics in plants. J. Exp. Bot. 67: 5291–5300.

Shen, Y., Wei, W., and Zhou, D.-X. (2015). Histone Acetylation Enzymes Coordinate Metabolism and Gene Expression. Trends Plant Sci. 20: 614–621.

Shi, F., Li, Y., Li, Y., and Wang, X. (2009). Molecular properties, functions, and potential applications of NAD kinases. Acta Biochim. Biophys. Sin. 41: 352–361.

Shilatifard, A. (2006). Chromatin Modifications by Methylation and Ubiquitination: Implications in the Regulation of Gene Expression. Annu. Rev. Biochem. 75: 243–269.

Sindhu, A., Chintamanani, S., Brandt, A.S., Zanis, M., Scofield, S.R., and Johal, G.S. (2008). A guardian of grasses: Specific origin and conservation of a unique disease-resistance gene in the grass lineage. Proc. Natl. Acad. Sci. 105: 1762–1767.

Singh, R.P., Huerta-Espino, J., Bhavani, S., Herrera-Foessel, S.A., Singh, D., Singh, P.K., Velu, G., Mason, R.E., Jin, Y., Njau, P., and Crossa, J. (2011). Race non-specific resistance to rust diseases in CIMMYT spring wheats. Euphytica 179: 175–186.

Slaughter, A., Daniel, X., Flors, V., Luna, E., Hohn, B., and Mauch-Mani, B. (2012). Descendants of Primed Arabidopsis Plants Exhibit Resistance to Biotic Stress. Plant Physiol. 158: 835–843.

Smith, D., Hooker, A., and Lim, S. (1970). Physiological races of Helminthosporium maydis. Plant Dis. Report. 54: 819–822.

Song, G. and Walley, J.W. (2016). Dynamic Protein Acetylation in Plant–Pathogen Interactions . Front. Plant Sci. 7: 421.

Song, W.Y., Wang, G.L., Chen, L.L., Kim, H.S., Pi, L.Y., Holsten, T., Gardner, J., Wang, B., Zhai, W.X., Zhu, L.H., Fauquet, C., and Ronald, P. (1995). A receptor kinase-like protein encoded by the rice disease resistance gene, Xa21. Science (80-. ). 270: 1804–1806.

Spielbauer, G., Li, L., Römisch-Margl, L., Do, P.T., Fouquet, R., Fernie, A.R., Eisenreich, W., Gierl, A., and Settles, A.M. (2013). Chloroplast-localized 6-phosphogluconate dehydrogenase is critical for maize endosperm starch accumulation. J. Exp. Bot. 64: 2231–2242.

Stone, J. (2001). Necrotroph. In Encyclopedia of Plant Pathology, Vol. 2, O. Maloy and T. Murray, eds (Wiley: New York), pp. 676–677.

Tada, Y., Spoel, S.H., Pajerowska-Mukhtar, K., Mou, Z., Song, J., Wang, C., Zuo, J., and Dong, X. (2008). Plant Immunity Requires Conformational Charges of NPR1 via S-Nitrosylation and Thioredoxins. Science (80-. ). 321: 952 LP-956.

Tatum, L.A. (1971). The Southern Corn Leaf Blight Epidemic. Science (80-. ). 173: 39.

Temme, N. and Tudzynski, P. (2009). Does Botrytis cinerea Ignore H2O2-Induced Oxidative Stress During Infection? Characterization of Botrytis Activator Protein 1. Mol. Plant-Microbe Interact. 22: 987–998.

Torres, M.A., Jones, J.D.G., and Dangl, J.L. (2005). Pathogen-induced, NADPH oxidase-derived reactive oxygen intermediates suppress spread of cell death in Arabidopsis thaliana. Nat Genet 37: 1130–1134.

Torres, M.A., Jones, J.D.G., and Dangl, J.L. (2006). Reactive Oxygen Species Signaling in Response to Pathogens. Plant Physiol. 141: 373–378.

Trabelsi, N., D'Estaintot, B., Sigaud, G., Gallois, B., and Chaudière, J. (2011). Kinetic and binding equilibrium studies of dihydroflavonol 4-reductase from Vitis vinifera and its unusually strong substrate inhibition. J. Biophys. Chem. 2: 332–344.

Turner, W.L., Waller, J.C., Vanderbeld, B., and Snedden, W.A. (2004). Cloning and Characterization of Two NAD Kinases from Arabidopsis. Identification of a Calmodulin Binding Isoform. Plant Physiol. 135: 1243–1255.

Tzin, V. and Galili, G. (2010). The Biosynthetic Pathways for Shikimate and Aromatic Amino Acids in Arabidopsis thaliana. Arab. B.: e0132.

Ullstrup, A. (1944). Further studies on a species of Helminthosporium parasitizing corn. Phytopathology 34: 214–222.

Ullstrup, A. (1941). Two physiologic races of Helminthosporium maydis in the corn belt. Phytopathology 31: 508–521.

Ullstrup, A.J. (1972). The Impacts of the Southern Corn Leaf Blight Epidemics of 1970-1971. Annu. Rev. Phytopathol. 10: 37–50.

Uppalapati, S.R., Ishiga, Y., Wangdi, T., Kunkel, B.N., Anand, A., Mysore, K.S., and Bender, C.L. (2007). The Phytotoxin Coronatine Contributes to Pathogen Fitness and Is Required for Suppression of Salicylic Acid Accumulation in Tomato Inoculated with Pseudomonas syringae pv. tomato DC3000. Mol. Plant-Microbe Interact. 20: 955–965.

Usadel, B. et al. (2005). Extension of the Visualization Tool MapMan to Allow Statistical Analysis of Arrays, Display of Coresponding Genes, and Comparison with Known Responses. Plant Physiol. 138: 1195–1204.

Usadel, B., Poree, F., Nagel, A., Lohse, M., Czedik-Eysenberg, A., and Sti, M. (2009). A guide to using MapMan to visualize and compare Omics data in plants: a case study in the crop species, Maize. Plant. Cell Environ. 32: 1211–1229.

Usuda, H. (1988). Adenine Nucleotide Levels, the Redox State of the NADP System, and Assimilatory Force in Nonaqueously Purified Mesophyll Chloroplasts from Maize Leaves under Different Light Intensities. Plant Physiol. 88: 1461–1468.

Valsangiacomo, C. and Gessler, C. (1988). Role of the cuticular membrane in ontogenic and Vf-resistance of apple leaves against Venturia inaequalis. Phytopathology: 1066–1069.

Vogt, T. (2010). Phenylpropanoid Biosynthesis. Mol. Plant 3: 2–20.

Waller, J.C., Dhanoa, P.K., Schumann, U., Mullen, R.T., and Snedden, W.A. (2009). Subcellular and tissue localization of NAD kinases from Arabidopsis: compartmentalization of de novo NADP biosynthesis. Planta 231: 305–317.

Walley, J.W., Rowe, H.C., Xiao, Y., Chehab, E.W., Kliebenstein, D.J., Wagner, D., and Dehesh, K. (2008). The Chromatin Remodeler SPLAYED Regulates Specific Stress Signaling Pathways. PLoS Pathog 4: e1000237.

Walton, J.D. (2006). HC-toxin. Phytochemistry 67: 1406–1413.

Walton, J.D. (1996). Host-selective toxins: agents of compatibility. Plant Cell 8: 1723–1733.

Walton, J.D., Earle, E.D., and Gibson, B.W. (1982). Purification and structure of the host-specific toxin from Helminthosporiumcarbonum race 1. Biochem. Biophys. Res. Commun. 107: 785–794.

Walton, J.D., Ransom, R., and Pitkin, J.W. (1997). Northern Corn Leaf Spot: Chemistry, Enzymology, and Molecular Genetics of a Host-Selective Phytotoxin. In Plant-Microbe Interactions, G. Stacey and N.T. Keen, eds (Springer US: Boston, MA), pp. 94–123.

Wang, C., Zhang, X., and Mou, Z. (2016). Comparison of nicotinamide adenine dinucleotide phosphate-induced immune responses against biotrophic and necrotrophic pathogens in Arabidopsis thaliana. Plant Signal. Behav. 11: e1169358.

Wang, Q. et al. (2010). Acetylation of Metabolic Enzymes Coordinates Carbon Source Utilization and Metabolic Flux. Science (80-. ). 327: 1004–1007.

Wigge, B., Krömer, S., and Gardeström, P. (1993). The redox levels and subcellular distribution of pyridine nucleotides in illuminated barley leaf protoplasts studied by rapid fractionation. Physiol. Plant. 88: 10–18.

Wight, W.D., Kim, K.-H., Lawrence, C.B., and Walton, J.D. (2009). Biosynthesis and Role in Virulence of the Histone Deacetylase Inhibitor Depudecin from Alternaria brassicicola. Mol. Plant-Microbe Interact. 22: 1258–1267.

Wight, W.D., Labuda, R., and Walton, J.D. (2013). Conservation of the genes for HC-toxin biosynthesis in Alternaria jesenskae. BMC Microbiol. 13: 1–11.

Williams, B., Kabbage, M., Kim, H.-J., Britt, R., and Dickman, M.B. (2011). Tipping the Balance: *Sclerotinia sclerotiorum* Secreted Oxalic Acid Suppresses Host Defenses by Manipulating the Host Redox Environment. PLoS Pathog 7: e1002107.

Wolpert, T.J., Dunkle, L.D., and Ciuffetti, L.M. (2002). HOST-SELECTIVE TOXINS AND AVIRULENCE DETERMINANTS: What's in a Name? Annu. Rev. Phytopathol. 40: 251–285.

Wolpert, T.J., Macko, V., Acklin, W., Jaun, B., Seibl, J., Meili, J., and Arigoni, D. (1985). Structure of victorin C, the major host-selective toxin from Cochliobolus victoriae. Experientia 41: 1524–1529.

Xiong, Y., Peng, X., Cheng, Z., Liu, W., and Wang, G.-L. (2016). A comprehensive catalog of the lysine-acetylation targets in rice (Oryza sativa) based on proteomic analyses. J. Proteomics 138: 20–29.

Xu, L., Zhao, Z., Dong, A., Soubigou-Taconnat, L., Renou, J.P., Steinmetz, A., and Shen, W.H. (2008). Di- and tri- but not monomethylation on histone H3 lysine 36 marks active transcription of genes involved in flowering time regulation and other processes in Arabidopsis thaliana. Mol Cell Biol 28.

Yan, J., Lipka, A.E., Schmelz, E.A., Buckler, E.S., and Jander, G. (2015). Accumulation of 5-hydroxynorvaline in maize (Zea mays) leaves is induced by insect feeding and abiotic stress. J. Exp. Bot. 66: 593–602.

Yan, Y., Christensen, S., Isakeit, T., Engelberth, J., Meeley, R., Hayward, A., Emery, R.J.N., and Kolomiets, M. V (2012). Disruption of OPR7 and OPR8 Reveals the Versatile Functions of Jasmonic Acid in Maize Development and Defense. Plant Cell 24: 1420–1436.

Yang, F., Zhang, Y., Huang, Q., Yin, G., Pennerman, K.K., Yu, J., Liu, Z., Li, D., and Guo, A. (2015). Analysis of key genes of jasmonic acid mediated signal pathway for defense against insect damages by comparative transcriptome sequencing. Sci. Rep. 5: 16500.

Yoder, O. and Gracen, V. (1975). Segregation of pathogenicity types and host-specific toxin production in progenies of crosses between races T and O of Helminthosporium maydis (Cochliobolus heterostrophus). Phytopathology 65: 273–276.

Yoshida, H. and Sugita, K. (1992). A novel tetracyclic peptide, trapoxin, induces phenotypic change from transformed to normal in sis-oncogene-transformed NIH3T3 cells. Japanese J. Cancer Res. 83: 324–328.

Young, H. (2008). The mode of action of HC-toxin, a disease determinant of the maize pathogen Cochliobolus carbonum race 1.

Zechmann, B. (2014). Compartment-specific importance of glutathione during abiotic and biotic stress . Front. Plant Sci. 5: 566.

Zhang, K., Sridhar, V. V, Zhu, J., Kapoor, A., and Zhu, J.-K. (2007a). Distinctive Core Histone Post-Translational Modification Patterns in Arabidopsis thaliana. PLoS One 2: e1210.

Zhang, X., Bernatavichute, Y. V, Cokus, S., Pellegrini, M., and Jacobsen, S.E. (2009). Genome-wide analysis of mono-, di- and trimethylation of histone H3 lysine 4 in Arabidopsis thaliana. Genome Biol. 10: R62.

Zhang, X., Clarenz, O., Cokus, S., Bernatavichute, Y. V, Pellegrini, M., Goodrich, J., and Jacobsen, S.E. (2007b). Whole-Genome Analysis of Histone H3 Lysine 27 Trimethylation in *Arabidopsis*. PLoS Biol 5: e129.

Zhang, Y., Song, L., Liang, W., Mu, P., Wang, S., and Lin, Q. (2016). Comprehensive profiling of lysine acetylproteome analysis reveals diverse functions of lysine acetylation in common wheat. Sci. Rep. 6: 21069.

Zhao, S. et al. (2010). Regulation of Cellular Metabolism by Protein Lysine Acetylation. Science (80-. ). 327: 1000–1004.

Zhou, C., Zhang, L., Duan, J., Miki, B., and Wu, K. (2005). HISTONE DEACETYLASE19 Is Involved in Jasmonic Acid and Ethylene Signaling of Pathogen Response in Arabidopsis. Plant Cell 17: 1196–1204.

Zhou, M., Wang, W., Karapetyan, S., Mwimba, M., Marques, J., Buchler, N.E., and Dong, X. (2015). Redox rhythm reinforces the circadian clock to gate immune response. Nature 523: 472–476.

Zhou, W., Chen, X., He, K., Xiao, J., Duan, X., Huang, R., Xia, Z., He, J., Zhang, J., and Xiang, G. (2016). Histone deacetylase inhibitor screening identifies HC toxin as the most effective in intrahepatic cholangiocarcinoma cells. Oncol. Rep. 35: 2535–2542.

Zhu, Q.-H., Shan, W.-X., Ayliffe, M.A., and Wang, M.-B. (2015). Epigenetic Mechanisms: An Emerging Player in Plant-Microbe Interactions. Mol. Plant-Microbe Interact. 29: 187–196.

Zhu, Z. et al. (2011). Derepression of ethylene-stabilized transcription factors (EIN3/EIL1) mediates jasmonate and ethylene signaling synergy in Arabidopsis. Proc. Natl. Acad. Sci. U. S. A. 108: 12539–12544.